REVIEW OF EFFECTS OF SUPERCOMPACTED WASTE AND HETEROGENEOUS WASTE EMPLACEMENT ON WIPP REPOSITORY PERFORMANCE

FINAL REPORT

Prepared by:

Trinity Engineering Associates
8832 Falmouth Drive
Cincinnati, Ohio 45231-5011

Under

Contract 68-D-00-210
Work Assignment 3-04

Prepared for:

U.S. Environmental Protection Agency
Office of Radiation and Indoor Air
Washington, DC 20460

Mr. Tom Peake
Work Assignment Manager

March 17, 2004

TABLE OF CONTENTS

LIST OF FIGURES AND TABLES

EXECUTIVE SUMMARY

This report presents a Trinity Engineering Associates (TEA) review of the proposed U.S. Department of Energy (the Department or DOE) emplacement of supercompacted waste at the Waste Isolation Pilot Plant (WIPP) in southeastern New Mexico. TEA is under contract to the U.S. Environmental Protection Agency (the Agency or EPA) to provide WIPP technical support. The supercompacted waste would be shipped from the Advanced Mixed Waste Treatment Facility (AMWTF), currently undergoing testing at the Idaho National Engineering and Environmental Laboratory. At the time of initial Agency certification, the WIPP was in a pre-operational status and the standard waste that was to be emplaced was modeled in performance assessment as homogeneous in physical and chemical properties. Upon becoming operational, it has become clear that waste from some generator sites could have different physical and chemical properties than the standard waste, and that such waste would tend to be shipped to WIPP in disposal campaigns that may result in a clustering of similar waste types within the repository. This emplacement process may result in an increased probability that one intruding borehole may encounter waste that is chemically and physically quite different from another intruding borehole, with a possible difference in releases.

These issues are reviewed in this report in the context of high strength, supercompacted waste from the AMWTF. The standard waste envisioned at the time of initial Agency certification was generally uncompacted, homogeneous, degraded, and compressible. The supercompacted wastes are highly rigid, may degrade more slowly, and are not expected to further compress during repository creep closure. In addition, the supercompacted waste is volumetrically significant and chemically dissimilar from the average standard waste assumed in the initial certification, with above average cellulose, plastic and rubber (CPR) concentrations and below average radionuclide concentrations.

The possible effects of these waste types on repository performance were evaluated by the Department in a special Advanced Mixed Waste (AMW) performance assessment. As a result of its assessment, the Department concluded that waste heterogeneity is not important to WIPP performance assessment and that AMWTF waste can be appropriately modeled as homogeneous standard waste. TEA's review of that assessment considered the differences in waste inventory, the effects of changes in waste mechanical characteristics, the heterogeneity in waste placement in the repository, the effects on chemical conditions in the repository, the ability of the Department to adequately predict waste room closure, and the adequacy of the Department's analysis of features, events, and processes to be considered in the performance assessment.

Not all information regarding emplacement of supercompacted AMWTF waste that has been requested by the Agency has been received from the Department at this time and several issues remain that have not been completely resolved. However, based on the information available at this time, TEA believes that emplacement of supercompacted and uncompacted AMWTF wastes at WIPP is not likely to affect the ability of the repository to meet the Agency-mandated release limits and will not have a significant impact on overall repository performance. The ability of the repository to successfully isolate waste from the environment is substantial and releases resulting from intrusion events are expected to be lower for AMWTF waste than for standard waste. This

is because of the higher strength and lower radionuclide inventories of the supercompacted waste. The remaining issues that have not been resolved concern the generation of CO_2 and the amount of MgO that must be added to the supercompacted waste to sequester it, and the effect of an increased room-scale permeability on direct brine releases.

1.0 INTRODUCTION

This report presents a Trinity Engineering Associates (TEA) review of the proposed U.S. Department of Energy (the Department or DOE) emplacement of supercompacted and heterogeneous waste at the Waste Isolation Pilot Plant (WIPP) in southeastern New Mexico. TEA is under contract to the U.S. Environmental Protection Agency (the Agency or EPA) to provide WIPP technical support. At the time of initial Agency certification, the WIPP was in a pre-operational status and the waste that was to be emplaced was assumed in the Department's performance assessment to be generally homogeneous in physical and chemical characteristics. Upon becoming operational, it has become clear that waste may be shipped to WIPP in disposal campaigns from the various source sites. This has resulted in a clustering of similar waste types within the repository on a scale that may alter the original performance assessment assumptions of random placement and homogeneity in determining releases from borehole intrusions. The waste has also been emplaced in a variety of container types and some waste is proposed by the Department to be emplaced in a supercompacted form that would have different physical characteristics than standard waste and may also alter the original performance assessment assumptions of homogeneity.

This report presents TEA's evaluation of the Department's conclusion that the original performance assessment assumptions remain appropriate in view of these differences. Much of the information in this report was obtained from Revisions 0 and 1 of the Sandia National Laboratories (SNL) report *Effects of Supercompacted Waste and Heterogeneous Waste Emplacement on Repository Performance* (Hansen et al. 2003a and 2003b). Those reports were prepared for the Department in response to an Agency request for additional information (EPA 2003). Information supporting this evaluation was also obtained from cited references and from technical exchange meetings with Department and SNL staff members on October 21 and 22, 2003, in Idaho Falls, Idaho, on November 18 and 19, 2003, in Carlsbad, New Mexico, and on January 20 through 23, 2004, in Albuquerque, New Mexico.

2.0 BACKGROUND INFORMATION

The Department's original performance assessment, presented in its 1996 Compliance Certification Application (DOE 1996), and the Agency-mandated Performance Assessment Verification Test (PAVT; SNL 1997a and 1997b), both assumed that waste containers would degrade rapidly in the WIPP repository environment and that the waste and the emplaced containers would not be physically strong. Under these circumstances, the waste would be expected to compress and to a degree mix under the force of halite creep during room closure to a waste mass that, on the average, can be considered homogeneous. These assumptions, along with the assumption of random placement, supported treating the waste as a homogeneous, well-mixed material in performance assessment. These assumptions may be challenged by the disposal of wastes of different types and the potential for large-scale clustering of such waste in the repository. These conditions result in the possibility that one intruding borehole may encounter waste that is chemically and physically quite different from another intruding borehole, with a possible difference in releases. These issues have been reviewed by TEA in the context of high strength waste from the proposed disposal of supercompacted waste at WIPP and the historic receipt and disposal of large quantities of similar wastes within a single waste panel.

The Department's analysis of the effects of supercompacted waste and heterogeneous waste emplacement (Hansen et al. 2003a and 2003b) included an analysis of pipe overpack waste from the Rocky Flats Environmental Technology Site (RFETS). Pipe overpacks are stainless steel cylinders that are considerably more rigid than the standard waste containers modeled in the original WIPP certification performance assessment. Although pipe overpack waste is mentioned when reviewing the Department's analysis, the focus of this report is on the influence of supercompacted waste.

2.1 Supercompacted Waste

The Department has requested the Agency to approve emplacement of supercompacted waste at the WIPP in a letter dated December 10, 2003 (Docket A-98-49, Item II-B-15). Supercompacted waste would be processed at the Advanced Mixed Waste Treatment Facility (AMWTF), currently undergoing testing at the Idaho National Engineering and Environmental Laboratory (INEEL). The AMWTF is designed to retrieve, characterize, repackage, and compact 55-gallon drums of contact-handled, mixed transuranic debris waste, and place the compacted drums into 100-gallon drums for disposal at WIPP (Hansen et al. 2003b, p. 15). Non-debris waste would also be processed at the AMWTF but would not be compacted. The uncompacted waste would be placed in standard 55-gallon drums or in standard waste boxes for shipment and disposal at WIPP (Hansen et al. 2003b, p. 17). The Agency approved disposal of the uncompacted AMWTF waste on June 11, 2003, assuming all additional requirements were also met (Docket A-98-49, Item II-B3-56).

The 55-gallon drums of debris waste would be compressed vertically, resulting in flattened cylinders called "pucks." The supercompacted pucks would have final volumes expected to range from 15 to 35 gallons. Each 100-gallon drum is expected to contain from 3 to 5 pucks, with an average of 4 pucks per drum (Hansen et al. 2003b, p. 15). Both the 55-gallon drums and the 100-

gallon disposal containers would be made of steel. A photograph of several supercompacted pucks is presented in Figure 2-1.

The 55-gallon drums of supercompacted waste would be compacted under a nominal pressure of about 60 MPa, which is considerably greater than the maximum compactive pressure of approximately 15 MPa exerted by halite creep at the WIPP repository (Hansen et al. 2003b, p. 23). As a result, the Department expects no additional compaction of this waste during repository creep closure. The presence of supercompacted waste would alter the time-dependent creep closure of waste rooms. The homogeneous waste model does not include the possible effects of spatially varying room closure or the specific mechanical or chemical characteristics of these supercompacted wastes.

Figure 2-1. Supercompacted waste pucks as generated in the AMWTF (from Hansen et al. 2003b, Figure 2-1)

2.2 Heterogeneous Emplacement

The operational plan of the WIPP is to emplace waste as it arrives. The WIPP site has limited above-ground waste storage capability so waste must be placed underground promptly for shipments to continue at a normal pace. Waste streams from individual sites, particularly pipe overpack waste from RFETS, have arrived at the WIPP in a short period of time, leading to local concentrations of the same waste stream in a particular area of the repository (Hansen et al. 2003a, p. 13). For example, approximately 43% of the containers in Panel 1 include a pipe overpack (Hansen et al. 2003b, p. 18). The 19,875 m^3 of supercompacted AMWTF waste will account for about 12 percent of the total available volume of 168,485 m^3 for contact-handled (CH) waste at WIPP, and the 40,944 m^3 of uncompacted AMWTF waste will account for about 24 percent of the total volume. Together, the Department expects the total volume of AMWTF waste (60,819 m^3) to account for 36% of the total available volume of CH waste at WIPP (Hansen et al. 2003b, p. 18). Local waste stream concentrations may be inconsistent with the assumptions of random placement and repository-wide homogeneity. The Department analyzed the effect of heterogeneous waste emplacement of supercompacted AMWTF wastes in a separate Advanced Mixed Waste (AMW) performance assessment. A primary purpose of TEA's review

of AMWTF waste emplacement at WIPP is to evaluate the potential impacts of departures from the mechanical and chemical homogeneity assumptions that were made in the initial WIPP compliance certification.

3.0 WASTE INVENTORY

This section presents an overview and evaluation of the inventory of AMWTF waste. TEA has compared inventory information provided by the Department in Hansen et al. (2003a and b) with supporting inventory information from the 1996 and draft 2003 certification and recertification applications.

3.1 DOE Inventory Characterization

3.1.1 AMWTF Waste

All AMWTF waste to be emplaced at WIPP will be contact-handled, transuranic (CH-TRU) waste. The inventory of supercompacted AMWTF debris waste is based on a total of 52,440 100-gallon containers being shipped to the WIPP (Leigh and Lott 2003a, p. 5). The total emplaced volume of these wastes, based on an inner volume of 0.379 m^3 per 100-gallon container, is 19,875 m^3. However, the actual supercompacted waste volume is reported by INEEL to be 11,635 m^3 (Leigh and Lott, 2003a, p. 5), which is 41 percent less than the container volume due to unused void space within the 100-gallon containers. The inventory for uncompacted AMWTF non-debris waste is based on a total of 7,138 ten-drum overpacks and 3,573 standard waste boxes being shipped to the WIPP (Leigh and Lott, 2003b, Table 7). The total emplaced volume of these uncompacted wastes is 40,944 m^3, based on inner volumes of 4.79 m^3 per ten-drum overpack and 1.89 m^3 per standard waste box (Hansen et al. 2003b, p. 18). The Department's currently projected, total waste volume of 60,819 m^3 for the AMWTF waste is more than double the volume of 28,607 m^3 used in the CCA and PAVT (DOE 1996, Appendix BIR) for all INEEL waste streams. Because of continuing inventory changes, discrepancies between the 1996 CCA and the more recent inventory data are expected.

Table 3.1 compares the Department's estimates of the emplaced volumes for supercompacted and uncompacted AMWTF waste from INEEL with the total volume of non-AMWTF CH-TRU waste to be contained in the WIPP repository. These comparisons are also shown as percentages. Supercompacted AMWTF waste is expected to be 11.8 percent of the total volume of CH-TRU waste emplaced at WIPP and uncompacted AMWTF waste is expected to be 24.3 percent of the total volume. These emplaced volumes are computed on a waste package basis calculated using the total inner volumes of the waste containers.

Table 3.1. Emplaced Waste Volumes in the WIPP Repository

Waste Type	Repository Totals
Total volume of CH-TRU waste from all sources	168,500 m^3
Volume of supercompacted waste from INEEL	19,875 m^3
Volume percent of supercompacted waste from INEEL	11.8 %
Volume of uncompacted waste from INEEL	40,944 m^3
Volume percent of uncompacted waste from INEEL	24.3 %
Volume of non-AMWTF waste from INEEL and all other sites	107,681 m^3
Volume percent of non-AMWTF waste from INEEL and all other sites	63.8 %

Modified from Hansen et al. 2003b, Table 8

The Department's analysis of the AMWTF waste inventory (Hansen et al. 2003b, Section 3.2) focused on the radioactivity, which is important in calculating direct releases, and the density of cellulosics, plastics, and rubbers (CPR), which is important for the repository gas generation that drives certain types of releases. The radioactive and CPR components in AMWTF wastes are significantly different from those in waste streams from other sources.

3.1.1.1 Radioactivity in AMWTF Wastes

The radioactivity of AMWTF wastes reported by the Department is compared with the radioactivity of non-AMWTF wastes for important radionuclides in Table 3.2. The concentration was calculated as mass per total container volume and may therefore underestimate the actual concentration in the waste because of the void space in the containers. This comparison shows that the average radionuclide concentrations in both the supercompacted and uncompacted AMWTF wastes are an order of magnitude less than the average concentration in all non-AMWTF waste streams.

Table 3.2. Radionuclide Loadings in CH TRU WIPP Waste

Radionuclide	Uncompacted AMWTF Waste	Supercompacted AMWTF Waste[1]	All CH-TRU Without AMWTF Supercompacted Waste[1]
^{229}Th (Ci/m^3)	Not calculated	5.41E-5	3.23E-6
^{230}Th (Ci/m^3)	Not calculated	5.86E-9	6.81E-7
^{233}U (Ci/m^3)	Not calculated	4.44E-2	2.38E-3
^{234}U (Ci/m^3)	Not calculated	9.85E-5	1.12E-3
^{238}Pu (Ci/m^3)	Not calculated	2.54E0	1.05E+1
^{239}Pu (Ci/m^3)	Not calculated	2.00E0	4.18E0
^{240}Pu (Ci/m^3)	Not calculated	1.70E-1	6.98E-1
^{241}Pu (Ci/m^3)	Not calculated	3.95E-3	1.62E+1
^{242}Pu (Ci/m^3)	Not calculated	5.66E-4	1.04E-4
^{241}Am (Ci/m^3)	Not calculated	3.74E-1	2.65E0
Total (Ci/m^3)	5.89 E0[2]	5.13E0[2]	44.8E0[2]
Radionuclide Activity (Ci)	2.41E+05[2]	1.02E+05[2]	4.92E+06[2]
Emplaced Volume (m^3)	40,944[2]	19,875[2]	109,737[2]

1. Based on Leigh 2003d, Attachment 1.
2. Modified from Hansen et al. (2003a) and personal communication Leigh, October 2003.

3.1.1.2 CPR Concentrations in AMWTF Wastes

The densities of CPR materials in AMWTF wastes reported by the Department are compared with the densities in non-AMWTF wastes in Table 3.3. The CPR densities were calculated by dividing the total masses of cellulosics, plastics, and rubbers in the waste containers by the total volume of each type of container. These densities represent the total mass of waste divided by the total container volume and may therefore underestimate the actual density of the waste because of the void space in the containers. The data show that while the CPR density in the supercompacted waste is an order of magnitude higher than for waste streams from other sources, the density in the uncompacted AMWTF waste is an order of magnitude lower than that of waste from other sites. These calculated densities are based on waste volumes presented in Leigh and Lott (2003a and b).

Table 3.3. Average Densities of Cellulosic, Plastic, and Rubber Materials in Emplaced, Contact-Handled Waste

Waste Type	Density of Cellulose (kg/m^3)	Density of Plastic (kg/m^3)	Density of Rubber (kg/m^3)	Density of Plastic Packaging (kg/m^3)
Supercompacted AMWTF waste[1]	302.67	204.54	79.91	0.0
Uncompacted AMWTF waste in ten-drum overpacks[2]	2.68	3.55	0.01	19.11
Uncompacted AMWTF waste in standard waste boxes[3]	2.73	3.56	0.01	16.0
Non-AMWTF waste streams from INEEL and all other sites[3]	33.65	26.49	7.12	17.93

1. Leigh and Lott, 2003a
2. Leigh and Lott, 2003b
3. Leigh, 2003a

3.2 TEA Inventory Evaluation

TEA's evaluation of waste inventory data focused on available information for AMWTF waste as presented in Appendix DATA of the Department's draft 2004 WIPP Compliance Recertification Application (DOE 2003). TEA's evaluation of the AMWTF inventory information supporting the AMW performance assessment is presented in Section 3.2.1. As part of this evaluation, four elements of the AMWTF waste were reviewed: (1) inventory volumes; (2) radioactivity; (3) CPR concentrations; and (4) ligand, phosphate, nitrate, and sulfate concentrations. These reviews are presented in Section 3.2.2. The conclusions related to TEA's evaluation of the inventory data are summarized in Section 3.2.3. TEA assessed data transfer from the Draft Final CRA to the AMWTF documents, and whether the Hansen et al. (2003a and b) AMWTF inventory data were supported by the Draft Final CRA (DOE 2003) inventory data. An adequacy analysis of the Draft Final CRA inventory data was not included in this investigation.

3.2.1 Evaluation of AMWTF Waste

3.2.1.1 Evaluation Methodology

TEA evaluated the following documents to verify the volumes, radionuclide content, and CPR content of the supercompacted AMWTF waste streams that were presented by the Department in Hansen et al. (2003a and b).

- *Final Draft CRA, Annex C of Attachment F to Appendix DATA* (DOE 2003). This annex provided a list of Appendix BIR (DOE 1996) waste streams that were combined to create the supercompacted AMWTF waste stream (IN-BN–510) as well as waste streams from Appendix BIR that were combined to create the uncompacted AMWTF waste stream.

- *Final Draft CRA, Annex E of Attachment F to Appendix DATA: Table DATA-F-E-1 for CH-TRU Waste Streams and Table DATA-F-E-2 for RH-TRU Waste Streams* (DOE 2003). These tables present data for emplaced waste streams included in the current WIPP disposal inventory for the 20 radionuclides considered most important to performance assessment for CH-TRU waste, and the 10 radionuclides considered most important to performance assessment for RH-TRU wastes. The data were compiled from Annexes J and K, and include the associated scaled volumes and radionuclide concentrations scaled and decayed to December 2001.

- *Final Draft CRA, Annex J of Attachment F to Appendix DATA* (DOE 2003). This annex provides a list of waste stream profile information for all AMWTF waste streams currently identified for disposal at the WIPP. The profile information includes waste stream volumes, waste material densities, and radionuclide concentrations.

- *Calculation of Waste Stream Volumes, Waste and Container Material Densities and Radionuclide Concentrations for Waste Stream IN-BN-510 at INEEL for the Compliance Recertification Application* (Leigh and Lott 2003a). This document provides information regarding the supercompacted waste stream volume, material densities, and radionuclide concentrations.

- *Radionuclide Densities in CH Waste Streams from TWBID Rev. 2.1 Version 3.1.2 Data Version 4.09, Letter Response to Dr. L.H. Brush, Attachment 1* (Leigh 2003d). The table in Attachment 1 of this document provides the half-life decayed, scaled concentrations for 13 radionuclides in the supercompacted AMWTF IN-BN-510 waste stream. This table is equivalent to Table 2 of Leigh and Lott (2003a).

- *Attachment TWBIR2 to the Compliance Certification Application* (DOE 1996). This attachment was used to recalculate the precursor waste stream volumes and waste material densities used to develop the supercompacted AMWTF waste stream information.

TEA evaluated the inventory data used in the AMW performance assessment by comparing the information in Hansen et al. (2003a and b) and their direct sources with information presented in

the aforementioned attachments and annexes to the Department's draft final Compliance Recertification Application (DOE 2003).

3.2.1.2 Inventory Volumes

Comparison of CRA to Hansen et al. Volumes. The inventory volumes reported by Hansen et al. (2003a and b) for both the supercompacted and uncompacted AMWTF wastes (19,875 m^3 and 40,044 m^3, respectively) were compared to totals cited in the annexes to Attachment F of the Department's Draft Final CRA (DOE 2003). The volume of 19,875 m^3 for the supercompacted waste stream IN-BN-510 as presented in Annex J of Attachment F was identical to the volume reported in Hansen et al. TEA then attempted to verify conversion of the pre-compacted waste volume to the final supercompacted waste volume based upon data provided in Hansen et al. Hansen et al. indicate that a total of 52,440 100-gallon containers would be used in the supercompacted waste stream. TEA attempted to generate this same number of drums based upon the total pre-compaction volume of 46,463 m^3 of waste presented in Annex J. Assuming that all pre-compacted waste would be contained in 55 gallon drums with a volume of 0.208 m^3 per container, a total of 223,374 55-gallon containers would require compaction. If an average of four compacted 55 gallon drums fit in each 100-gallon container, then a total of 55,844 100-gallon containers would be needed for the supercompacted waste. This is slightly but not substantially different from the 52,440 100-gallon containers predicted in Hansen et al. The total volume of uncompacted waste was reported as 41,083 m^3 in Annex J. Again, this is slightly but not substantially different from the 40,944 m^3 predicted in Hansen et al.

Comparison of Hansen et al. Supporting Documents to the Hansen et al. Volumes. The inventory volumes reported by Hansen et al. (2003a and b) for both the supercompacted and uncompacted AMWTF wastes (19,875 m^3 and 40,044 m^3, respectively) were compared to totals cited in Hansen et al.'s supporting documents. The volume of supercompacted waste reported in Leigh and Lott (2003a) was identical to the volume reported in Hansen et al.

In summary, the supercompacted AMWTF waste volumes presented in Leigh and Lott (2003a) corresponded identically with data presented in Hansen et al. (2003a and 2003b) and in the Draft Final CRA.

3.2.1.3 Radioactivity

As described in Table 3.2, the average radionuclide concentration in the supercompacted and uncompacted AMWTF waste is considerably less than the average concentration in all non-AMWTF waste streams. This is to be expected, because the Department intends to blend lower-activity waste with higher-activity TRU waste for both the supercompacted and uncompacted AMWTF wastes to meet transportation requirements. Currently, most of the unprocessed waste does not meet the requirements for transportation to and disposal at WIPP. For example, some of the waste has not been characterized sufficiently or is in boxes or drums that are unsuitable for shipping in the TRUPACT-II containers certified for WIPP. Some waste requires repackaging to meet the minimum concentration of alpha-emitting radionuclides specified for the "transuranic" category in WIPP's waste acceptance criteria.

Comparison of CRA to Hansen et al. (2003b) TEA attempted to trace the radionuclide concentration values in selected source references to the data in Hansen et al. (2003b) for both

supercompacted and uncompacted AMWTF waste. Using Leigh (2003d) and the Draft Final CRA's Appendix DATA, Attachment F, Annex E (DOE 2003), TEA was able to verify transfer of data for the 10 EPA radionuclides from these data sources to Table 3.2 of Hansen et al. (2003b) for the supercompacted waste stream IN-BN-510. Several discrepancies, however, were noted.

While some of the non-decayed, non-scaled radionuclide concentrations reported in Leigh and Lott (2003a) and in the Draft Final CRA's Appendix DATA, Attachment F, Annex J (DOE 2003), are the same as the decayed and scaled data reported in Annex E and in Hansen et al. (2003b), other radionuclide concentrations changed as a result of the decay and scaling corrections. The discrepancies are likely affected by differences in decay and scaling factors, but could also be influenced by reporting errors or ingrowth. Insufficient information was presented in the Department's documentation for TEA to determine why some decay-corrected, scaled radionuclide concentrations changed and some did not. Not all radionuclide concentrations listed in Hansen et al.'s Table 13 (2003a) for the category *All CH-TRU Without Supercompacted Waste* could therefore be replicated. It was verified, however, that the total decayed and scaled radionuclide concentrations in Hansen et al.'s Table 13 (2003a) for this category is equivalent to those found in Attachment F of the Draft Final CRA (DOE 2003). Table 3.4 compares the radionuclide values listed in Leigh (2003d), in the Draft Final CRA Annexes E and J (DOE 2003), and in Hansen et al. (2003a).

Table 3.4. Comparison of Radionuclide Concentrations in Supercompacted Waste Stream IN-BN-510 by Source Document

Radionuclide	Leigh and Lott 2003a (not scaled or decayed) (Ci/m^3)	Draft Final CRA Appendix DATA Attachment F Annex J, Waste profiles for IN-BN-510 (not scaled or decayed) (Ci/m^3)	Leigh 2003d (scaled and decayed) (Ci/m^3)	Draft Final CRA Appendix DATA Attachment F Annex E (total conc./total volume, scaled and decayed) (Ci/m^3)	Hansen et al. 2003a (scaled and decayed) (Ci/m^3)
^{229}Th	Not Reported	Not Reported	5.41E-05	5.41E-05	5.41E-05
^{230}Th; ^{230}Th	Not Reported	Not Reported	5.86E-09	5.86E-09	5.86E-09
^{233}U; ^{233}U	4.44E-02	4.44E-02	4.44E-02	4.44E-02	4.44E-02
^{234}U	Not Reported	Not Reported	9.85E-05	9.85E-05	9.85E-05
^{238}Pu	2.81E+00	2.81E+00	2.54E+00	2.54E+00	2.54E+00
^{239}Pu	2.00E+00	2.00E+00	2.00E+00	2.00E+00	2.00E+00
^{240}Pu	1.69E-01	1.7E-01	1.7E-01	1.7E-01	1.7E-01
^{241}Pu	7.38E-03	7.38E-03	3.95E-03	3.95E-03	3.95E-03
^{242}Pu	5.66E-04	5.66E-04	5.66E-04	5.66E-04	5.66E-04
^{229}Th; ^{241}Am	3.82E-01	3.82E-01	3.74E-01	3.74E-01	3.74E-01

As indicated above, general radionuclide information for the supercompacted waste as presented in the Draft Final CRA (DOE 2003) could be traced to Hansen et. al (2003a and b), although the specific decay calculations could not be confirmed. Values for the uncompacted AMWTF waste could not be confirmed due to a lack of data in supporting documents as well as in Hansen et al.

Comparison of the AMWTF Supporting Documents to Hansen et al. TEA attempted to trace radionuclide concentration values for supercompacted waste from selected references to Hansen et al. (2003a and b) for the purpose of testing data transfer. TEA was able to verify accurate transfer of radionuclide concentration data from Leigh (2003d) to Hansen et al. for the ten radionuclides described in Table 3.2. TEA then attempted to verify the values in Leigh (2003d, Attachment 1) for supercompacted AMWTF waste by comparing those values with the values reported in Leigh and Lott (2003a, Table 2) and in Lott (2003b, Table E-1). Leigh and Lott (2003a) present radionuclide concentration data for supercompacted AMWTF waste recalculated for a waste stream volume of 19,875 m^3. Lott (2003b) presents radionuclide data in terms of scaled total Curies. Lott (2003b) also presents scaled waste stream volumes. TEA was able to verify that the supercompacted radionuclide concentrations reported in Leigh and Lott (2003a) and Lott (2003b) were accurately transferred. Using Lott (2003b, Table E-1) and Leigh and Lott (2003b, Tables 11 and 12), TEA then attempted to confirm radionuclide concentrations for the uncompacted AMWTF waste. For some radionuclides, such as Pu-238, Pu-239, and Pu-240, the values were consistent across the two reference documents. However, inconsistencies were found for Am-241. The nature and origin of these inconsistencies could not be determined from the available documentation.

3.2.1.4 CPR Concentrations

Comparison of CRA to Hansen et al. TEA used waste material parameter densities and volumes found in the Draft Final CRA's Attachment F, Annex J (DOE 2003) to verify the average densities for cellulosics, plastics, and rubber as presented in Hansen et al. (2003a and b). Uncompacted waste stream densities in Hansen et al. and Annex J compared with minor differences, as shown in Table 3.5.

Table 3.5. Comparison of Uncompacted CPR Densities between Hansen et al. and Annex J

Waste Material Parameter	Annex J Density Value (kg/m^3)	Hansen et al. (2003a) Density Value (kg/m^3)
Cellosics	2.71	2.68
Plastic	3.58	3.55
Rubber	0.02	0.01
Plastic Packaging	18.55	18.91

Table 3.3 indicates that the average density of CPR in supercompacted AMWTF waste is approximately an order of magnitude higher than in non-AMWTF waste. Also, the average density of CPR in the uncompacted AMWTF waste is much lower than from other sources. This result is expected because the supercompacted waste is concentrated debris waste consisting

largely of man-made materials, while the uncompacted, non-debris waste is largely soils and sludges (Hansen et al. 2003a, Section 2.3). The calculated densities of CPR materials in the supercompacted waste stream as documented in Annex J were identical to those reported in Hansen et al. (2003a). However, the pre-compacted waste stream volumes and densities that would allow TEA to compare the pre-compacted and compacted volumes and densities were not available in Annex J.

Comparison of AMWTF Supporting Documents to Hansen et al. For supercompacted AMWTF waste, TEA compared the results in Leigh and Lott (2003a) against the values reported by Hansen et al. (2003a and b). The values in Leigh and Lott agree with the values in Hansen et al.

Comparison of TWBIR2 to AMWTF Supporting Documents and Hansen et al. The density of supercompacted waste as presented in Hansen et al. (2003a and b) was compared to the calculated densities obtained from TWBIR2 (DOE 1996) for the waste streams that were combined to form the supercompacted waste stream IN-BN-510. The densities obtained from the TWBIR2 calculations were corrected to account for the compaction process assuming that all the precompacted waste containers were 55 gallon drums and that an average of four compacted drums would be placed in each 100 gallon container. Table 3.6 illustrates the comparative densities obtained from TWBIR2 and Hansen et al.

Table 3.6. Comparison of Supercompacted CPR Densities between Hansen et al. and TWBIR2

Waste Material Parameter	TWBIR2 Density (kg/m^3)	Hansen et al (2003a) Density (kg/m^3)
Cellosics	280.4	302.67
Plastic[1]	250.2	204.54
Rubber	58.9	79.91

3.2.1.5 Ligands, Phosphate, Nitrate, and Sulfate

Hansen et al. (2003b, p. 40) indicate that supercompacted AMWTF waste does not contain ligands. This is supported by inventory information examined by Crawford and Leigh (2003) indicating that the only ligands in the AMWTF waste streams are in the uncompacted waste. Crawford and Leigh (2003) state that RFETS waste that was shipped to INEEL for processing contains a small quantity (25.6 kg) of the ligand EDTA. The EDTA was used over a 20-year

[1]The plastics total from TWBIR2 represents the total plastic material in the waste (185.5 kg/m3) plus the plastic packaging material in the compacted drums (64.7 kg/m3). Hansen et al. (2003b, Table 13) reported a plastic packaging density of 0 kg/m^3 because the plastic liners in the compacted 55 gallon drums were no longer considered to be packaging material.

period as a complexing agent for generating saltcrete waste and because of the long period of use, this ligand was likely widely distributed in the saltcrete and is present in low concentrations (Crawford and Leigh, 2003). TEA believes that the concentration of ligands assumed for WIPP brine in the AMW performance assessment is conservatively high because it was based on the assumption that the entire ligand inventory in the repository would dissolve in the minimum amount of brine required for a release (Brush and Xiong 2003b). The performance assessment calculations are therefore conservative and the possible presence of small quantities of ligands in AMWTF uncompacted waste should not affect repository performance. Appendix BIR (DOE 1996) also indicates the presence of phosphate, nitrate and sulfate in INEEL waste. Hansen et al. (2003a and b) make no statement regarding the presence or absence of these three constituents in AMWTF waste.

3.2.2 Evaluation Conclusions

TEA generally verified the accuracy of transferring waste volume and concentration data from the Draft Final CRA (DOE 2003) to the AMW performance assessment. Although discrepancies were identified between various supporting documents, the general assumptions regarding CPR content and radionuclide content as presented in Hansen et al. (2003a and b) were consistent with the inventory information presented in the Draft Final CRA. That is, the relatively high CPR and low radionuclide concentrations in supercompacted AMWTF waste were substantiated, as were the relatively low CPR and low radionuclide concentrations in uncompacted AMWTF waste. The inventory information used in the AMW performance assessment for supercompacted AMWTF waste was found to be generally confirmed by TEA's review. TEA concludes that the supercompacted waste inventory information used in the AMW performance assessment is consistent in general magnitude with information presented in the Draft Final CRA, and conclusions drawn by Hansen et al. concerning the effects of the increased CPR concentrations of these wastes appear to be supported by the Draft Final CRA inventory.

4.0 WASTE MECHANICAL AND EMPLACEMENT CHARACTERISTICS

4.1 DOE Mechanical and Emplacement Assumptions

4.1.1 AMWTF Supercompacted Waste

The AMWTF will compact 55-gallon drums of debris waste and place the compacted drums into 100-gallon disposal drums for shipment to WIPP. Compaction is performed in a 2,000 metric ton press (BNFL 2003, p. 1). As previously mentioned, this press subjects the waste to a pressure of about 60 MPa, which is considerably higher than the maximum of about 15 MPa due to room closure (Hansen et al. 2003b, p. 23). The Department therefore expects the individual pucks to be more rigid and have lower porosities than standard waste. The Department believes that the lower porosities will provide greater resistance to brine penetration, which is expected to make the supercompacted waste more resistant to degradation and corrosion (Hansen et al. 2003b, p. 50). Because of its compaction and resistance to degradation, the Department also expects the shear and tensile strengths of the supercompacted waste to be equal to or higher than that for standard waste (Hansen et al. 2003b, p. 49). The Department also notes that because of its mechanical and physical form, the room-scale permeability of supercompacted waste will be at least as great as that of standard waste, and may be higher (Hansen et al. 2003b, p. 45). This conclusion is based on the ability of the rigid waste to maintain open channels between stacks of supercompacted waste (Hansen et al. 2003b, p. 46).

The 100-gallon disposal drums for supercompacted waste have a 35-inch (89 cm) outside height and a 32-inch (81 cm) outside diameter. An uncompacted 55-gallon drum has a similar height but a 24-inch (61 cm) diameter. The weight of an empty 100-gallon drum is 95 pounds (43 kg) and, as previously stated, the inner volume is 0.379 m^3 (Hansen et al. 2003b, p. 16). The 100-gallon drums would be shipped to and emplaced at WIPP in groups of six (two layers of three drums each) or three (one layer of three drums). This configuration is operationally efficient because its footprint is similar to the footprints of a standard seven-pack of 55-gallon drums, a ten-drum overpack, and a standard waste box.

Assuming that only supercompacted waste is placed in a waste room, the initial waste room porosity was calculated by the Department to be about 0.743. This porosity was determined based on the void space between and within the 100-gallon drums and includes consideration of the MgO backfill (Hansen et al. 2003b, Section 3.1.4). During waste room closure, the free space in the room is expected to close rapidly and deform the 100-gallon drum outer containers (Hansen et al. 2003b, p. 30). However, because of the high, 60 MPa compaction pressure used to create the waste pucks, the pucks themselves are expected to remain rigid and not deform under the much lower, 15 MPa maximum pressure of the creeping halite. The Department believes that packages of supercompacted waste would therefore tend to hold the waste room open and preserve the structural integrity of the supercompacted waste stack during creep closure (Hansen et al. 2003b, p. 23).

The primary release mechanisms of cavings and spallings are sensitive to waste strength. Because of the expected greater shear strength of supercompacted waste, the Department has

concluded that the waste shear strength values used in calculating cavings releases for standard waste are conservatively low and do not need to be changed for supercompacted waste (Hansen et al. 2003a, p. 52). Similarly, because of the expected greater tensile strength of supercompacted waste, the Department has concluded that the waste tensile strength values used in calculating spallings releases for standard waste are also conservatively low and do not need to be changed for supercompacted waste (Hansen et al. 2003a, p. 53). The Department also concluded that because of the greater strength and higher room-scale permeability of the supercompacted waste, the stuck pipe and gas erosion release scenarios, which were screened out of the CCA and PAVT performance assessments for standard waste, are even less likely to occur for supercompacted waste and therefore do not need to be considered (Hansen et al. 2003a, p. 53).

The effect of a higher room-scale permeability is believed by the Department to reduce spallings and direct brine releases (Hansen et al. 2003b, p. 46). For spallings releases, this is because the pressure gradients that cause tensile failure near the borehole are reduced as the waste permeability increases (Hansen et al. 2003a, p. 46). For direct brine releases, this conclusion was based on modeling results that showed that a thin layer of the highest assumed waste permeability had minimal effect on the calculated release (Hansen et al. 2003a, p. 47). The Department therefore concluded that applying the standard waste release calculations to supercompacted waste is either conservative because it would tend to overestimate releases, or has a minimal effect.

4.1.2 AMWTF Uncompacted Waste

Although uncompacted AMWTF waste is not the focus of this report, a description is included here because it is referenced in some of the Department's waste loading scenarios in the AMW performance assessment. The uncompacted AMWTF waste will be placed in either ten-drum overpacks or standard waste boxes for shipment to and emplacement at WIPP (Hansen et al. 2003b, Section 2.4). These containers have similar footprints to and can readily be commingled with the 100-gallon drum three or six packs and the 55-gallon drum seven packs in the repository. The uncompacted AMWTF waste is assumed by the Department to have the same characteristics as standard, uncompacted waste from other sites. Assuming that only uncompacted waste is placed in a waste room, the initial waste room porosity was estimated by the Department to be 0.848, which is the same as for standard waste (Hansen et al. 2003b, Table 4). The uncompacted waste package is expected to compress readily during room closure

4.1.3 Waste Heterogeneity in Performance Assessment

The WIPP waste was represented in the CCA and PAVT as randomly placed and homogeneous. Although it is now evident that waste tends to be shipped to and emplaced in the WIPP in groups of similar types from specific generator sites, the Department continues to assume homogeneity in performance assessment through the use of average values for mechanical and chemical waste

properties. The Department cites 40 CFR 194.24(d)[2] as justification for assuming homogeneity (Hansen et al. 2003b, p. 8).

Average values were used for many waste-related parameters in the CCA and PAVT performance assessments. For example, the structural analysis assumed that all waste was placed in 55-gallon drums (Hansen et al. 2003b, p. 20). The waste and waste containers were assumed to rapidly degrade to a very weak, composite material that had the same mechanical and hydrological properties throughout the repository. Although actinide solubilities were sampled, the calculations assumed a homogeneous chemical environment throughout the repository. Gas generation models assumed that the reactants in the waste (iron-based metals for corrosion reactions and CPR for biodegradation) were uniformly distributed throughout the repository (Hansen et al. 2003a, p. 6).

The Department studied the effect of waste heterogeneity on direct release calculations by varying the assumptions and representation of waste in several direct release models. Given an intrusion, cuttings and cavings releases were calculated in the CCA and PAVT performance assessments by randomly selecting three waste streams for the three-drum stack penetrated by an exploration borehole. For the purpose of evaluating the effects of heterogeneity, the Department recalculated these releases by assuming that all three drums are from the same waste stream. Spallings releases were calculated in the CCA and PAVT performance assessments by assuming that the radioactivity in the released material is the average radioactivity in the WIPP repository at the time of intrusion. For the purpose of evaluating the effects of heterogeneity, the Department recalculated these releases by assuming that the release has the same activity as the single waste stream selected in the cuttings and cavings release study. The Department did not study the effect of heterogeneity on direct brine releases because the brine is assumed to be well-mixed and therefore have the same radionuclide concentration throughout the repository (Hansen et al. 2003a, pp. 56-57).

The cuttings and cavings releases from a random selection of three waste streams were found to be similar to releases from a randomly selected single waste stream (Hansen et al. 2003b, Figure 44). The spallings release computed using the average radioactivity in all CH waste streams was found to be higher than the release computed using a single, randomly selected waste stream (Hansen et al. 2003b, Figure 45). In both cases, these observations held for all but the lowest probability releases. Based on these results, the Department concluded that spatial correlations are either not significant, as in the case of cuttings and cavings, or are non-conservative, as in the case of spallings, and can be omitted from performance assessment.

[2]40 CFR Part 194.24(d): The Department shall include a waste loading scheme in any compliance application, or else performance assessments conducted pursuant to § 194.32 and compliance assessments conducted pursuant to § 194.54 shall assume random placement of waste in the disposal system.

4.2 TEA Review of DOE Mechanical and Emplacement Assumptions

4.2.1 AMWTF Supercompacted Waste

4.2.1.1 Review of Waste Properties

TEA believes that the AMWTF waste pucks will be more rigid and are likely to initially have higher shear and tensile strengths than standard waste. This is because the compaction process will deform and impart additional strength to the waste. The approximately 60 MPa normal stress in the supercompaction process is four times greater than the lithostatic pressure of approximately 15 MPa exerted by creep closure of the WIPP repository panels. TEA also agrees that unless the supercompacted waste significantly degrades, it would not be expected to be further compacted by creep closure in the repository and would act as an essentially rigid, unyielding material. A higher shear strength is supported by the Mohr-Coulomb failure criterion, which relates shear strength to normal stress and identifies an increase in shear strength with an increasing normal stress (Lambe and Whitman 1969, p. 307). Tensile strength is not predicted by the Mohr-Coulomb failure criterion to increase with increasing normal stress because the Mohr-Coulomb model is designed for granular materials and does not consider grain deformation. However, the tensile strength is expected to increase as a result of the deformation and intermeshing of the metals and other non-granular materials in the supercompacted AMWTF waste that occurs during compaction.

TEA also believes that the AMWTF waste pucks will initially have lower porosities and permeabilities than standard waste. Waste porosity will decrease significantly during the supercompaction process, with a resultant decrease in permeability. The average height of a 55-gallon waste drum is expected to decrease to about 22 percent of the original height in the supercompaction process, from 0.89 m to about 0.20 m (Park and Hanson 2003b, p. 22). If the initial uncompressed waste porosity is assumed to be the same as for standard waste, about 68 percent (Stone 1997a, p. 3), and the drum diameter does not change during compaction, then compressing the waste to 22 percent of its initial height will require compressing the solid fraction as well as the voids. If the solid fraction compresses the same relative amount as the voids, the compressed porosity of the supercompacted waste would be about 15 percent (0.68 x 0.22). If the voids compressed more than the solid fraction, the initial compressed porosity would be lower. By comparison, the initial porosity of standard waste is about 68 percent, as stated above.

The end state porosity of supercompacted waste is uncertain. If degradation of the supercompacted waste is minor within the regulatory time frame, its porosity after 10,000 years would remain about 15 percent or less. By comparison, the Department's constitutive model for degraded standard waste predicts a 15 percent porosity under an average triaxial load of only about 6.4 MPa (Stone 1997a, Figure 6). This is less than the equilibrium lithostatic pressure at the repository level of about 15 MPa. If equilibrium stress conditions prevail in the repository after 10,000 years, creep closure would be complete and a 15 MPa lithostatic pressure could be high enough to reduce the end state porosity of standard waste to well below 15 percent. The Department's SANTOS model, however, predicts a higher standard waste porosity of about 23 percent and an average triaxial load of about 4.0 MPa after 10,000 years (Stone 1997a, Figure 6).

Although TEA believes that SANTOS may overestimate waste porosity, it is clear that the endstate porosity of standard waste as determined by the SANTOS model is also uncertain. The accuracy of the SANTOS calculations is currently being reviewed by SNL.

TEA agrees that corrosion and biodegradation of the supercompacted waste may be slower in the interior of the pucks than for standard waste. This is because corrosion and biodegradation processes are considerably enhanced by the presence of brine, and the generally lower permeability of the supercompacted waste would inhibit brine migration through the supercompacted waste as compared with standard waste. Although the slower brine migration rates may be offset by an increased capillary rise in the pucks due to a generally lower porosity, TEA considers the increased brine saturation resulting from the wicking effect already incorporated in BRAGFLO to be adequately conservative. However, as discussed in Section 7, a possible change in the wicking effect was not identified as relevant in the Department's FEPs analysis and was not addressed in the AMW performance assessment. Also, the greater surface area of iron associated with the supercompacted AMWTF waste may increase the rate of anoxic corrosion and the production of hydrogen gas in the repository. This is further discussed in Section 5. Although no supercompacted waste porosity or permeability data were provided by the Department to support its conclusion that the mechanical effects of puck degradation could be completely ignored, if degradation does occur, the properties of the supercompacted waste are expected to become more like those of standard waste.

At the Agency's request, additional supporting information regarding the Department's room-scale permeability assumptions were presented by SNL in the November 18 and 19, 2003, Carlsbad meeting. The Department provided numerical modeling results and described mining practices based on the rigid pillar concept, wherein stress concentrations on the top of a rigid pillar in a mine relieve stresses and reduce creep rates in the near vicinity of the pillar. As applied to the WIPP, stacks of pucks would act as rigid pillars during creep closure. The overburden stresses would be concentrated on the pillars and relieve stresses in the near vicinity until creep closure was completed. The Department believed that the reduced stresses would reduce horizontal creep rates adjacent to the pillars and the lower creep rates would increase the time required for significant horizontal loads to develop on the pucks. These loads in turn are needed to provide the back pressure required to reduce the porosity and permeability of the halite in the waste room. TEA agrees that the rigid pillar concept provides a reasonable conceptual model for the near term room closure behavior around supercompacted waste, but questions whether that behavior would endure for 10,000 years. In particular, TEA questions the accuracy of the Department's SANTOS modeling results that show a minimum porosity of about 35 percent remaining in a room full of ideally packed supercompacted waste pucks after 10,000 years, assuming no gas generation. This value appears high considering the low porosity of the compressed waste itself and the long period of time.

The Department presented an extrusion analog at the November 18 and 19, 2003, Carlsbad meeting when explaining the delayed movement of highly viscous halite into the interstitial spaces between columns of supercompacted waste pucks and their deformed containers. Viscous creep of halite into the spaces between the supercompacted waste pucks would be considerably slowed by friction against the sidewalls. TEA agrees that halite creep into the spaces between waste pucks would be slower than into a room of highly compressible waste, but the Department

did not provide information to support its modeling assumption that no halite would enter the interstitial spaces through either creep or spalling within the 10,000-year regulatory time frame.

TEA believes that, in the absence of gas generation, the room-scale porosity and permeability of supercompacted AMWTF waste will be at least as high as for standard waste in the near term but not necessarily for the entire 10,000-year period of regulatory concern. This is because the interstitial space between waste pucks will initially be open and provide relatively high permeability conduits. This space is not likely to rapidly fill with halite, and the rigidity of the pucks may allow it to retain a relatively high porosity and permeability for an extended time. In addition, the conceptual model wherein stress concentrations on the top of a rigid pillar relieve stresses and reduce horizontal creep rates in the vicinity of that pillar appears to be reasonable in the near term. However, the Department has not adequately evaluated the degree to which the interstitial spaces will be filled by halite within 10,000 years. If equilibrium stress conditions occur in the repository within 10,000 years, the interstitial spaces may be tightly filled with low permeability halite that could seal the interstitial void spaces between pucks and serve as a barrier to flow. In its letter of February 9, 2004, the Agency requested the Department to provide additional justification to support its qualitative assessment of parameter values for the supercompacted waste. Additional discussion of room scale permeability and its possible effect on direct brine releases is presented in the following section.

4.2.1.2 Review of Impacts on Releases

Spallings Releases. TEA agrees with the Department that the spallings strength parameters used in the PAVT are appropriate for use in the AMW performance assessment but has continuing concerns about the appropriateness of using repository-wide average waste properties when calculating spallings releases. The spallings conceptual model used in the PAVT is appropriate for continuing use despite its limitations because it allows comparison with an established baseline. Although a borehole does not need to penetrate the waste to a significant depth for spallings to occur, the waste must be sufficiently degraded to have adequately reduced strength and particle size for a spallings release. The higher waste strength and possibly reduced degradation rate expected in supercompacted waste indicate that spallings releases would tend to be lower than for standard waste and continued use of the model as developed for standard waste is conservative.

Cuttings and Cavings Releases. TEA accepts the Department's conclusions regarding the suitability of the cuttings and cavings model used in the AMW performance assessment. The Department's continued assumption that waste would be released from the repository as drill cuttings may be conservative for supercompacted waste because it is not certain that the drill bits typically used for penetrating soft rock in the Delaware Basin would be able to penetrate a column of supercompacted waste pucks. Similarly, the Department's continued assumption that cavings releases would continue to occur at the same volume may also be conservative for supercompacted waste, given the higher shear strength of that waste and the uncertainty that a drill bit would penetrate it. The continuing use of the repository average radionuclide content is also conservative for the supercompacted AMWTF waste, given its lower than average radionuclide content.

AMW performance assessment results showed that cuttings and cavings releases based on three randomly selected waste streams were similar to releases that came from a single, randomly selected stream (Hansen et al. 2003b, Figure 44). TEA therefore considers the current approach of sampling from three waste streams to be appropriate. However, spallings releases based on the average repository waste concentration were shown to be generally greater for high probablility releases and lower for low probability releases than if the waste came from a single, randomly selected stream (Hansen et al. 2003b, Figure 45). This is because spallings release calculations based on repository-wide averages do not show the increased releases at low probabilities that are evident when heterogeneity is considered. These larger, low probability releases are consistent with the presence of a few low volume, non-AMWTF waste streams with very high radioactivity in the updated waste inventory (Hansen et al. 2003a, p. 64). Although the magnitude of the spallings releases may have been elevated by higher gas pressures related to the high CPR concentrations in the AMW performance assessment, the effects of these low volume, high radioactivity waste streams are also seen in the cuttings and cavings release curves which are not affected by repository pressure. These effects are seen because cuttings and cavings releases are not based on repository-wide average waste properties (Hansen et al. 2003b, Figure 44). These results provide examples of the kind of lower probability effects that would be seen and the greater understanding of WIPP performance that would be gained if increased heterogeneity were introduced into performance assessment.

Stuck Pipe and Gas Erosion. TEA questioned the Department's conclusions regarding stuck pipe and gas erosion releases as explained in the Department's summary reports (Hansen et al. 2003a, Sections 4 and 5; Hansen et al. 2003b, Section 3.8). Stuck pipe occurs when high gas pressures cause low permeability waste to be pressed against the drill string with sufficient force to stop normal drilling. Release occurs when the waste-encrusted drill pipe is pulled from the borehole. Gas erosion occurs in low permeability waste when escaping gas causes waste to enter the wellbore, where it is eroded and carried to the ground surface by the moving drill fluid. Neither scenario was considered in the CCA or PAVT because the waste permeability was considered to be too high (Hansen et al. 2003b, Section 3.8). However, the Department's contention that the increased room scale permeability of the supercompacted AMWTF waste would preclude these two release scenarios is not viable because it ignores the possibility that a higher room-scale permeability may not persist for 10,000 years, or that a borehole could directly penetrate a low permeability puck instead of the higher permeability void space between pucks.

These alternative possibilities were discussed at the November 18 and 19, 2003, Carlsbad meeting. The Department stated that the stuck pipe and gas erosion scenarios have in common the requirements of low permeability *and* a weak waste material. The Department contended that although the supercompacted waste pucks may have low permeabilities, they are too strong to support these release mechanisms. The Department stated that the low permeability of the waste will retard corrosion and biodegradation, and the waste must be degraded to sufficiently reduce its strength for these mechanisms to occur. In addition, the aforementioned uncertainty of whether a drill bit designed for the soft Delaware Basin strata would be able to penetrate a supercompacted waste puck was raised. In view of these multiple considerations, TEA has concluded that it was appropriate to exclude these scenarios from the AMW performance assessment.

Direct Brine Release. TEA questioned the Department's conclusions regarding direct brine releases as explained in the Department's summary reports (Hansen et al. 2003a, Sections 4 and 5; Hansen et al. 2003b, Section 3.9). This is primarily because the Department's rationale for not changing the direct brine release model did not account for the potentially higher room-scale permeability of the supercompacted waste.

A direct brine release occurs when repository fluid pressures are sufficiently high to force contaminated brine up a penetrating borehole to the ground surface. Under otherwise equivalent conditions, a higher waste room permeability will allow more brine to flow to a borehole than a lower permeability. The Department's belief that room scale permeability with supercompacted AMWTF waste will be at least as high as standard waste appears to be based on the assumption that the interstitial void and compressible spaces between waste pucks will not be sealed with creeping halite but will remain relatively open throughout the regulatory time frame. In support of its position, the Department stated that higher values of permeability lead to lower direct brine releases (Hansen et al. 2003b, p. 46). TEA does not accept this argument because the layered model upon which the Department's position is based (Hansen et al. 2003b, p. 46) was designed for standard waste rather than supercompacted waste and had a lower overall transmissivity than standard waste. The layered model has an increased permeability above the CCA/PAVT average in a thin upper layer of undegraded waste but a reduced permeability in a thick lower layer of degraded, compressed waste. The total system transmissivity was 25 percent lower in the layered model than if the constant, standard waste permeability had been used (it was reduced from 4.8 x 10^{-13} m to 3.75 x 10^{-13} m), so naturally a direct brine release would be reduced. It would be more appropriate to have concluded that the reduced direct brine release was the result of waste degradation.

TEA has agreed that the waste pucks themselves will have relatively low permeabilities throughout the regulatory time frame (see Section 4.2.1.1). The principal issue related to long-term waste room permeability is the rate at which the interstitial void spaces between waste pucks will be filled with halite. The rate of halite creep into these spaces is likely to be relatively slow because of the narrowness of the spaces and the drag forces exerted by the sidewalls. The most likely scenario is that the spaces will be first be filled with spalling halite, which will be slowly compacted by halite creep exerting both horizontal stress pushing the pucks closer together and vertical stress through extrusion into the voids. The permeability of the voids would be progressively reduced during the regulatory time frame by this process, and at the same time the waste containers and possibly the pucks themselves would be corroding and degrading. These processes could, over time, cause the supercompacted waste to acquire the physical properties of standard waste. Although it is not understood is how rapidly these processes would occur, the rigidity of the supercompacted waste pucks is likely to maintain a higher room-scale porosity and permeability for a longer period of time than would be found for standard waste.

Hansen et al. (2003b, Section 3.9) state that the CCA/PAVT assumption that the brine within the waste is well mixed is not challenged by the proposed emplacement of supercompacted AMWTF waste and the approach for calculating direct brine releases was therefore not changed in the AMW performance assessment. However, if the room-scale permeability remains equal to or higher than that of standard waste over an extended period of time, as conceptualized by the Department (Hansen et al. 2003b, p. 45), direct brine releases are also likely to be greater. Direct

brine releases would be expected to increase with increasing room scale permeability until the release becomes controlled by the wellbore. Although the effect of increased direct brine releases on total repository releases may be small because direct brine releases are typically considerably lower than cuttings, cavings, and spallings releases, the impact of increased direct brine releases is currently being evaluated by SNL.

In the course of its review, TEA also identified two other issues related to direct brine releases but not directly related to supercompacted AMWTF waste emplacement. TEA notes that direct brine releases do not occur unless there is a reasonably high gas pressure in the repository and the Department's SANTOS modeling has shown that the porosity, and presumably also the permeability, are similar for all waste forms at higher gas pressures (Hansen et al. 2003b, Figures 11-12). Under the SANTOS modeling assumption of pore swelling under increasing gas pressure, direct brine releases could be little influenced by a higher room-scale permeability with supercompacted waste. However, TEA questions the validity of these SANTOS results. TEA believes that while high gas pressures may retard halite creep, they are unlikely to reverse it. Rather, gas pressure is likely to increase in the repository to near lithostatic pressures until relieved by initiating fractures in the surrounding halite and anhydrite.

TEA also questions the appropriateness of basing the direct brine release concentration on the repository average waste inventory rather than on the panel average inventory. SNL stated and TEA agrees that determining direct brine releases based on the waste inventory in a single panel rather than on the average inventory in the repository would principally affect the extremes of the CCDF curves rather than the mean. However, SNL has no prediction of waste loading by panel.

4.2.2 AMWTF Uncompacted Waste

The Department treated AMWTF uncompacted waste in the same manner as standard waste in the AMW performance assessment. TEA considers this approach to be acceptable because the waste is uncompacted and placed in standard, 55-gallon drums for disposal in the same manner as standard waste. It is non-debris waste and is expected to have a variety of forms, with mechanical properties within the range of properties for standard waste (Hansen et al. 2003b, p. 17).

The Department plans to ship AMWTF uncompacted waste drums in several packages, including ten-drum overpacks. The Department appears to have based its inventory of CPR in the AMW performance assessment on the assumption that a ten-drum overpack occupies the same repository volume as three seven-drum overpacks (Leigh 2003, p. 8). However, the Agency has observed that one ten-drum overpack occupies the same repository space as only two seven-drum overpacks. This discrepancy may have resulted in underestimating the quantity of waste assumed to be placed in a panel in the AMW performance assessment. SNL evaluated this discrepancy by determining the impacts on hypothetical "realistic" and "conservative" waste packing scenarios (Leigh 2004). The realistic scenario assumes a panel filled with a mixture of AMWTF waste and other CH-TRU waste, in which the fraction of AMWTF waste is equivalent to the fraction of the highest-volume single waste stream in Panel 1. The conservative scenario assumes a panel filled with a mixture of AMWTF waste and other CH-TRU waste, in which the fraction of AMWTF waste is equivalent to the fraction from the highest-volume generator site (RFETS) in Panel 1

(Leigh 2003c). SNL concluded that this discrepancy resulted in a 7 percent increase in the mass of CPR, oxyanions, and complexing agents for the realistic case and a 16 percent increase for the conservative case (Leigh 2004). SNL calculated roughly proportional reductions in MgO safety factors, which dropped to 2.44 for the realistic scenario, 1.71 for the conservative scenario, and 1.57 for a scenario with a panel filled with only INEEL mixed waste (Hansen and Snider 2004, Table 1). TEA notes that SNL's value of 1.57 is already below the Agency-approved safety factor of 1.67. Furthermore, it cannot be determined whether Leigh's scenarios are in fact "realistic" or "conservative" because the Department has not related them to likely shipment schedules of AMWTF waste and waste from other generator sites. This Agency observation provides an example of how an unforeseen, systematic increase in CPR in a waste panel would reduce the MgO safety factor. The uncertainty in waste loading and the effects on the MgO safety factor are further discussed in Section 5.2.1.2.

The effect of increased CPR loading resulting from the ten-drum overpack stacking discrepancy on the AMW performance assessment was also reviewed by SNL. This review found that the range of CPR mass used in the assessment included the increased mass of CPR resulting from this discrepancy (Hansen and Snider 2004, p. 3). The increase in CPR mass therefore had already been incorporated in the modeling. TEA accepts this finding and concludes that the ten-drum overpack stacking discrepancy did not affect the AMW performance assessment calculations.

5.0 REPOSITORY CHEMICAL CONDITIONS

5.1 DOE Analysis of Chemical Conditions

The Department concluded that supercompacted AMWTF waste contains relatively high concentrations of CPR and iron-based metals compared to average CH waste, as shown in Table 5.1. However, the Department also concluded that supercompacted AMWTF waste contains relatively low radionuclide concentrations compared to average CH waste, as shown in Table 3.2, as well as no ligands, sulfates, or nitrates (Leigh 2003a and 2003b). The Department evaluated the potential effects of AMWTF waste on chemical conditions in the repository by analyzing its likely effects on MgO safety factors, the concentrations of organic ligands that could affect the solubilities of actinides in WIPP brines, brine radiolysis, and anoxic corrosion of iron-based metal. In its analysis, the Department considered four cases (Hansen et al. 2003a, Sections 4.2.1-4.2.2):

- A homogeneous repository;
- A panel filled with a mixture of AMWTF waste and other CH-TRU waste, in which the fraction of AMWTF waste is equivalent to the fraction of the highest-volume single waste stream in Panel 1 ("realistic Panel X");
- A panel filled with a mixture of AMWTF waste and other CH-TRU waste, in which the fraction of AMWTF waste is equivalent to the fraction of the highest-volume generator site (RFETS) in Panel 1 ("conservative Panel X"); and
- A panel filled with AMWTF waste (uncompacted and supercompacted AMWTF wastes).

The relative amounts of the different waste types in each scenario are summarized in Table 5.2.

Table 5.1. Densities of CPR, Iron Metal, and Container Steel and Plastics in Standard CH Waste and Supercompacted AMWTF Waste

Waste Constituent	Average CH waste[1] (kg/m^3)	Supercompacted[2] AMWTF waste (kg/m^3)
Cellulosics	58	302.67
Plastics	42	204.54
Rubbers	14	79.91
Iron-Base Metal/Alloys	110	261.1
Container Plastics	16	0
Container Steel	170	119.75

[1]From Lott (2003)

[2]From Leigh and Lott (2003)

Table 5.2. Waste Percentages in the Homogeneous Repository and in the Realistic-Panel, Conservative-Panel, and All-AMWTF-Waste-Panel Scenarios

Waste	Homogeneous Repository[1]	Realistic Panel[1]	Conservative Panel[1]	All AMWTF Waste Panel[2]
Supercompacted AMWTF Waste	11.8	13.4	27.2	32.7
Uncompacted AMWTF Waste	24.3	27.7	56.1	67.3
Non-AMWTF Waste	63.8	58.3	15.4	0

[1]From Hansen et al. (2003b) Table 8; it is assumed that these percentages do not total to 100% because of rounding

[2]Calculated from supercompacted and uncompacted waste volumes reported in Leigh and Lott (2003a and 2003b)

5.1.1 MgO Safety Factors

MgO backfill is used in the WIPP repository to increase pH and maintain carbon dioxide (CO_2) fugacities at low levels, creating conditions that contribute to relatively low actinide solubilities in the WIPP brines. The MgO safety factor is the available number of moles of MgO divided by the maximum number of moles of carbon dioxide that could be produced by microbial degradation of CPR. The original MgO safety factor calculated for the CCA was 1.95, indicating that the amount of MgO available for reaction in the repository was nearly twice the maximum amount of carbon dioxide that could be generated by microbial degradation. The Agency later approved a reduction in the amount of MgO in the repository through removal of the MgO mini-sacks, which reduced the MgO safety factor to 1.67 (EPA 2001).

The Department calculated the MgO safety factors shown in Table 5.3 for the four cases considered for the AMWTF waste analysis. The Department also reported recalculated MgO safety factors for a homogeneous repository with MgO mini-sacks (CCA) and without MgO mini-sacks, assuming that CPR would be degraded by microorganisms according to the following sequential reactions:

$$C_6H_{10}O_5 + 4.8\ H^+ + 4.8\ NO_3^- \rightarrow 7.4\ H_2O + 6\ CO_2 + 2.4\ N_2 \qquad (1)$$

$$C_6H_{10}O_5 + 6\ H^+ + 3\ SO_4^{2-} \rightarrow 5\ H_2O + 6\ CO_2 + 3\ H_2S \qquad (2)$$

$$C_6H_{10}O_5 + H_2O \rightarrow 3\ CH_4 + 3\ CO_2 \qquad (3)$$

where $C_6H_{10}O_5$ represents cellulose (Hansen et al. 2003a, p. 37).

Reactions (1) and (2) produce one mole of carbon dioxide for each mole of organic carbon that is consumed, whereas reaction (3) produces only 0.5 moles of carbon dioxide per mole of organic carbon consumed. In the Agency's safety factor calculations (EPA 2001), it was assumed that all microbial gas generation would proceed via reactions (1) and (2). However, Wang and Brush (1996) calculated that reaction (3) would account for over 95% of the possible microbial gas generation in the WIPP because the quantity of CPR will greatly exceed the quantities of sulfate and nitrate in the waste and waste containers (Hansen et al. 2003a, p. 37). This assumption,

adjusted for the current inventory projections of sulfate and nitrate, was used by the Department to calculate the MgO safety factors in Table 5.3.

Table 5.3. Amounts of MgO in the Repository and MgO Safety Factors Reported in Hansen et al. (2003b, Table 9)

Repository/Panel Assumptions	MgO in Repository (kg)	MgO Safety Factor
Homogeneous Repository with Mini-Sacks (CCA)[1]	7.766×10^7	3.73
Homogeneous Repository Without Mini-Sacks (January 2001)[1]	6.713×10^7	3.23
Homogeneous Repository[2]	6.713×10^7	2.45
"Realistic" Panel[2,3]	7.674×10^7	2.66
"Conservative" Panel[2,3]	7.674×10^7	2.02
Panel with All AMWTF Waste[2,4]	7.674×10^7	1.66

[1]CCA inventory
[2]Current inventory
[3]Calculated based on the projected number of waste 7-packs in repository for PA
[4]AMWTF waste included both supercompacted and uncompacted waste

5.1.2 Actinide Solubilities

Based on the MgO safety factors presented in Table 5.3, the Department determined that virtually all carbon dioxide produced by microbial degradation would be consumed by reaction with MgO. Therefore, pH and carbon dioxide fugacity values in a panel containing AMWTF waste would not differ from values predicted for a homogeneous repository (Hansen et al. 2003a, p. 39).

Supercompacted AMWTF waste is reported to contain no ligands, so ligand concentrations are highest for the homogeneous repository case (Hansen et al. 2003b, p. 40). The Department calculated actinide solubilities for the homogeneous repository, and compared these values to solubilities calculated for the CCA and PAVT. These results are shown in Table 5.4. The effects of complexation by organic ligands were included in the new solubility calculations reported by Hansen et al. (2003b, p. 40) for the homogeneous repository. The earlier values did not include the effects of actinide complexation by organic ligands because the thermodynamic data for these reactions were unavailable at the time of the CCA and PAVT.

5.1.3 Anoxic Corrosion

Although supercompacted AMWTF waste will have relatively high loadings of steel compared to average CH waste, the Department predicts that AMWTF waste will not have significant effects on the gas generation rate from anoxic corrosion of steels and other iron-based metals (Hansen et al. 2003b, p. 41). Because MgO backfill is expected to maintain low carbon dioxide fugacities and pH values at conditions used to predict anoxic corrosion rates for the PAVT, the Department does not expect hydrogen production rates for AMWTF waste to deviate from the rates used in the PAVT (Hansen et al. 2003b, p. 41).

Table 5.4. Comparison of Actinide Solubilities (M) Reported for PAVT and AMW Performance Assessments

Actinide Oxidation State	Brine	PAVT	AMW (microbial vectors)	AMW (nonmicrobial vectors)
III	Salado	1.2×10^{-7}	3.07×10^{-7}	3.07×10^{-7}
III	Castile	1.3×10^{-8}	1.69×10^{-7}	1.77×10^{-7}
IV	Salado	1.3×10^{-8}	1.19×10^{-8}	1.24×10^{-8}
IV	Castile	4.1×10^{-8}	2.47×10^{-8}	5.84×10^{-9}
V	Salado	2.4×10^{-7}	1.02×10^{-6}	9.72×10^{-7}
V	Castile	4.8×10^{-7}	5.08×10^{-6}	2.13×10^{-5}
VI	Salado	8.7×10^{-6} [1]	8.7×10^{-6}	8.7×10^{-6}
VI	Castile	8.8×10^{-6}	8.8×10^{-6}	8.8×10^{-6}

[1]Value incorrectly listed in Table 11 of Hansen et al. (2003b) as 8.7×10^{-5}

5.1.4 Radiolysis

The Department assessed the effects of AMWTF waste on brine radiolysis by comparing radionuclide loadings in AMWTF waste to average loadings in all CH waste and to average loadings in CH waste without supercompacted waste. Of the 10 radionuclides determined to be the most likely to have radiolytic effects on the brine (thorium-229, thorium-230, uranium-233, uranium-234, plutonium-238, plutonium-239, plutonium-240, plutonium-241, plutonium-242, and americium-241), seven occur in the AMWTF waste at loadings that are less than the average CH waste loading (Hansen et al. 2003b, p. 42). The total loading of these 10 radionuclides in the supercompacted waste (5.13 Ci/m^3) is lower than the loading in CH waste without supercompacted waste (Hansen et al. 2003b, p. 42), primarily because of lower loadings of plutonium-238, plutonium-239, plutonium-241, and americium-241 in the supercompacted waste. Consequently, the Department predicted that a waste panel with a higher proportion of AMWTF waste would have less brine radiolysis than a panel with average CH waste (Hansen et al. 2003b, p. 42). The Department therefore does not expect AMWTF waste to change chemical conditions in the repository through brine radiolysis.

5.1.5 Implementation of Gas Generation

WIPP performance assessment calculations include two gas generation mechanisms: microbial degradation of organic compounds in the waste and anoxic corrosion of iron-based metals.

5.1.5.1 Microbial Gas Generation

Microbial degradation of CPR in the waste is treated as uncertain for performance assessment calculations. Significant microbial activity has been modeled for both the PAVT and the AMW performance assessments as occurring with a probability of 0.5 (Hansen et al. 2003b, p. 42). In vectors where significant microbial activity occurs, one-half include complete degradation of only the cellulosics materials in the waste. Thus, half of the performance assessment realizations include no significant microbial degradation of CPR, one-quarter of the realizations include

complete microbial degradation of cellulosics, and one-quarter of the realizations include complete microbial degradation of cellulosics, plastics, and rubbers.

Table 5.5. Densities of Cellulosic, Plastic, and Rubber Materials in CH-TRU Waste

Waste Type	Density of Cellulose (kg/m^3)	Density of Plastic (kg/m^3)	Density of Rubber (kg/m^3)	Density of Plastic Packaging (kg/m^3)	Total Density of CPR (cellulosics equivalent, kg/m^3)[1]
Supercompacted Waste	302.67	204.54	79.91	0.0	730.30
Uncompacted Waste in Ten-Drum Overpacks	2.68	3.55	0.01	19.11	41.21
Uncompacted Waste in Standard Waste Boxes	2.73	3.56	0.01	16	35.99
All Non-AMWTF Waste Streams	33.65	26.49	7.12	17.93	116.28

From Hansen et al. (2003b, Table 13)

[1] Calculated assuming each kg of plastics is equivalent to 1.7 kg of cellulosics and each kg of rubber is equivalent to 1 kg of cellulosics (Wang and Brush 1996).

As shown in Table 5.5, supercompacted AMWTF waste has relatively high loadings of CPR, whereas uncompacted AMWTF waste has relatively low CPR loadings. Therefore, non-homogeneous placement of AMWTF waste could cause spatially variable gas generation rates within the repository (Hansen et al. 2003b, p. 43). To determine how heterogeneous placement of AMWTF waste could affect the AMW performance assessment realizations that include significant microbial gas generation, an uncertain parameter was defined as the fraction of a single panel's volume that is filled with AMWTF waste (supercompacted and uncompacted). This parameter was given a uniform distribution between 0.2 and 1.0 to bracket the inventory fractions for both the "realistic Panel X" and "conservative Panel X" cases considered in the AMWTF report. This parameter was then sampled for the performance assessment calculations (Hansen et al. 2003b, p. 43).

Gas generation by microbial degradation is implemented by the BRAGFLO code. For BRAGFLO modeling, the scale of the heterogeneity of the CPR content of the waste was set at a single panel. In the BRAGFLO grid, the waste was divided into three regions, one representing the waste panel and two regions that represented the rest of the repository (i.e., the other nine panels).

BRAGFLO represents CPR degradation as a zero-order reaction, so the microbial gas generation rate is constant regardless of CPR concentration (Hansen et al. 2003a, p. 45). Therefore, in BRAGFLO calculations of gas generation reactions, greater amounts of CPR cause gas generation to proceed for longer periods of time at a constant rate and result in more total gas generation in areas of the repository with greater CPR concentrations. The Department justified the use of a zero-order reaction rate for CPR degradation instead of a first-order reaction rate (which would depend on the CPR concentration) by assuming that the low porosity of supercompacted waste would limit access of brine to the waste, which in turn would limit the reaction rate.

5.1.5.2 Anoxic Corrosion of Iron-Based Metals

Iron corrosion is assumed to occur in all performance assessment calculations. In those calculations, a uniform distribution of iron was assumed throughout the repository. Although some waste streams (such as AMWTF supercompacted waste) contain relatively high iron-based metal concentrations, the Department indicated that the assumption of uniform iron-based metal distribution is justified because in all previous performance assessment calculations at least 25 percent of the steel remained after 10,000 years. The Department stated that gas generation due to iron corrosion is limited by the availability of brine rather than the inventory of iron, and a non-uniform distribution of iron would not increase the total amount of gas produced (Hansen et al. 2003b, p. 44).

5.2 TEA Review of Chemical Conditions

In analyzing chemical conditions, TEA has assumed that the inventory information presented by the Department is correct. However, supercompaction of AMWTF waste will result in higher densities of CPR, iron-based metals, and radionuclides than if the waste was placed in WIPP without supercompaction. These higher densities could have an effect on chemical conditions in the WIPP repository. The likely effects of the AMWTF waste on repository chemical conditions are considered in the following sections.

5.2.1 Gas Generation from CPR Degradation

The amount of CPR present in the repository influences the total amount of gas that can be generated by microbial degradation. The Department has assumed that methanogenesis will be an important microbial degradation reaction in the WIPP repository. The extent to which CPR degradation occurs through methanogenesis in the repository will affect the amount of carbon dioxide produced, which in turn could influence chemical conditions in the repository if an inadequate amount of MgO is present to react with the carbon dioxide.

5.2.1.1 Methanogenesis

The Department has conducted a series of long-term experiments to investigate the microbial degradation of CPR in the WIPP repository. Because methanogenesis had not been observed in these experiments at the time of the CCA, the Department conservatively assumed that all CPR microbial degradation would occur through denitrification or sulfate reduction (reactions 1 and 2, Section 5.1.1), and each mole of carbon in the CPR could therefore be converted to a mole of carbon dioxide. This assumption maximized the amount of carbon dioxide that could be produced, ensuring that regardless of the reactions that occurred during microbial degradation of CPR, an adequate amount of MgO would be present in the repository to react with carbon dioxide produced by CPR degradation and control chemical conditions within predicted limits.

Since the time of the CCA and PAVT, methanogenesis has been observed in some of the microbial degradation experiments. The Department maintains that this has conclusively demonstrated that methanogenesis will occur in the WIPP repository environment. The

Department also asserts that only limited amounts of CPR degradation will occur through sulfate reduction and denitrification because of the relatively small amounts of sulfate and nitrate in the waste. Consequently, once the sulfate and nitrate inventories in the waste are consumed, the Department states that CPR degradation will either cease or will proceed through methanogenesis. Because methanogenesis produces only 0.5 moles of carbon dioxide for each mole of CPR carbon that is degraded, CPR degradation by the methanogenesis reaction would significantly reduce the amount of carbon dioxide that could be produced. Thus, if microbial degradation of CPR occurs through methanogenesis, a smaller amount of MgO will be required to control carbon dioxide fugacities and pH and maintain the predicted chemical conditions in the repository.

TEA believes that the Department's consideration of the sulfate available for CPR degradation by sulfate reduction (Reaction 2, Section 5.1.1) in the AMW performance assessment did not take into account the natural sulfate that may be present in the brine and in the Salado formation. Both GWB and ERDA-6 brines contain significant concentrations of sulfate (approximately 0.17 M; Brush and Xiong 2003a). In addition, sulfate minerals such as anhydrite ($CaSO_4$) are present in the Salado formation, both in the anhydrite marker beds and intermixed with the halite (Lambert 1992; Pfeifle and Hurtado 1998). The sulfate present in the brine will be available for microbial degradation of CPR via reaction (2). As this sulfate is consumed by the reaction, the assumption of equilibrium within the repository requires that sulfates present in the Salado formation dissolve to maintain equilibrium between the minerals in the Salado and the brine in contact with the waste. Because sulfate minerals are present in the Salado formation, it is possible that sufficient sulfate will be available for complete CPR degradation through reactions that convert all carbon in the CPR to carbon dioxide.

In response to the Agency's letter of December 9, 2003, SNL acknowledged that natural sulfate in the Salado and Castile brines and minerals had not been considered in the AMW performance assessment and presented an evaluation of the effects of excess sulfate during the January 20-23, 2004, Albuquerque meeting. SNL's evaluation assumed a time scale of hundreds of years for complete CPR degradation and included the effects of two pathways for additional sulfate to enter the repository: (1) the advection of sulfate in the maximum cumulative volume of brine that was predicted to flow into the repository in the S2 simulation of the AMW performance assessment, and (2) the diffusion of sulfate from the solids in the surrounding halite and interbeds into the repository. The S2 simulation includes brine inflow from a Castile brine pocket and should approximate a near-maximum inflow volume. Assuming that only the sulfate in the waste was available for sulfate reduction resulted in 94.5 percent of the CPR in a homogeneous repository being degraded by methanogenesis. Assuming that sulfate in the brine *and* waste was available for sulfate reduction reduced the CPR being degraded by methanogenesis to 88.7 percent. SNL estimated the additional amounts of sulfate that could be available from the Salado solid phases by calculating a range of diffusion lengths (0.06 to 0.6 m) based on a range of effective diffusion coefficients (10^{-13} to 10^{-11} m^2/sec), and assuming that all sulfate within these diffusion lengths would be available for the sulfate reduction reaction. Including diffusive sources of sulfate further reduced the CPR being degraded by methanogenesis to as low as 62.7 percent.

Subsequent to the January 20-23, 2004, Albuquerque meeting, SNL modified and documented its sulfate study in Kanney et al. (2004). The modifications included assuming a longer time scale (2,000 years) and a constant effective diffusion coefficient (4.48×10^{-12} m^2/sec), which resulted in a longer diffusion length (1.06 m). The two pathways for natural sulfate described above were retained in this new analysis and discussion was presented regarding additional sulfate transport through possible repository-induced fracture pathways in the disturbed rock zone (DRZ) and anhydrite interbeds. These pathways were evaluated for cases where repository gas pressure was less than lithostatic and where the gas pressure exceeded lithostatic, but were rejected as not being significant.

For cases where the gas pressure is less than lithostatic, SNL cited a report by F.D. Hansen (2003) indicating that, for a room mined up to Clay Seam G, creep closure would heal any potential pathways to Marker Bed 139 within 50 years. Hansen was quoted as further stating that in fewer than 100 years the state of stress in the salt around the waste rooms would approach equilibrium and the DRZ around the greater areas of the waste rooms would be largely healed. SNL stated that healing of the salt strata between the anhydrite interbeds in the vertical DRZ will effectively isolate them from the repository. SNL also believes that healing of the ribs in the lateral DRZ will take significantly longer time but that the maximum extent of the lateral DRZ is on the order of 3 m (Kanney et al. 2004, p. 9).

For cases where the gas pressure exceeds lithostatic, SNL believes that any pressure-induced fracturing will not provide brine pathways because significant brine volumes will not be able to enter the fractures as long as the gas pressure is high, and the fractures will close and seal if the pressure drops (Kanney et al. 2004, pp. 10, 11). SNL also believes that the flow of brine from the thinner Anhydrite B (at the waste room ceiling) and Anhydrite A (about 2 m above Anhydrite B (Stein 1985)) will be limited by pressure and capillarity (Kanney et al. 2004, p. 11).

TEA agrees that advection, dissolution, and diffusion in brine are the major mechanisms for transporting natural sulfate into the repository. TEA also agrees that basing the quantity of available sulfate on the maximum available brine volume and ignoring mass transfer limitations in dissolution and diffusion are conservative. However, TEA questions certain details of the approach that should be resolved before SNL's calculations can be accepted as adequately bounding sulfate availability. These questions primarily concern the questionable basis for the assumed rate of room closure and the associated degree of DRZ healing, a lack of consideration of the anhydrite-rich beds immediately above the repository, and a lack of consideration of the effect of increased iron surface area or the conservatism of the microbial degradation rates in determining an appropriate time scale for the sulfate reduction reaction.

The timing of room closure and the associated degree of DRZ healing cited by Kanney et al. (2003) are related to the accuracy of SANTOS model predictions which are currently being reviewed by the Agency and SNL. If the SANTOS model predictions are found to be inaccurate, the conclusions cited by Kanney et al. may not be supported. In addition, the belief that the vertical DRZ would essentially heal within fewer than 100 years may be inconsistent with the approved conceptual model implemented in the CCA and PAVT performance assessments, which incorporate a DRZ that endures for 10,000 years with permeabilities that can be orders of magnitude higher than for intact halite. Even if the vertical DRZ rapidly heals to the extent that

additional vertical brine flow is not of concern, SNL's diffusion length of about 1 m is not consistent with the approximately 3 m cited extent of the lateral DRZ. The lateral DRZ includes stress fracturing, provides advective access to Anhydrite B, and will endure significantly longer than the vertical DRZ (Kanney et al. 2004, p. 9).

TEA agrees that pressure-induced fractures are more likely to conduct brine away from the repository rather than toward it, and that brine flow into the repository from the thinner anhydrite layers immediately above the waste rooms is likely to be small compared with the volume of brine inflow assumed in SNL's calculations. However, TEA believes that structural disruptions during room closure, such as a roof collapse that would bring sulfate-bearing minerals such as anhydrite into direct contact with waste room brines, cannot be ruled out. Additional sulfate could be derived in this manner from Anhydrite Interbeds A and B, and from the anhydrite-rich halite between these interbeds (Stein 1985). As the sulfate in the brine is consumed by the reduction reaction, the tendency of the system to maintain chemical equilibrium requires that sulfates present in minerals accessible to repository brines dissolve. These sources of additional natural sulfate were not considered in SNL's analysis.

The assumption that all sulfate around the repository within an approximately 1 m diffusion length would be available for reaction was considered by SNL to account for sulfate that may be dissolved from the Salado as well as sulfate that may diffuse from the Salado (Kanney et al. 2004, p. 13). The approximately 1 m diffusion length was based in part on the assumption that CPR degradation would be essentially complete within 2,000 years (Kanney et al. 2004, Sections 2.3.1 and 3.2.1). The 2,000-year time scale is used by SNL to establish limits for the volume of brine inflow and diffusion length that need to be considered as sources of sulfates. However, the assumption that CPR degradation would be essentially complete within 2,000 years does not hold for waste panels with the increased iron surface areas that would be present with supercompacted AMWTF waste. Stein and Zelinski (2004, Figure 2) show that CPR biodegradation endures for over 10,000 years for an increasing number of vectors because of decreased brine saturation as the iron surface area increases. TEA has agreed that the effects of increased iron surface areas can be ignored in performance assessment for purposes of gas generation impacts because the prolonged CPR degradation reaction conservatively results in less overall gas generation (see Section 5.2.2). However, ignoring a prolonged CPR degradation reaction for purposes of limiting the sulfate reduction reaction is not conservative and inappropriate. In addition, the microbial degradation rates used in BRAGFLO are consistent with the higher initial reaction rates observed in microbial degradation experiments. Use of these higher initial rates is conservative from the standpoint of estimating gas generation rates, but use of the lower, long-term rates would be more conservative for the purpose of determining the length of time available for sulfate diffusion.

The MgO safety factors calculated by SNL fall below the Agency-approved value of 1.67 (EPA 2001) for *every* waste loading scenario considered in SNL's analysis when natural sulfates are included. SNL's calculated safety factors range from 0.94 for the EPA loading scenario (50 percent supercompacted AMWTF waste and 50 percent standard waste) to 1.40 for the SNL realistic Panel X scenario described in Section 5.2.1.2 (Kanney et al. 2004, Table 12). TEA believes that uncertainties in the quantities of CPR present in a waste panel and in the extent to which sulfate reduction will occur are sufficiently great that the Agency-approved safety factor

of 1.67 is the minimum that should be maintained. MgO safety factors are further addressed in Section 5.2.1.2.

TEA concludes that the aforementioned SNL study by Kanney et al. (2004) provides useful information but clearly demonstrates that reductions in the effect of methanogenesis due to the availability of natural sulfates can have a significant adverse effect on MgO safety factors. TEA also believes that not all potential sources for natural sulfates to enter the repository were considered in SNL's analysis and that an acceptable bounding analysis has therefore not been performed. In its letter of February 9, 2004, the Agency requested the Department to perform a bounding analysis that adequately addressed all potentially significant chemical conditions and sulfate pathways. In the absence of such an analysis, TEA believes that the Department should assume that all carbon in CPR could be completely converted to carbon dioxide and that no methanogenesis occurs.

5.2.1.2 MgO Safety Factors

The Department considered several different scenarios when calculating MgO safety factors for the AMWTF waste (Snider 2003a and 2003b). The scenarios considered included a homogeneous repository, a "realistic panel," a "conservative panel," and a panel with all AMWTF waste. The realistic scenario was developed by setting the relative amount of supercompacted waste equal to the percentage in Panel 1 from the largest single waste stream. The conservative scenario was developed by setting the relative amount of supercompacted waste equal to the percentage in Panel 1 from the largest single generator site. The all-AMWTF-waste scenario includes both supercompacted and uncompacted AMWTF wastes in proportion to the total volumes of each waste type.

Although the scenarios considered by the Department cover a range of percentages of supercompacted waste in a panel, as shown in Table 5.2, the Department has not related these scenarios to likely shipment schedules of AMWTF waste and waste from other generator sites. Thus, the applicability of these scenarios, and whether they are in fact "realistic" or "conservative," cannot be determined. In these calculations, it was also assumed that supercompacted and uncompacted waste from the AMWTF would be shipped to the repository in amounts proportional to their total volumes. Based on information provided by the Department at the EPA/DOE October 21 and 22, 2003, Idaho meeting, shipments of uncompacted waste are in fact likely to be completed several years before shipments of supercompacted waste. During the last few years of operation of the AMWTF, it is likely that only supercompacted waste will be generated, and this waste will be placed in WIPP with waste from other generator sites. This latter scenario is likely to differ significantly in terms of MgO safety factors from the scenarios considered by the Department (Hansen et al. 2003b, Section 3.2.1), because average non-AMWTF CH waste has significantly higher CPR densities than uncompacted AMWTF waste.

The MgO safety factors were calculated by TEA for two scenarios. In the first scenario, a homogeneous 10-panel repository was assumed. In the second scenario, it was assumed that equal volumes of supercompacted AMWTF waste and non-AMWTF waste were placed in a single panel. These calculations were performed for situations in which all carbon in the CPR

reacted to form carbon dioxide (without methanogenesis), and also for situations in which methanogenesis occurred.

When calculating the amount of sulfate available for reduction according to reaction (2), Snider (2003a and b) did not consider the sulfate available in the brine. In TEA's calculations, the amount of sulfate dissolved in the maximum amount of brine released up a borehole during an intrusion scenario (1.46×10^5 m^3; Snider 2003a and b) was added to the sulfate present in the waste inventory. The mass of sulfate was calculated from the volume of brine and the concentration of sulfate in ERDA-6 brine (0.17 M; Brush and Xiong 2003a). The Department has also not considered the possible dissolution of sulfate minerals (such as anhydrite) from the Salado Formation into the brine as another potential source of sulfate for reduction. For the purposes of TEA's calculations with methanogenesis reported in Table 5.6, sulfate was assumed to be unavailable from sulfate mineral dissolution. The quantity of MgO was assumed in the calculations to be the amount approved on removal of the MgO minisacks (74,000 tons; EPA, 2001), corrected for the reactive portion of the Premier MgO (0.846; Snider 2003) and for the amount of MgO that would dissolve in the maximum volume of brine that would escape up the borehole. For the single-panel calculations, it was assumed that 7,400 tons of MgO would be placed in the panel. The results of these calculations are summarized in Table 5.6.

Table 5.6. MgO Safety Factors Calculated with Approved Quantity of MgO

Repository/Panel Assumptions	MgO Safety Factor Without Methanogenesis	MgO Safety Factor With Methanogenesis
Homogeneous Repository	1.30	2.37
Panel with Equal Amounts of Supercompacted AMWTF Waste and Non-AMWTF Waste	0.49	0.82

From EPA 2001

For a homogeneous repository without methanogenesis, the MgO safety factor in TEA's calculations was 1.30, which is significantly lower than the previously approved MgO safety factor of 1.67 (EPA 2001). The homogeneous repository calculations were carried out assuming the supercompacted AMWTF waste would be evenly distributed throughout the repository. Because Panel 1 is closed and Panel 2 is likely to be filled before supercompacted AMWTF waste begins to arrive at WIPP, the supercompacted waste is likely to be placed only in the remaining eight panels (Snider 2003b). Larger proportions of supercompacted waste in these eight panels would reduce the MgO safety factor to even lower values than shown in Table 5.6 for the 10-panel homogeneous repository scenario. For the single panel containing half supercompacted waste, the safety factors calculated both with and without methanogenesis were significantly less than 1, indicating that the amount of MgO in the panel would be insufficient to control chemical conditions in the panel if all CPR underwent microbial degradation.

The calculated MgO safety factors are sensitive to the estimated CPR density in the waste. Any significant changes to the inventory estimates of CPR density in CH waste from the AMWTF and from other waste generator sites could result in significant changes in the MgO safety factor. An example is provided by the potential CPR increases of 7 to 16 percent resulting from the discrepancy in the emplacement of ten-drum overpacks discussed in Section 4.2.2. Because the Department has not provided information demonstrating the confidence that can be associated

with the current CPR inventory estimates, TEA believes that calculated MgO safety factors of at least 1.67 should continue to be maintained to ensure that high brine pH and relatively low carbon dioxide fugacity are maintained in the repository. Methanogenesis may not occur because of the presence of excess sulfate in the system, so MgO safety factors calculated assuming all carbon could be converted to carbon dioxide should be used to determine the required amount of MgO for maintaining the required repository chemical conditions until the Department provides adequate bounding calculations for the extent to which sulfate reduction will occur.

Because of the relatively high CPR density in supercompacted waste, significantly greater quantities of MgO may be required than the amounts currently placed in each panel to ensure that chemical conditions are adequately controlled in the repository. For example, in a panel containing equal amounts of supercompacted AMWTF waste and standard waste, 23,770 tons of MgO would be required to maintain the currently approved MgO safety factor of 1.67. This amount of MgO is more than three times the currently approved amount of 7,400 tons per panel (assuming a 10-panel repository; EPA, 2001). Alternatively, the required amount of MgO for maintaining a safety factor of 1.67 can be calculated for each three-pack of 100-gallon supercompacted AMTWF waste drums. Using the masses of CPR per 100-gallon drum provided by Leigh (2003c), approximately 1.28 MgO supersacks will be required per 3-pack. If three 3-packs are placed in a single stack, this stack would require 3.84 MgO supersacks to be consistent with the currently approved MgO safety factor.

The waste placed in WIPP will be in the form of various waste packages, such as 7-packs of 55-gallon drums, standard waste boxes, 3-packs of 100-gallon drums of supercompacted AMWTF waste (HalfPACTs), ten-drum overpacks of non-debris AMWTF waste, and RH waste canisters. The amount of MgO required per waste package to maintain a safety factor of 1.67 will depend on the amounts of CPR present in the waste packages. The minimum mass of MgO required per waste package to achieve this safety factor is illustrated in Figure 5-1 as a function of the CPR mass in each waste package (cellulosics equivalent).

More MgO must be added to the repository than illustrated in Figure 5-1 to allow for the MgO dissolved in brine that may be released from the repository. Such releases can occur through anhydrite interbeds or intrusion boreholes and the MgO removed from the repository would not be available to react with CO_2. The volume of brine that could leave the repository can conservatively be set equal to the volume of brine that could enter the repository. The amount of MgO that would be dissolved in the maximum volume of brine that could enter the repository is 4.81×10^5 kg (Snider, 2003a and 2003b). This would require the placement of an additional 253 MgO supersacks in the repository.

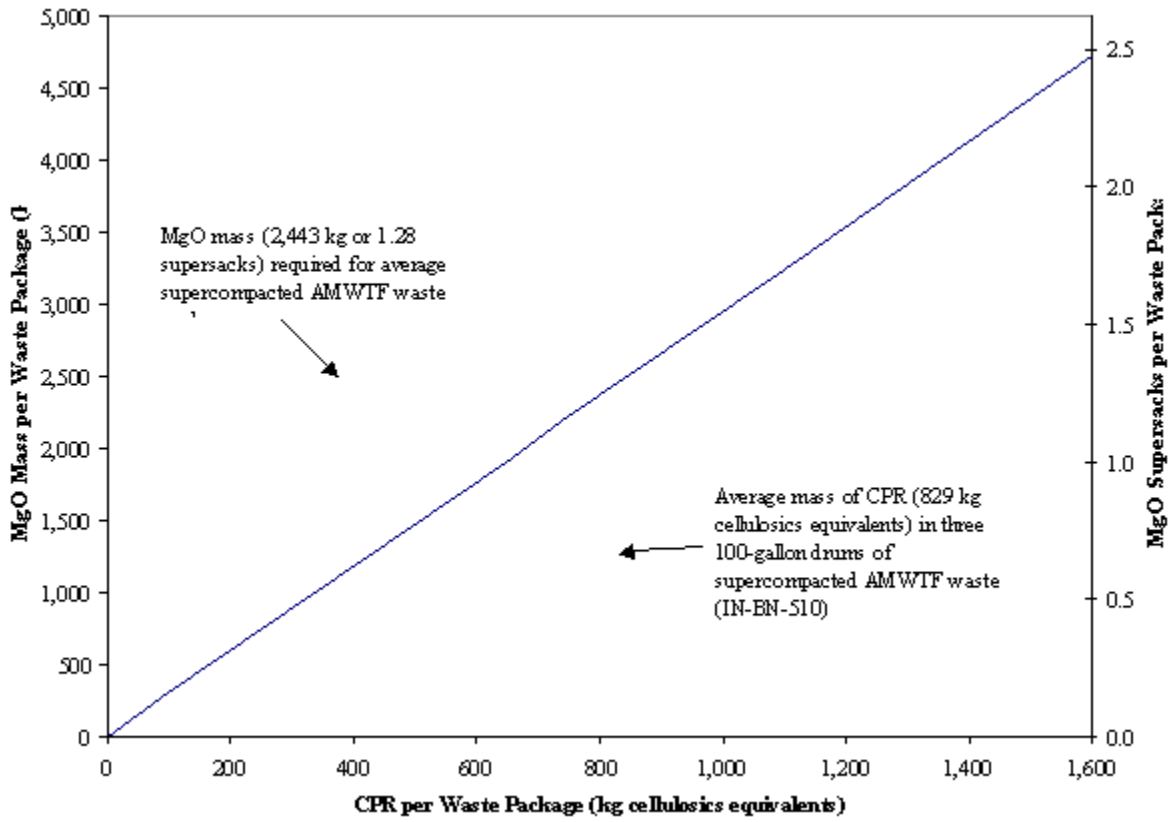

Figure 5-1. Minimum mass of MgO required per waste package.

5.2.1.3 Implementation of Gas Generation from CPR Degradation

The probability of significant microbial gas generation from degradation of CPR has been assumed to be 0.5, based on consideration of the limited available evidence at the time of the CCA regarding: whether microbes capable of consuming the emplaced organic materials will be present and active; whether sufficient electron acceptors will be present and available; and whether enough nutrients will be present and available (Wang and Brush 1996). Since the time of the CCA and PAVT, experimental evidence has indicated that a microbial population capable of consuming the CPR is likely to always be present in the repository, as stated by SNL personnel during the November 18 and 19, 2003, Carlsbad technical exchange meeting. Consequently, it is appropriate to re-evaluate the assumed probability of significant microbial degradation of CPR in the WIPP repository.

In the BRAGFLO code, CPR degradation is modeled as a zero-order reaction, that is, the CPR degradation rate is constant regardless of the amount of CPR. The Department justifies this assumption by stating that the low porosity of the supercompacted waste will limit the access of

brine to the CPR. However, the Department has not presented any evidence to support this assumption. TEA evaluated this issue along several lines of reasoning. The degradation rates for CPR are sampled across a range that accounts for uncertainty, and the sampled values conservatively represent the more rapid rates that would be expected in early times. The total volume of gas produced by CPR degradation depends on the volume of CPR in the repository, which is allowed to vary, and is independent of the degradation rate. In addition, a previous evaluation of the sensitivity of performance assessment results to humid and inundated microbial degradation rates indicated that performance assessment is relatively insensitive to these parameters (EPA 1998). For these reasons, TEA believes that continuing to model CPR degradation as a zero-order reaction is reasonable.

5.2.2 Gas Generation from Anoxic Corrosion

The Department states that supercompacted waste contains relatively high loadings of steel, but would not increase the rate of hydrogen gas (H_2) production (Hansen et al. 2003b, p. 41). The Department assumes a constant 6 m^2 surface area of iron-based metal in the repository for each 55-gallon drum of waste. This surface area includes the inner and outer surface areas of the drum, as well as the surface area of iron-based metals in the waste.

The surface area of iron associated with supercompacted waste can be estimated from the surface areas associated with each puck (6 m^2), plus the surface area of the 100-gallon drum (approximately 6.6 m^2). If each 100-gallon drum contains an average of four pucks (SNL 2003b, p. 15), the estimated total surface area per 100-gallon drum of supercompacted waste will be 30.6 m^2. Three 100-gallon drums will occupy a space roughly equal to the space occupied by a seven-pack of 55-gallon drums (Hansen et al. 2003b, p. 17). Thus, the relative increase in iron surface area when a seven-pack of 55-gallon drums is replaced by a three-pack of AMWTF supercompacted waste is:

$$(30.6\ m^2 \times 3)/(6\ m^2 \times 7) = 2.19 \qquad (4)$$

This value indicates that the surface area of iron associated with supercompacted waste could be more than twice the iron surface area associated with 55-gallon waste drums occupying the same repository volume. Because the anoxic corrosion rate is linked to the surface area of iron (Wang and Brush 1996), the increased iron surface area of supercompacted AMWTF waste has the potential to affect gas generation rates in the repository.

Anoxic corrosion is assumed to occur in all performance assessment realizations. The gas generation rate from iron corrosion (K) is calculated by BRAGFLO using the equation:

$$K = S_b*(CORRWCO2)*B*(ASDRUM)*(DRROOM/VROOM) \qquad (5)$$

Where:

S_b	= brine saturation
CORRWCO2	= corrosion rate in m/s
B	= 141,000 moles Fe/m^3 Fe (molar density of iron metal)
ASDRUM	= 6 m^2/drum (surface area of iron metal per drum)
DRROOM/VROOM	= 1.9 drums/m^3 in the repository

In the BRAGFLO corrosion rate calculations, the gas generation rate (K) is calculated as a function of the sampled corrosion rate and the brine saturation, assuming a constant value of the iron surface area per unit volume in the repository (calculated from ASDRUM*DRROOM/VROOM). Because the amount of iron surface area per unit repository volume in the supercompacted waste is twice the value associated with standard CH waste, the effect on the calculations of assuming an unchanged iron surface area is the same as reducing by a factor of two the range of corrosion rates that are sampled by BRAGFLO. Previous analysis of the sensitivity of performance assessment to changes in the upper bound of the sampled range of anoxic corrosion rates has indicated that performance assessment results are sensitive to this upper bound (EPA 1998). The Department's assumption that the increased surface area of iron in supercompacted AMWTF waste will not affect iron corrosion rates appears to be neither reasonable nor conservative.

In response to the Agency's letter of December 9, 2003, the effect of an increased iron surface area was addressed by SNL during the January 20-23, 2004, Albuquerque meeting and later documented in a report by Stein and Zelinski (2004). SNL's analyses were conducted using the AMW performance assessment model. SNL's initial analysis assumed a tenfold increase in surface area and therefore increased the inundated corrosion rate by a factor of ten. However, the final corrosion rate used in BRAGFLO is also a function of the humid corrosion rate and brine saturation, resulting in a less than tenfold increase in most realizations. The results were compared with the AMW baseline case in which the iron surface area was not increased. The results showed that the additional brine consumed by the increased iron corrosion rate dried the repository to the extent that CPR degradation, which also depends on the availability of brine, was significantly reduced (Stein and Zelinski 2004, pp. 2, 3). The net result was reduced overall gas production with more gas produced at early times due to a higher reaction rate, and less produced at later times due to an increase in the quantity of CPR that did not degrade. This result increased repository pressure at early times and reduced repository pressure at later times. Because the probability of an early borehole penetration is small, SNL concluded that not changing the anoxic corrosion rate in the AMW performance assessment was conservative. The Agency observed that this conclusion was based on an excessively large increase in the iron surface area, and requested that the analysis be performed with a 2.2 times increase in the iron surface area.

A followup analysis, also documented in Stein and Zelinski (2004), was performed pursuant to the Agency's request. The results of the 2.2 times increase (2x run) in the iron surface area were intermediate between those for no increase (0x run) and a 10 times increase (10x run). The increase in gas production rate from anoxic corrosion was generally greater for the 10x runs than for the 2x runs; however, the total gas production from anoxic corrosion was only slightly

affected in both the 2x and 10x runs (Stein and Zelinski 2004, Figure 1). The reduction in gas production from microbial degradation of CPR was generally greater for the 10x runs than for the 2x runs, indicating that as the iron surface area increases, the number of vectors with incomplete biodegradation increases because of the decreasing brine saturation (Stein and Zelinski 2004, Figures 2 and 5). The net result of increasing the iron surface area is a general increase in the total amount of gas produced during approximately the first 2,500 years, followed by a general decrease thereafter (Stein and Zelinski 2004, Figures 3 and 4). Gas pressure in the representative panel varied in a manner consistent with gas production. The cases with increased iron surface area generally showed higher gas pressures during approximately the first 1,500 years, followed by generally lower pressures thereafter (Stein and Zelinski 2004, Figures 6 and 7). SNL concludes that while release scenarios that are sensitive to repository pressure (spallings and direct brine releases) may increase in a first intrusion that occurs during the first approximately 1,500 years, after the first intrusion the pressures are generally lower than in the AMW baseline case and the spallings and direct brine releases would generally be expected to be lower (Stein and Zelinski 2004, p. 12). TEA agrees with these results and with SNL's conclusion that total repository releases will not significantly increase due to an increased iron surface area and may decrease because of lower long-term pressures and brine saturations.

5.2.3 Gas Viscosity

Including methanogenesis as the principal biodegradation reaction for CPR in performance assessment represents a change from the assumptions presented in the CCA and PAVT. Previously, the principal gas assumed to be generated by such reactions was CO_2, which was assumed to have been completely removed from the repository by the MgO backfill. This left H_2 generated from anoxic corrosion of iron-based metals as the primary gas, thus it was reasonable to assume that all gas in the repository behaved as H_2. Including methanogenesis in performance assessment, and assuming that the CO_2 is still effectively sequestered by MgO, will result in a mixture of primarily H_2 and methane (CH_4) gases in the repository. The higher viscosity of CH_4 could result in an increase in viscosity of the gas mixture by as much as a factor of 2, depending on the proportion of each gas present.

The effects of increased gas viscosity were discussed by SNL during the November 18 and 19, 2003, Carlsbad meeting and the January 20-23, 2004, Albuquerque meeting. In the Carlsbad meeting, SNL observed that changes in gas viscosity would have the same effect on gas mobility as inverse changes in DRZ permeability. Increasing the gas viscosity by a factor of two would have the same effect as decreasing the sampled ranges of DRZ permeabilities by a factor of two. SNL observed that the sampled ranges of DRZ permeabilities were so large, covering four orders of magnitude for the DRZ around the panel closures and seven orders of magnitude for the DRZ around a waste room, that an additional change of a factor of two would make no significant difference. In response to further Agency questions, SNL evaluated the effects of increased gas viscosity in several BRAGFLO realizations and presented the results at the Albuquerque meeting and in a report by Kanney et al. (2004). SNL's evaluation indicated that despite the higher viscosities of CO_2 and CH_4 gases, exclusive use of the properties of H_2 did not significantly affect gas pressure in the repository. Because gas pressure is a principal driver for spallings and direct brine releases, this result indicates that predicted releases would also not be significantly affected by using the properties of hydrogen. TEA accepts this conclusion and agrees that

assuming the properties of hydrogen for repository-generated gas does not significantly affect performance assessment results.

5.2.4 Effects of Brine Radiolysis and Ligand Concentrations on Actinide Solubilities

The Department stated that supercompacted AMWTF waste contains no ligands and has reported total radionuclide loadings of most alpha-emitting radionuclides that are less than the average for CH waste without supercompacted waste. The Department's statements concerning lower radionuclide loadings and the absence of ligands were supported by TEA's inventory evaluation. See Section 3.2.1.5 for additional information.

5.2.5 Effects of AMWTF Waste on Repository Chemical Conditions

The AMWTF waste could affect the chemistry of the WIPP repository because of the higher densities of waste constituents brought about by the supercompaction process. However, even after supercompaction, the AMWTF waste is reported to have lower ligand and radionuclide densities than average CH waste. Therefore, repository chemical conditions are unlikely to be affected by higher ligand concentrations or increased brine radiolysis associated with the supercompacted AMWTF waste.

The higher density of CPR in the supercompacted AMWTF waste could significantly affect repository chemical conditions. Because of this higher density, MgO safety factors calculated for a panel with supercompacted AMWTF waste would be lower than for a panel without AMWTF waste. When calculating MgO safety factors, the Department has included methanogenesis as the major CPR degradation reaction because of the relatively low densities of nitrate and sulfate in the WIPP inventory. However, sufficient sulfate may be present in brines and in minerals in the Salado formation to allow most CPR degradation to take place via sulfate reduction, which would increase the amount of carbon dioxide generated by CPR degradation and decrease MgO safety factors. Even when sulfate is not available from minerals within the Salado formation and methanogenesis occurs, it appears possible that some panels within the repository could contain high enough densities of CPR to generate carbon dioxide in excess of the amount that can be sequestered by the currently approved amount of MgO. Thus, it appears possible that repository chemical conditions may not be adequately controlled in a panel with a relatively high, but potentially realistic, emplacement of supercompacted AMWTF waste. As previously stated, TEA believes that the Department has not presented an adequately bounding calculation for the extent of sulfate reduction that may occur and until such a calculation is provided, no methanogenesis should be assumed to occur and the appropriate amount of MgO needed to maintain a safety factor of 1.67 should be emplaced in each repository panel.

6.0 WASTE ROOM CLOSURE

6.1 DOE Analysis of Waste Room Closure

In the Department's AMW performance assessment calculations, room closure initially proceeds as if the room were open. The free air space is eliminated early by creep closure without resistance from the waste package. Eventually the salt contacts the waste package stacks and deforms the waste package according to the relevant waste package response model. At the same time, the conceptual models for corrosion and gas generation allow internal pressure to build within the room. Thus, room closure owing to salt creep is modified by the structural response of the waste and by gas generation. These competing conditions (creep closure, waste package rigidity, and gas generation) yield porosity histories for each waste package configuration that are compiled into a porosity surface for incorporation into the Department's AMW performance assessment calculations (Hansen et al. 2003b, Section 3.1).

Analyses performed during the CCA showed that lateral deformation of a configuration of drums caused by the inward movement of the walls of the disposal room is sufficient to eliminate space between the drums early in the closure process at low stress levels (DOE 1996, Appendix PORSURF, Attachment 1). This same logic was followed for conceptualizing the behavior of the standard wastes during the recent AMW performance assessment modeling. The AMWTF wastes, however, were configured in the model by placing the waste containers in the center of the room and surrounding them with the compressible standard wastes, the compressible volume of the 100-gallon supercompacted waste containers, and the MgO backfill. This configuration allowed the compressible waste and MgO porosity to be reduced during room closure.

The standard waste response to creep closure was calculated as part of the assessment of the effects of raising the repository to Clay Seam G (Park and Holland, 2003). Calculations for five additional emplacement configurations, consisting of only pipe overpack waste, only supercompacted waste, and mixes of supercompacted and standard waste, are reported by Park and Hansen (2003b). For each waste emplacement configuration, the Department performed 13 separate calculations in which the gas generation rate was varied from the base rate by factors (f) ranging from 0.0 (no gas generation) to 2.0 (twice the base rate listed in Table 5 of Hansen et al. 2003b).

Based on its closure analyses, the Department concluded that, in general, the standard waste configuration is the most structurally compliant, that the initial porosity of standard waste is the highest, and that standard waste compresses to the lowest porosity of all waste types. This is because standard waste offers the least resistance to deformation. In contrast, the Department's modeling indicates that the case with only supercompacted waste packages has the lowest initial porosity but a higher long-term porosity than standard waste. The Department notes that the rigidity of the supercompacted waste prevents room closure after it is contacted by the surrounding halite (Hansen et al. 2003b, Section 3.1.6).

The porosity histories calculated by the Department for the mixed standard and supercompacted waste emplacement configurations and the all-supercompacted configuration show that the configurations with supercompacted waste retain a generally higher porosity during creep closure

than standard waste (Hansen et al. 2003b, Figure 9). In the case of a room of only supercompacted waste, the free space of the room diminishes rapidly until the creeping salt and deforming outer containers impinge on the pucks. The configurations with mixed standard and supercompacted waste show different porosities in the transient period while the room closes. However, the Department indicates that the long-term porosity of these cases is similar to the all-supercompacted-waste configuration.

Park and Hansen (2003b) present porosity history results for all 13 gas generation rates used in the Department's AMW performance assessment calculations. As sufficient gas is generated, room closure reverses and porosity increases. As gas generation rates increase, the Department's modeling predicts that all waste package configurations tend toward similar long-term porosities (Hansen et al. 2003b, Figures 10-12).

Conceptually, the processes of salt creep, brine flow, gas generation, and room closure are coupled in the AMW performance assessment. The computational model for creep closure is implemented in the BRAGFLO code by means of a porosity surface. A porosity surface is essentially a look-up table that determines the value of room porosity based on pressure, time, and gas generation rate. BRAGFLO can use a different porosity surface for each waste material represented in the BRAGFLO grid (Hansen et al. 2003b, Figure 16).

In the Department's room closure modeling, the BRAGFLO grid includes two waste materials, WAS_AREA and REPOSIT, having identical hydrologic properties but different porosity surfaces. WAS_AREA was assigned to the representative waste panel, and REPOSIT was assigned to the two regions modeled as the rest of the repository (Hansen et al. 2003b, p. 34). Because the future placement of waste is uncertain, the Department treated the porosity surface for the waste materials in the BRAGFLO grid as uncertain by sampling from a set of possible porosity surfaces for each waste package configuration. The Department believes that this uncertainty reflects the subjective uncertainty of the spatial arrangement of the waste packages, as well as the subjective uncertainty in the response models for the waste packages. Rather than attempting to represent this uncertainty as a continuous range of surfaces, the Department chose the following set of four porosity surfaces, three of which were intended to represent bounding elements in the set of possible porosity surfaces.

1. Standard Waste Model. The standard waste model represents a room filled with a homogeneous mix of waste in 55-gallon drums, identical to the assumptions for the CCA and PAVT. The standard model represents a bounding case of high initial porosity and structurally compliant waste packages.

2. Combined Waste Model. This model assumes that stiff and structurally compliant wastes are mixed within a room. Supercompacted waste is used for the stiff waste, and standard waste is used for the compliant waste. A mix of 2/3 supercompacted waste and 1/3 standard waste (by volume) was selected for this model.

3. Supercompacted Waste Model. This model assumes that all waste is structurally similar to supercompacted waste. This model reflects a bounding case where the initial porosity is low and the waste packages are stiff.

4. Pipe Overpack Model. This model assumes all waste is structurally similar to pipe overpacks. This model represents a bounding case where initial porosity is high and the waste packages are stiff. Results from the porosity surface calculations for 12" pipe overpacks were used for this model.

The Department introduced a new, discrete, random variable to select the porosity surface for the representative waste panel in each BRAGFLO realization. This random variable is implemented as the parameter WAS_AMW/CLOSMODl, with the distribution being 30 percent for the first three waste models described above and 10 percent for the pipe overpack model. The Department believes that this distribution is consistent with the expectation that the waste yet to be shipped to WIPP will not include a significant number of pipe overpacks, and hence only one panel (out of 10 total panels) was modeled with the pipe overpack porosity surface. To preserve the widest range of variability in the selection of porosity surfaces, the other three porosity surfaces were assigned equal probabilities.

The rest of repository in BRAGFLO represents the other nine waste panels. The porosity surface for the rest of repository was selected by a discrete random variable, implemented by the parameter WAS_AMW/CLOSMOD2, and assigned equal, 50 percent, probabilities for selecting either the standard waste model or the combined waste model (2/3 supercompacted waste and 1/3 standard waste). The Department has not represented the porosity surfaces for pipe overpacks and for only supercompacted waste in this distribution because the waste in the rest of repository cannot consist solely of these stiff waste forms (the emplaced volume of supercompacted waste, 19,875 m^3, is insufficient to fill more than two waste panels). The two remaining porosity surfaces were assigned equal probabilities to preserve the widest range of variability (Hansen et al. 2003b, Section 3.1.7).

The Department treats the parameters WAS_AMW/CLOSMOD1 and WAS_AMW/CLOSMOD2 as uncorrelated to allow for all combinations of porosity surfaces in the performance assessment calculations. The Department acknowledges that it is possible that some combinations of waste forms may be more or less likely in the inventory than the probability resulting from these distributions. However, the Department notes that there is little basis for assigning probabilities to combinations of probability surfaces, and the assumption of independence simplifies the sensitivity analysis to determine the significance of the variability in porosity surfaces.

The Department believes that the selection of a discrete distribution using bounding elements captures the range of uncertainty in the various porosity surfaces. The use of bounding elements results from the observation that porosity surfaces created for standard waste, supercompacted waste, and pipe overpack waste do not exhibit monotonic relationships (continuously increasing or deceasing). This means that porosity evolution in the repository does not vary between two hypothetical bounding surfaces but could exhibit a wide range of variability depending upon the waste type.

In addition to uncertainty in the spatial distribution of waste in the repository, there is also uncertainty about the deformational characteristics of the various waste containers, such as the ten-drum overpacks (Hansen et al. 2003b, p. 36). The Department believes that the bounding

elements in their assessment capture the uncertainty in waste container characteristics. Therefore, the Department concludes that implementation of this approach in the AMW performance assessment accounts for the possibilities that waste containers may range from stiff to compliant.

The Department has also conducted analyses to assess the structural response of waste-filled disposal rooms raised to Clay Seam G, 2.43 meters above the level of current disposal operations (Park and Holland, 2003). The Department's Clay Seam G analysis is based on that of Stone (1997a). The calculational procedures and data described by Stone were used in the Clay Seam G analysis. The Department's initial calculations replicated Stone's room pressure and porosity histories for various gas generation rates for a period of 10,000 years following excavation and waste emplacement. The data used in the Department's Clay Seam G analysis, such as stratigraphy, waste characterization, gas generation potential and material response, are identical to the data used in Stone (1997a).

The quasi-static, large deformation finite-element code SANTOS version 2.1.7 (Stone 1997b) was used in the Clay Seam G analysis to produce porosity surfaces (an example is shown in Figure 1 of Park and Holland 2003). As presented above, porosity surfaces generated by SANTOS are used in BRAGFLO analyses that simulate the brine and gas flow in the Salado Formation (see Figure 2 of Park and Holland, 2003).

6.2 TEA Review of Waste Room Closure

In the CCA, creep closure was accounted for in BRAGFLO by changing the porosity of the waste disposal area according to a look-up table of porosity, called a porosity surface, that was generated using the SANTOS code. The porosity surface is constructed from a minimal set of nonlinear finite element analyses in which the gas generation potential is varied to generate porosity time history curves. Disposal room porosities and gas pressures are calculated for each of the assumed histories as a function of time. SANTOS modeling results in a three-dimensional porosity surface representing changes in gas pressure and porosity over the 10,000-year simulation period.

The room closure analyses performed by Park and Hansen (2003b) in support of the AMW performance assessment did not include raising future repository panels to Clay Seam G. Based on the description of Krieg's (1984) constitutive model for clay seams, the presence of Clay Seam G as a horizontal, low friction surface may lead to different stress and displacement distributions than predicted by Park and Hansen's modeling. Because of the limited shear resistance offered by the clay seam, the upper part of the disposal room wall may move more readily into the disposal room, thereby decreasing the disposal room porosity at a faster rate. However, TEA expects that the effects of a more rapid upper wall movement will be largely limited to early time, before vertical room closure effectively blocks horizontal movement along the clay seam. Park and Holland's (2003) structural evaluation of raising the repository panels to Clay Seam G reached a similar conclusion. The porosities of the raised room were found to be lower for low gas pressures, but all differences were less than 5 percent and were considered to be small (Park and Hansen 2003, p. 48). TEA therefore concludes that raising the repository to Clay Seam G will not significantly affect the disposal room porosity.

In the CCA conceptualization of creep closure, the excavation begins to close immediately and causes the volume of the waste room to become smaller. If the room were empty, rather than partially filled with waste, the Department believed that closure would proceed to the point where the void volume created by the excavation would be eliminated and the surrounding halite would eventually return to its undisturbed, uniform stress state. The Department also indicated that in a waste-filled room, the waste will be compressed by the creeping halite and eventually contact the surrounding rock. The rate of closure will decrease and eventually cease as the strength of the waste becomes sufficient to support the rock above the room (DOE 1996, Appendix PORSURF). Initially, uncompressed waste can support only small loads, but as the room continues to close after contact with the waste, the waste will compress and support a greater portion of the weight of the overburden. Conceptually, compression will continue until mechanical equilibrium is reached. TEA believes that this conceptual model is appropriate for WIPP performance assessment. However, the ability of the Department's SANTOS code to accurately implement this model is currently under review.

The Department concluded that the initial porosity of the standard waste is the highest and compresses to the lowest porosity of all the waste types. Alternatively, the Department predicts that the supercompacted waste package configuration has the lowest initial porosity but has a higher long-term porosity than does the standard waste configuration. These conclusions are based on SANTOS modeling results and are supported by the aforementioned rigid pillar concept. In the rigid pillar concept, stress concentrations on the top of a rigid pillar in a mine relieve stresses and reduce creep rates in the near vicinity of the pillar. As applied to the WIPP, stacks of pucks would act as rigid pillars during creep closure. The overburden stresses would be concentrated on the pillar and relieve horizontal stresses in the near vicinity. The Department believes that the reduced horizontal stress would reduce horizontal creep rates adjacent to the pillars, increasing the time required for significant horizontal loads to develop on the pucks. These reduced horizontal loads would prevent the open space and/or backfill between the stacks of drums and between the drums and the room walls from being compressed to the same extent as standard wastes. TEA accepts the stress redistribution associated with a rigid pillar as an appropriate conceptual model for the near-term behavior of rooms with rigid wastes, but questions the SANTOS modeling results that the stress concentrations would persist and not be essentially eliminated by halite creep after 10,000 years.

As noted above, TEA has questioned the ability of the Department's SANTOS code to adequately model creep closure of a waste room and determine the waste porosity and room volume as a function of time. TEA believes that SANTOS and its secondary codes may underestimate the stress applied to the waste as well as the waste room volume during creep closure. These concerns may be especially important in the SANTOS closure predictions for supercompacted AMWTF waste because of the large horizontal strains that must be modeled before the walls contact the waste, the resistance to movement provided by an unrealistically extensive contact area between the vertical and horizontal creep components, and the potentially large residual void spaces remaining outside the waste resulting from the relatively large size of the deformed grid cells.

TEA performed an independent calculation to verify the porosity history for standard waste during room closure as shown in Figure 21 of Park and Holland (2003). Standard waste should provide the best vehicle for this verification because it is the most deformable. This calculation is

relevant to the porosity history of supercompacted AMWTF waste because the same modeling approach was used. Direct measurements of the deformed standard waste grid dimensions in Park and Holland's Figures 16 to 19 were made on larger scale versions than provided in their report. The measured dimensions were then scaled using the known initial waste grid dimensions from Park and Holland's Figure 9. The calculation results reveal that potential errors may occur when the disposal room is highly distorted, as in the case of $f = 0$ (no gas generation) in Park and Holland's Figure 16. In that figure, one can see that the waste becomes highly compressed. At 10,000 years, the figure suggests that the halite has completely encapsulated the waste and that the void space between the halite and the waste is virtually non-existent. An approximation of the porosity of the standard waste at 10,000 years with no gas generation is shown below.

Compressed waste half width	= 2.85 m
Compressed waste height	= 1.23 m
Half width compressed waste volume	= 2.85 x 1.23 = 3.51 m^3/m
Volume of the solid waste fraction	= 551.2 m^3
Effective length of the waste	= 87.85 m
Half-width solid volume	= 551.2/(87.85)(2) = 3.14 m^3/m
Porosity	= (3.51-3.14)/3.51 = 0.11

The compressed waste half width measured from Park and Holland's Figure 16 (2003) is 2.85 m. The half width is used because the model assumes a line of symmetry that bisects the waste and repository room. The compressed waste height measured in Park and Holland's Figure 16 is 1.23 meters. The compressed waste volume per unit waste room length is obtained by multiplying the width of the waste by the height. This results in a volume of 3.51 m^3 per meter of waste room length. The volume of the solid waste fraction and the effective length of the wastes is reported by Park and Holland as 551.2 m^3 and 87.85 m, respectively. To obtain the half-width of the solid volume, the quotient of the volume of the solid waste fraction and the effective length of the waste is divided by two. This results in a half-width solid volume of 3.14 m^3 per meter of waste room length. Therefore, to obtain the porosity, the difference between the half width compressed waste volume (3.51 m^3/m) and the half-width solid volume (3.14 m^3/m) is divided by the half width compressed waste volume (3.51 m^3/m). TEA's calculated porosity of 0.11 is smaller than the value of 0.23 in Park and Holland's Figure 21, suggesting that waste porosities may be overestimated by SANTOS. As a result of this difference, the Agency requested the Department to evaluate the uncertainty in the room-scale porosity of supercompacted AMWTF waste on repository conditions by performing bounding calculations with BRAGFLO using constant porosities that are independent of SANTOS.

The Department's analysis of the effects of waste porosity on the AMW performance assessment was documented by SNL in Hansen et al. (2004). This analysis was conducted by determining waste porosities for bounding conditions of supercompacted AMW waste emplacement and subsequent movement during creep closure, and sampling porosities from that range for use as constant values in BRAGFLO calculations. The porosity values were sampled from a uniform distribution that ranged from 9.1 percent to 23 percent. SNL based the high end of the range on a panel filled with supercompacted waste in an ideal arrangement of 3-packs or 6-packs as originally emplaced in the repository, with no further rearrangement during creep closure (Hansen et al. 2004, Figure 1). Assuming the waste pucks themselves have zero porosity, SNL's calculated room-scale porosity for this scenario was 52.9 percent, which is equivalent to a

BRAFGLO porosity of 23 percent (Hansen et al. 2004, p. 9). SNL based the low end of the range on a panel filled with supercompacted waste in which the individual 100-gallon waste containers have been moved together during creep closure into an ideal packing that minimizes the void space between containers. (Hansen et al. 2004, Figure 2). Again assuming the waste pucks themselves have zero porosity, SNL's calculated room-scale porosity for this scenario was 30.9 percent, which is equivalent to a BRAFGLO porosity of 9.1 percent (Hansen et al. 2004, p. 10).

In all calculations, the representative waste panel was assumed by SNL to be completely filled with supercompacted AMWTF waste and the rest of the repository was assumed to be filled with standard waste. Although porosity was independently sampled for these two model regions, SNL performed the sampling using the same distribution. Runs were made with and without correlations between porosity and biodegradation to evaluate a possible correlation between porosity and repository gas pressure. SNL called these the PORC and PORU runs, respectively. The CPR concentration assumed for the representative waste panel was consistent with a panel filled with only supercompacted AMW waste, while SNL assigned the remaining CPR inventory to the rest of the repository.

SNL compared the results of the PORC and PORU runs with those of the AMW and CRA performance assessments. Porosities tended to be lower at 10,000 years than in the AMW performance assessment calculations but similar to those in the CRA calculations (Hansen et al. 2004, Figures 3 and 4). SNL considered these differences to be due to uncertain waste configurations in the AMW calculations. Although brine saturation in the undisturbed case was similar among all runs, saturations tended to be higher in early times in the PORC and PORU runs (Hansen et al. 2004, Figure 5). SNL attributed this to the lower early time porosities in the PORC and PORU runs. Brine saturations in the disturbed case, where a borehole intersects a Castile brine pocket, tended to be lower for the PORC and PORU runs than for the AMW and CRA runs (Hansen et al. 2004, Figures 7 and 8). SNL believed this was due to the lower porosity of the PORC and PORU runs, which allowed a smaller volume of Castile brine to enter the repository. This smaller volume would be consumed more quickly by corrosion and degradation reactions, and more rapidly build up gas pressure that would slow brine inflow (Hansen et al. 2004, p. 21). The amount of gas generated in the repository was similar for all runs (Hansen et al. 2004, Figures 11 through 13), but the gas pressures were more variable.

The mean pressures in the PORC and PORU runs were similar to those of the AMW and CRA runs but their ranges were slightly wider (Hansen et al. 2004, Figures 14 through 17). SNL attributed the higher pressures in both the undisturbed and disturbed scenarios to a generally lower porosity in the PORC and PORU runs while the gas production tended to be the same (Hansen et al. 2004, pp. 26, 27). The low end of the pressure range tended to be similar to the AMW results in the undisturbed scenario and lower than the AMW case in the disturbed scenario (Hansen et al. 2004, Figures 15 and 17). SNL attributed the lower pressures in the disturbed scenario to runs where there is relatively little gas generated and where the constant porosity value is larger than the SANTOS-calculated porosity in the AMW and CRA runs (Hansen et al. 2004, p. 27). Although release CCDFs were not calculated for the PORC and PORU runs, SNL noted that the differences in pore pressure may result in differences in direct brine and spallings releases. However, SNL observed that the 90^{th} percentile, high end pressures in the undisturbed scenario are similar to those in the CRA run, the 10^{th} percentile, low end pressures in the disturbed scenario are similar to those in the AMW run, and the mean pressures are similar to

both the CRA and AMW runs for both scenarios. Based on these observations and the similarity in brine saturations, SNL concluded that direct releases to the ground surface would be similar to those calculated for the CRA and AMW performance assessments (Hansen et al. 2004, p. 33). In comparing the mean CCDFs for these two performance assessments (Hansen et al. 2004, Figure 21), SNL concluded that there is little difference. Although the higher pressures in the PORC and PORU runs resulted in higher brine flows across the Land Withdrawal Boundary than in the CRA or AMW runs, SNL found that transport in all vectors remained below the threshold amount (Hansen et al. 2004, p. 32).

TEA generally agrees with the conclusions SNL has drawn from its porosity studies. The studies were appropriately designed to evaluate reasonable bounding conditions for the room-scale porosity of supercompacted AMWTF waste. The principal results from these studies are repository gas pressure and brine saturation which affect spallings and direct brine releases. Spallings releases are sensitive to repository gas pressure and direct brine releases are sensitive to both gas pressure and brine saturation. Mean repository gas pressures for the PORC and PORU runs were similar for those for the CRA and AMW runs and brine saturations were similar except at early times (less than 1,000 years). This indicates that mean spallings and direct brine releases will not be strongly affected by the uncertainty in the room-scale porosity of supercompacted AMWTF waste. TEA believes that the relatively small number of vectors with higher gas pressures would have an observable effect on the extreme spallings and direct brine release CCDFs, but the similarity to the highest pressures observed in the CRA runs indicates that overall repository performance would not be affected. TEA therefore concludes that Hansen et al.'s (2004) study has adequately demonstrated that repository performance is relatively insensitive to uncertainty in the room-scale porosity of supercompacted AMWTF waste.

6.3 Implementation of SANTOS Code

SANTOS is a finite element program designed to compute the quasistatic, large deformation, inelastic response of two-dimensional planar or axisymmetric solids or engineering structures. The code is derived from the transient dynamic code PRONTO 2D. The solution strategy used to compute the equilibrium states is based on a self-adaptive dynamic relaxation solution scheme, which is based on explicit central difference pseudo-time integration and artificial mass proportional damping. SANTOS uses a uniform strain, 4-node quadrilateral element with an hourglass solution scheme to control spurious deformation modes. Finite strain constitutive models for many common engineering materials are available. A robust master-slave algorithm for modeling sliding contacts is implemented. An interface for coupling to an external code is also provided.

6.3.1 Background

SANTOS Version 2.0 was originally validated for the CCA on the Cray platform. In April 2002, SANTOS was migrated to the Linux platform running on a PC. The Department re-evaluated the code using the same acceptance criteria defined in the SANTOS Verification and Qualification Document (SNL 1997d). Since the CCA, the Department has made unspecified changes to the code. The Department, however, has not tested the new functionalities associated with the changes in the code because it does not plan to use them to support the WIPP recertification (CRA1) performance assessment. The Department also intends to use SANTOS calculations that

have been performed on the Compaq Alpha 8400 running a True 64 Unix Operating System. Therefore, the Department also validated SANTOS on this system by using the same acceptance criteria defined in the SANTOS Verification and Qualification Document identified above.

SANTOS is designed to simulate salt creep that results in a time-dependent reduction of disposal room volume. Creep is attributed to differences in principal stresses in the salt induced by room excavation. The pre-excavation stress state is hydrostatic, characterized by the equality of principal stresses. After excavation, the salt flows like a viscous fluid until the stress state becomes hydrostatic once again. Volumetric strain of the salt is considered elastic, similar to fluids that lack volumetric viscosity.

Total room volume is composed of two parts: a solid part equal to the volume of solid waste placed in a room, and a void part equal to the room volume less the solid volume. Fluid pressure in the room void space and resistance of solid waste to compression impede room volume reduction. The room solid volume is considered constant, although decomposition of the solid waste by chemical and biological processes occurs in time. These processes generate gas pressure in addition to the pressure increase caused by compression of air trapped within a sealed room. Pressure generation caused by waste decomposition is governed by the ideal gas law and waste decomposition rate, which varies in time.

Gas pressure within the room may be generated in excess of the weight of the overlying strata and cause room volume reduction to cease and, indeed, to begin a relative expansion. This creates the possibility that fracturing of less ductile anhydrite beds near repository rooms will occur, providing additional volume for pressure relief.

The importance of salt creep and related room void volume and gas pressure variation is in their effect on direct brine and spall release volumes. Void volume relates to gas and brine storage, while gas pressure directly influences fluid flow rates within the repository and the volume of waste released to the surface during a human intrusion event. The room closure rate is slow enough to not affect the active life of the repository (about 25 years), but is much faster than waste decomposition. During the CCA, it was assumed that closure is essentially complete within about one hundred years, while gas pressure build-up is maintained over hundreds of years.

6.3.2 DOE Test Methodology

The SANTOS Verification and Qualification Document (SNL 1997d) defines 21 test cases. These cases are designed to ensure that all requirements identified in the Requirements Document section of the SANTOS Quality Assurance Document (SNL 1997c) are satisfied. All of the tests were rerun using the same 21 cases and the results were compared with the analytic solution or solutions from other codes presented in the Verification and Qualification Document.

The 21 test cases systematically exercise various aspects of SANTOS including the large displacement, large strain capability needed for creep closure analysis. Problem 20 is of particular interest because of the benchmark comparisons of SANTOS with the SANCHO, SPECTRUM and ANSALT codes. The comparison problem (Problem 20) is the isothermal strip model of a half-room and half-pillar geometry that contains various strata (salt, anhydrite and

clay seams) represented by slide lines. SANTOS met the benchmark criteria. This same problem (Problem 20) was rerun by EPA during a technical qualification study at Sandia National Laboratories with identical results.

The SANTOS Verification and Qualification Document (SNL 1997d) also contains a number of example problems that demonstrate that the computer model successfully implements the numerical equations. Theoretically, there can be no guarantee that a computer code is free of coding errors or conflicts. However, numerous example problems and a long history of successful code application indicate that SANTOS is reliable. This inference means that the code functions as intended. Given physically realistic input data, the output data from an adequately discretized grid and a well-converged program run can be viewed with confidence.

Requirements are outlined in Sections 2.0 and 3.0 of the Quality Assurance Document for SANTOS (SNL 1997c). The 21 functional requirements described in Section 2.0 are those necessary for code usage in WIPP performance assessments. These include handling the two-dimensional, large displacement, finite strain, time-dependent response of salt and the inelastic response of other geologic media such as anhydrite. Modeling of contact surfaces is also a requirement, as is the consolidation of porous materials. The latter differs from a conventional soil mechanics (porous geologic medium) consolidation process, which requires a genuinely coupled material model. Compaction is a more apt description of this material model requirement that is intended for waste behavior.

The description of test cases, input files, and acceptance criteria exercise all portions of the code required in the list of Section 2.0 of the Quality Assurance Document for SANTOS (SNL 1997c). However, specific acceptance criteria are replaced by comparisons with known solutions or with solutions obtained independently using other computer codes. TEA considers this approach to be acceptable in that it provides a conventional way of validating computer codes through a series of comparisons with known analytical and numerical results that test various combinations of code options. There are no performance or attribute requirements for SANTOS relative to WIPP.

7.0 FEATURES, EVENTS, AND PROCESSES CONSIDERED IN PERFORMANCE ASSESSMENT

7.1 FEPs Changes Identified by DOE

The Department examined the original CCA Features, Events and Processes (FEPs) baseline to determine whether the AMWTF waste properties are accounted for within that original baseline. The results of that analysis were summarized in the AMWTF Report (Hansen et al. 2003b) and additional details were presented in a reference document (SNL 2002). That FEPs analysis was performed in accordance with the Department's *"FEPs Assessment Analysis Plan, AP-090"* (Wagner and Kirkes 2002). The reference document (SNL 2002) was the focus of TEA's review because it included the most detail regarding the Department's FEPs analysis.

The assessment was limited to evaluating whether the existing waste-related FEPs baseline was adequate. Impacts to performance presented by the AMWTF wastes were not evaluated. SNL began by searching the waste-related FEPs in the current baseline to determine whether there were any new FEPs associated with the AMWTF waste that were not identified in the CCA FEPs analysis. SNL then examined the FEPs baseline for FEPs that might be affected by the AMWTF waste. The affected FEPs were then evaluated to determine whether the CCA screening arguments were still valid and whether any decisions with respect to these FEPs required revision based on AMWTF waste characteristics. SNL then identified additional activities that should be conducted based on revised screening arguments and concluded by summarizing potential impacts to the CCA FEPs compliance baseline.

In the first step, SNL determined that no additional FEPs needed to be added to the baseline list, stating "The breadth of waste-related FEPs ensures that all important waste properties and interactions are accounted for in PA. Therefore, no new FEPs are necessary to account for the properties of supercompacted waste. The results of this step do not identify any new FEPs that should be added to the FEPs list" (SNL 2002, p. 12).

In the second step, FEPs potentially related to the AMWTF change were identified. Of the 237 FEPs identified in the original CCA FEPs analysis, SNL believed that 71 of those FEPs were potentially related to accepting AMWTF waste at the WIPP. Appendix A presents a list of SNL's 71 FEPs. Three duplicated FEPs presented in the SNL's original table have been removed in Appendix A.

SNL further evaluated the FEPs related to the AMWTF in the third step. This evaluation was based on the question "Does the proposed change [to AMWTF waste] invalidate, change, or render incomplete the screening arguments or decisions for FEPs identified in Step 2?" (SNL 2002, p. 22). SNL concluded of the 38 potentially related FEPs listed in Appendix A that were originally screened out from further consideration in the CCA performance assessment, none required changes in either their screening arguments or their associated screening decisions, and they were also screened out of the AMW performance assessment. In addition, the 33 potentially related FEPs that were screened into the CCA performance assessment were also screened into the AMW performance assessment but no changes to the screening information were considered

necessary. SNL concluded that "…the FEPs baseline is adequate in its current form to account for AMWTF waste" (SNL 2002, p. 22).

Possible implementation issues that could require special evaluation with respect to AMWTF waste were identified by SNL in Step 4. This step did not determine the impacts of these changes with respect to the AMW performance assessment, but instead identified areas that may merit further investigation. Each of the screened-in FEPs in Appendix A was evaluated to qualitatively determine if the differences in AMWTF waste potentially affected the way in which the AMW performance assessment should be conducted. This included potential changes in performance assessment parameters, models, and codes, as well as any resulting changes in predicted repository performance. Each FEP was assessed to determine if changes due to AMWTF waste were bounded or represented by current assumptions and interactions already considered in performance assessment (SNL 2002, p. 23). Table 7.1 presents those FEPs that were identified by SNL as requiring further investigation.

SNL stated that all assumptions listed in Table 7.1 are directly related to waste properties considered in performance assessment. SNL concluded that the following six waste characteristics were expected to be important to performance assessment:

- Solubility
- Formation of colloidal suspensions
- Gas generation
- Shear strength of waste
- Radioactivity of specific isotopes, and
- TRU activity at disposal

SNL concluded that the screening arguments and decisions within the original FEPs baseline are unaffected by the proposed disposal of AMWTF waste and that accepting AMWTF wastes at WIPP will not impact the FEPs baseline (SNL 2002, p. 24). However, SNL also stated that "…this assessment has identified issues that may require further investigation to determine if there are potential performance impacts associated with the AMWTF wastes. Disposing AMWTF waste may present slight changes in waste properties such as material parameter weights, fissile mass, shear strength (due to compacted drums), and waste composition (iron, cellulose, plastic and rubber content). It is recommended that an impact assessment to further investigate these potential effects be conducted" (SNL 2002, pP. 24-25).

When incorporating the results of SNL's FEPs analysis in its AMWTF report, SNL further concluded that the FEPs screened in were adequate to represent supercompacted AMWTF waste, and that none of the FEPs that had been screened out should be implemented in the AMW performance assessment (Hansen et al. 2003b, p. 11). Thus, the Department concluded that although no new FEPs needed to be added to the AMW performance assessment to accommodate the supercompacted waste in the inventory, some models, parameters, or numerical implementation of models may be affected and merited further consideration (Hansen et al. 2003b, p. 12).

Table 7.1. Screened-In WIPP FEPs Determined by SNL to Require Further Investigation

FEP ID	FEP	FEP Base Assumption	Possible Implementation Issues
W2	Waste Inventory	The quantity and type of radionuclides emplaced in the repository will dictate performance requirements	AMWTF waste may increase the fissile mass in localized areas within the repository.
W3	Heterogeneity of waste forms	The distribution of radionuclides within the different waste types could affect release patterns	Loading schemes and disposal schedules may present inconsistencies with random emplacement assumption.
W5	Container material inventory	Steel and other materials will corrode and affect the amount of gas generated	AMWTF waste will increase the corrodible metals content over previous estimates.
W32	Consolidation of waste	Salt creep and room closure will change waste permeability	Initial waste properties (densities) are different than those previously assumed.
W44	Degradation of organic material	Microbial breakdown of cellulosic material in the waste will generate gas	AMWTF waste may possess greater amounts of cellulosic material than previous estimates.
W49	Gases from Metal Corrosion	Anoxic corrosion of steel will produce hydrogen	Greater amounts of gas may be produced than those previously assumed.
W51	Chemical effects of corrosion	Corrosion of reactions will lower the oxidation state of brines and affect gas generation rates	Current reaction rates may need revision.
W64	Effect of metal corrosion	Metal corrosion will have an effect on chemical conditions in the repository by absorbing oxygen	Greater amounts of metal may require revision of coupled chemical processes.
W84	Cuttings	Waste material intersected by a drill bit could be transported to the ground surface	Intersection of an AMWTF 100 gallon overpack drums may cause cuttings releases to increase.
W85	Cavings	Waste material intersected by a drill bit could be transported to the ground surface	AMWTF waste may change waste properties thereby changing cavings into borehole.
W86	Spallings	Waste material entering a borehole through repository depressurization could be transported to the ground surface	AMWTF waste may have a different shear strength/physical properties than those assumed in the CCA.

From SNL 2002, Table 3

7.2 TEA Review of FEPs

TEA examined the Department's FEPs analysis to determine whether it was complete and adequate. TEA understands that the fundamental purpose of a FEPs analysis is to guide performance assessment by identifying those features, events, and processes that could impact performance. It is also understood that the Department's AMWTF FEPs analysis process was to first identify those FEPs that could possibly be impacted by AMWTF waste, and then to identify those FEPs related to AWMTF waste that require further investigation.

TEA found that SNL's FEPs assessment was incomplete and poorly executed. At least one FEP that should have been identified in the FEPs assessment and considered in the AMW performance assessment was not included. Several FEPs were included in the AMW performance assessment that were not identified as relevant in the FEPs analysis. In addition, the analysis documentation does not include adequate discussion or support for the conclusions and screening analysis results. While TEA agrees that, based on information available at the time of the FEPs analysis, no new waste-related FEPs needed to be added to the baseline list to deal with the inclusion of AMWTF waste, additional justification for the exclusion of waste-related FEPs from Appendix A is warranted. Without a more specific discussion pertaining to the exclusion of waste-related FEPs from further analysis, it is difficult to concur that an adequate FEPs analysis was performed.

Following are examples of FEPs whose exclusion from Appendix A was inadequately justified and inappropriate.

- The WIPP repository disposal geometry (FEP W1) influences brine flow and transport patterns but was not identified in the FEPs analysis as relevant. Performance assessment assumptions concerning waste distribution could change given the different physical and chemical characteristics of the AMWTF waste. While the Department's actual AMW performance assessment took disposal geometry into account, the original FEPs screening should have captured this element.

- Wicking (FEP W41) could be impacted by the new waste's physical and chemical form but was not identified as relevant in the FEPs analysis or in the AMWTF report. Further explanation for this exclusion should have been provided.

- FEP W42 deals with the impact that increases in gas pressure could have on fluid flow. The increased amount of CPR in AMWTF waste would affect potential gas generation. Although this FEP was addressed in the AMWTF performance assessment, it is unclear why it was not identified as relevant to accepting AMWTF waste at WIPP.

- FEPs W45-48 deal with the effects of temperature, pressure, radiation and biofilms on microbial gas generation. Since the supercompacted AMWTF waste contains more CPR than the average WIPP waste stream, it would appear that these FEPs are related to accepting AMWTF waste at WIPP and should have been identified as relevant.

- The stuck pipe and gas erosion release scenarios were not identified in the FEPs analysis as potentially relevant. These scenarios were identified by TEA and subsequently addressed in the Department's AMWTF report.

SNL determined that, of the FEPs presented in Appendix A, none of the 38 originally identified as being screened out of the CCA needed to be reconsidered based on AMWTF waste. TEA also believes that these conclusions were inadequately supported, as illustrated by the following examples.

- FEP W33 deals with the movement of containers within the repository. The possible lateral movement and crushing of the 100-gallon outer containers of supercompacted

AMWTF waste during creep closure was included in Appendix A but was screened out for consideration in the AMW performance assessment and was not included in the original AMW performance assessment. This FEP was further considered by SNL at the Agency's request.

- FEP W53 deals with radiolysis of cellulose. It was included in Appendix A but screened out for consideration in the AMW performance assessment. Because supercompaction could conceivably put radiological components in close proximity to cellulosics, the FEPs analysis should have recognized the potential significance of this FEP. Despite being screened out in the FEPs analysis, radiolysis was addressed in the AMWTF report.

- FEP W59 deals with precipitation of secondary minerals that could affect concentrations of radionuclides in brines. This FEP should have been screened in because the increased concentration of CPR in the supercompacted AMWTF waste could change chemical conditions in the repository.

- FEPs W68 and W69 deal with organic complexation and organic ligands. The ligands favor the formation of organic complexes that may increase radionuclide solubility. These two FEPs were included in Appendix A but were screened out for consideration in the AMW performance assessment. Despite being screened out in the FEPs analysis, the effect of organic ligands was addressed in the AMWTF report.

The number of FEPs that were addressed in the AMWTF report but excluded from SNL's FEPs analysis provides an additional indication that the Department's FEPs analysis does not appear to provide an adequate baseline for guiding development of the AMW performance assessment. However, despite the deficiencies in the FEPs analysis, TEA believes that with the exception of brine wicking, which is identified as an issue in this report, all significant FEPs were identified and analyzed in the Department's AMWTF report and AMW performance assessment. TEA therefore concludes that no additional evaluation of FEPs is required for AMWTF waste.

8.0 EFFECTS ON REPOSITORY PERFORMANCE

8.1 AMW Performance Assessment

The Department conducted a separate performance assessment to assess the effects of supercompacted wastes on repository performance. As previously noted, this has been called the AMW performance assessment. Two AMW performance assessments were conducted by SNL. As discussed below, the second assessment was conducted to correct errors in the CPR inventory identified in the first assessment, while all other aspects remained the same. Details of implementing the AMW performance assessment are presented in SNL (2003c).

The AMW performance assessments incorporated the following changes from the PAVT.

- **CPR Distribution.** The spatial distribution of CPR was treated as uncertain because of the increased CPR concentration in supercompacted waste (Hansen et al. 2003a, Section 4.3.1). Uncertainty in the CPR concentration was implemented by assuming that a single panel could contain from 20 to 100 percent AMWTF supercompacted and uncompacted waste by volume and by sampling the percentage from a uniform distribution. The random variable was implemented as parameter WAS_AMW/FRACAMW and was used to independently determine CPR concentrations for the representative waste panel and for the rest of the repository. This parameter was not correlated with the randomly selected porosity surface. Although the lack of correlation resulted in some combinations that were unrealistic, it did allow the sensitivity to this parameter to be independently determined. The CPR was assumed to be homogeneously distributed within these model regions (Hansen et al. 2003b, pp. 43-44).

- **Microbial Gas Generation Potential.** The microbial gas generation potential was allowed to vary depending on the concentration of CPR in the waste. Greater amounts of CPR would allow microbial gas generation to proceed for a longer period of time, causing more total gas to be generated in areas of the repository with greater CPR concentration (Hansen et al. 2003b, p. 44). This change did not require additional parameters and did not change the microbial gas generation rate.

- **Initial Room Porosity.** In developing the different porosity surfaces, the initial waste room porosity was varied consistent with the different waste materials (Hansen et al. 2003a, Section 4.1.4). These initial room porosities were incorporated into the respective porosity surface models.

- **Porosity Surface in Representative Panel.** New porosity surfaces were developed to represent differences in the mechanical properties of the waste and waste containers. A set of 13 porosity surfaces was generated for each of the six different waste emplacement configurations described below, with each porosity surface representing a different gas generation factor. However, in the AMW performance assessment realizations the set of porosity surfaces used in the representative waste panel in BRAGFLO was randomly selected from four out of the six emplacement configurations: all standard waste (probability 0.3), all supercompacted waste (probability 0.3), all 12-inch pipe overpack waste (probability 0.1), and a mix of 2/3 supercompacted and 1/3 standard waste (probability 0.3). The porosity

surfaces for the 6-inch pipe overpacks and the mix of 1/3 supercompacted and 2/3 standard waste were not used. The random variable was implemented as parameter WAS_AMW/CLOSMOD1 (Hansen et al. 2003b, pp. 34-35). The sampled porosity surface was associated with the waste material WAS_AREA (Hansen et al. 2003b, p. 34).

- **Porosity Surface in Rest of Repository.** The set of porosity surfaces was randomly selected from the two following emplacement configurations: all standard waste (probability 0.5), and a mix of 2/3 supercompacted and 1/3 standard waste (probability 0.5). The random variable was implemented as parameter WAS_AMW/CLOSMOD2 (Hansen et al. 2003b, p. 35). The sampled porosity surface was associated with the waste material REPOSIT. The same hydrologic properties were used in the rest of the repository and in the representative panel (Hansen et al. 2003b, p. 34).

The Department did not change the methodology of the AMW performance assessments in response to other conditions that varied from standard waste emplacement, generally on the basis of conservatism or insignificant effect. The following key elements of the performance assessments were not changed.

- **Features, Events, and Processes.** The Department's analysis of FEPs affected by supercompacted waste and heterogeneous emplacement found that no changes were warranted in the FEPs baseline and concluded that the current performance assessment system could be used to evaluate repository performance (Hansen et al. 2003b, Section 1.1).

- **Room Closure.** The Department concluded that the SANTOS code could be successfully used to evaluate creep closure under different emplacement configurations involving supercompacted wastes (Hansen et al. 2003a, Section 4.1).

- **Release Calculations.** The Department concluded that no new release scenarios were justified and that the models used to calculate cuttings, cavings, spallings, releases through the Culebra, and direct brine releases did not need to be changed. This conclusion was primarily based on conservatism, as discussed in Section 4.2.1 (Hansen et al. 2003b, Sections 3.6-3.9). However, the magnitudes of the releases changed because of changes in the waste inventory.

- **Waste Permeability.** The Department concluded that no change in room scale waste permeability was needed. This was primarily based on the Department's conclusion that the higher room scale permeability of rigid waste is conservative, as discussed in Section 4.2.1 (Hansen et al. 2003b, Section 3.4).

- **Waste Shear and Tensile Strength.** The Department concluded that no changes in waste shear and tensile strengths were needed. This conclusion was primarily based on the conservatively greater strength of rigid waste, as discussed in Section 4.2.1 (Hansen et al. 2003b, Section 3.5).

- **Microbial Gas Generation Rate.** The rate of microbial gas generation was held constant and unchanged despite the greater concentrations of CPR in the AMWTF supercompacted waste, on the basis that the lower porosity of this waste would retard brine flow and the consequent

waste degradation (Hansen et al. 2003a, p. 45). However, as stated above, the microbial gas generation potential was allowed to vary depending on the randomly selected concentrations of CPR.

- **Anoxic Gas Generation Rate and Potential.** The anoxic gas generation rate and potential were held constant and unchanged despite the greater quantities of iron-based metals in the AMWTF wastes. The generation rate was not changed on the basis that it is controlled by the fugacity of CO_2 and the pH, which would not change (Hansen et al. 2003b, p. 41). The generation potential was not changed on the basis that it is limited by repository conditions that do not allow the current inventory of iron to completely corrode during the 10,000-year regulatory time frame (Hansen et al. 2003b, p. 44).

- **Radionuclide Concentrations.** The radionuclide concentrations used in release calculations were not changed between the AMW and CRA performance assessments on the basis that the repository average concentrations used in the CRA were higher than the average AMWTF waste concentrations and were therefore conservative (Hansen et al. 2003b, p. 42).

- **Chemical Conditions.** The Department concluded that the conceptual models for repository chemistry were not affected by the presence of supercompacted waste. The Department concluded that the effect of ligands was inconsequential and that radionuclide solubilities would not change, that the MgO engineered barrier remained adequate to consume all CO_2 that could be produced, and that the actinide source term did not deviate significantly from values predicted for a homogeneous repository (Hansen et al. 2003b, Section 3.2).

The Department accounted for differences in waste type, container type, and mixtures of waste and container types by using the SANTOS code to develop porosity surfaces specific to the different emplacement configurations considered in the AMW performance assessments. As stated above, the configuration assumed in a particular realization was sampled to account for the variability in the spatial arrangement of the waste from panel to panel. The Department considered these cases to bound the effects of the different waste emplacement configurations (Hansen et al. 2003a, p. 33). Other container types such as standard waste boxes and container bundle configurations such as ten-drum overpacks, four-pack 85-gallon drums, and seven-pack 55-gallon drums were assumed to be bounded by the four general types that were considered. As discussed in Section 6, room closure was found to be reduced by the presence of stiff supercompacted waste in cases with little gas generation, but was not affected in cases with higher gas generation.

The AMW performance assessments were performed using the same code versions and parameter baseline being used in the WIPP recertification performance assessment, termed the CRA1 performance assessment. The AMW calculations used the same random seed as Replicate 1 of the CRA1 calculation to ensure that the calculations would have the same sampled values and would be directly comparable. The second AMW performance assessment also used the same waste inventory, which included the AMWTF waste and the waste already emplaced in Panel 1 (Hansen et al. 2003b, p. 56). Although BRAGFLO was run for all six intrusion scenarios in the AMW performance assessments, detailed results were presented by SNL for the undisturbed scenario (S1) and the disturbed scenario in which a drilling intrusion at 350 years also intersects a brine pocket below the repository (S2) (Hansen et al. 2003b, p. 57). These two

scenarios approximate the extreme conditions of brine availability in the repository. In both scenarios, the results for pressure, brine saturation, and porosity in the repository show approximately the same average values but a generally greater range of results for the AMW calculations. This was expected because the CRA1 calculations have a greater use of average parameter values, which tend to mask the possible extremes. Brine flow to the Culebra was similar in both S2 calculations.

With the exception of one realization in the first AMW performance assessment, the CCDFs are quite similar for Replicate 1 of both the AMW and CRA1 performance assessments. The single exception is due to a large direct brine release through a borehole that intersected the repository at early time (before 1,500 years). The release was driven by a combination of high CPR inventory and a high repository pressure and brine saturation that occurred at early time. These repository conditions developed when the intruded waste panel was randomly selected to contain standard waste, the "rest of the repository" was randomly selected to have a porosity surface consistent with a mix of 2/3 supercompacted waste and 1/3 standard waste, and a high gas generation rate was sampled. This combination of conditions resulted in pressures high enough to fracture the DRZ early in the simulation, increasing the DRZ permeability enough to elevate brine inflow and thus increase brine saturation (Hansen et al. 2003b, p. 69). Despite the exceptionally large direct brine release, no vectors in either the AMW or the CRA1 performance assessment replicate exceeded the regulatory limits.

The second AMW performance assessment was conducted to correct two errors: (1) the total mass of CPR in the first assessment was 2.5 times larger than the CRA total whereas it should have been the same as the CRA total because the CRA inventory included all waste, and (2) the relatively small amount of CPR in remote-handled (RH) waste was omitted from the first assessment and was added to the analysis. The resulting calculations showed generally lower gas pressures, lower porosities, and lower brine saturations. The aforementioned large direct brine release seen in the first assessment did not occur in the second assessment. The result of the second assessment was in lower spallings releases than in the CRA but slightly higher direct brine releases than in the CRA due to several early time intrusions. The effect on releases was small because they are dominated by cuttings and cavings which are independent of gas pressures.

The Department concluded that the AMW performance assessments demonstrate continued compliance with the Agency’s containment requirements in 40 CFR 194 with supercompacted waste specifically included in the inventory. The results were compared with those of CRA1 and the differences were considered by the Department to be minor. A sensitivity analysis showed that the uncertainties associated with the newly introduced AMW parameters were not significant contributors to the uncertainty in performance assessment results. The Department therefore concluded that the refinements made in the AMW performance assessment were not warranted and that the standard CCA/PAVT performance assessment conceptual and mathematical models remained appropriate for demonstrating compliance.

8.2 TEA Review of DOE AMW Performance Assessment

The final AMW performance assessment represents the Department’s implementation of the conceptual models and the conclusions from those models that were summarized in the previous

sections of this report. Based on the Department's conceptualization, the only changes made to address heterogeneity issues with the AMWTF wastes involved the changes in room closure due to the strength of the waste packages and the increased concentrations of CPR in the AMWTF waste. No changes were made to any of the release scenarios. TEA's conclusions regarding the final AMW performance assessment and supporting conceptual models are summarized below. The focus in TEA's review was on the proposed emplacement of supercompacted AMWTF waste. As discussed in Sections 4.2.2 and 4.2.3, the uncompacted AMWTF waste will be placed in standard, 55-gallon drums and is expected to have properties similar to those of standard waste.

8.2.1 Waste Inventory Issues

Inventory Change Documentation. At the November 18-19, 2003, technical review meeting in Carlsbad and in its letters of October 29 and December 9, 2003, the Agency requested documentation on how the waste inventory has changed since the CCA, why those changes have occurred, and a description of the process of blending LLW and TRU waste at the AMWTF. That documentation was provided by the Department on December 24, 2003. Although the provided information did not explain the basis for all of the AMWTF inventory changes that have occurred since the CCA, sufficient information was received to support the supercompacted AMWTF waste inventory for use in the Department's AMW performance assessment.

Inventory Accuracy Documentation. Additional information on the Department's methodology for estimating inventory volumes, radioactivity concentrations, CPR densities, and the presence or absence of complexing agents and other constituents was needed for TEA to assess the accuracy of the Department's inventory data. That information was received from the Department on January 10, 2004.

8.2.2 Mechanical and Emplacement Issues

Waste Strength. TEA believes that the supercompacted AMWTF waste pucks will be more rigid and will initially have higher shear and tensile strengths than standard waste. This is because of the high degree of compaction of the supercompacted AMWTF wastes. As discussed below, higher strength wastes are more resistant to release. As the containers and waste degrade, they may gradually assume strength properties similar to those of standard waste. Therefore, from a waste strength standpoint, TEA believes that the Department's approach in modeling the supercompacted waste as the weaker, standard waste, is acceptable because it will conservatively underestimate releases. See Sections 4.2.1 and 4.2.3 for additional discussion.

Waste Porosity and Permeability. TEA believes that the supercompacted AMWTF waste pucks will initially be less porous and have a lower average permeability than standard waste. This is because of the high degree of compaction of the supercompacted waste. However, the Department's assumed long-term structural integrity of this waste in the repository environment was not adequately supported. If the supercompacted waste degrades and loses structural integrity, it may become less porous than degraded standard waste because of its initial lower porosity. SNL evaluated the effects of porosity on repository releases by assuming a zero porosity for the waste pucks and randomly selecting values of interstitial, room-scale porosity from an appropriately bounded distribution. The results showed that, even if the waste puck

porosity is assumed to be zero, the repository brine saturations and gas pressures were sufficiently similar to those for the CRA and AMW performance assessments that spallings and direct brine releases, which are sensitive to these parameters, would not be significantly affected. TEA concludes that repository performance is relatively insensitive to waste porosity and permeability.

Cuttings and Cavings Releases. TEA agrees with the Department that the cuttings and cavings release models used in the CCA/PAVT remain appropriate for use in the AMW performance assessment. This is because (1) the radionuclide concentration in the supercompacted and uncompacted AMWTF waste streams is lower than the repository average and use of the repository average is therefore conservative; (2) it is not certain that a drill bit designed for penetrating the soft rock in the Delaware Basin would be able to fully penetrate a supercompacted waste puck and effect a complete cuttings or cavings release; and (3) cavings releases would be further reduced below that for standard waste because of the greater shear strength of supercompacted waste pucks. See Section 4.2.1 for additional discussion. In support of the random placement assumption, the Department adequately showed that cuttings and cavings releases based on three randomly selected waste streams were similar to releases from a single waste stream. See Section 4.2.4 for additional discussion.

Spallings Releases. TEA agrees with the Department that the assumption of standard waste physical and chemical properties for calculating spallings releases of supercompacted AMWTF waste is appropriate because it conservatively overestimates this type of release. This is because the greater shear and tensile strength of supercompacted AMWTF waste pucks will tend to limit spallings releases to below the volumes that would occur under equivalent conditions for standard waste. See Section 4.2.1 for additional discussion. In support of the random placement assumption, the Department showed that spallings radionuclide releases based on a single randomly selected waste stream were lower than standard waste releases for higher probability events and higher than standard waste releases for lower probability events. Because neither approach resulted in spallings releases near the regulatory limits, assuming the properties of standard waste for spallings releases is acceptable. See Section 4.2.4 for additional discussion of heterogeneity.

Stuck Pipe and Gas Erosion Releases. TEA agrees with the Department that the stuck pipe and gas erosion release scenarios do not have to be considered in the AMW performance assessment. This is because the greater strength of the supercompacted waste pucks will minimize the tensile failure required for these phenomena to occur. See Section 4.2.1 for additional discussion.

Direct Brine Releases. TEA does not accept the Department's rationale for concluding that no changes to the direct brine release model need to be made to address supercompacted AMWTF waste. This is because the Department did not consider the potentially higher room-scale permeability of supercompacted waste. TEA believes that the room-scale permeability of both standard and supercompacted waste will initially be relatively high and decrease over time as the waste and containers corrode and degrade. In addition, the higher initial room-scale permeability with supercompacted waste may be more rapidly reduced as the larger interstitial void spaces between pucks become filled with spalled halite that is subsequently compacted by halite creep. Although these processes will tend to create an end-state material that is substantially the same for both waste types, the relative rates of degradation and infilling have not been established. As

previously mentioned, the effect of a larger room-scale permeability on direct brine releases is currently being evaluated by SNL. See Section 4.2.1 for additional discussion.

Releases Through the Culebra. A release through the Culebra occurs when repository pressure is sufficient to drive brine up an intrusion borehole to the Culebra dolomite, where it may be subsequently transported to the land withdrawal boundary. Such releases were included in the AMW performance assessment and found to be similar to those in the CRA1 performance assessment (Hansen et al. 2003b, p. 61 and Figure 27). The Department's model for identifying such releases should not be affected by the proposed emplacement of supercompacted AMWTF waste and TEA accepts the use of that model in the AMW performance assessment.

Ten-Drum Overpacks. One ten-drum overpack of uncompacted AMWTF waste may occupy the same repository space as two seven-packs of standard drums rather than three seven-packs as assumed by the Department. Although this discrepancy resulted in underestimating the volume of waste in the repository, an analysis by SNL documented that the increase in CPR concentration did not exceed the amount assumed in the AMW performance assessment. The results of the performance assessment were therefore not affected. On the basis of this explanation, TEA agrees that the Department's discrepancy in the volume of ten-drum overpacks did not adversely affect the AMW performance assessment. See Section 4.2.2 for additional discussion.

Rigid Pillar Concept. The relatively weak horizontal pressure on supercompacted AMWTF waste stacks predicted by SANTOS modeling was stated by the Department to be consistent with the rigid pillar concept in mining. The Department used this concept to help support its conclusion that, in the absence of gas generation, the room-scale porosity and permeability of supercompacted AMWTF waste would be at least as high as for degraded standard waste during the entire 10,000-year regulatory time frame. Although TEA questions whether the rigid pillar effects would endure for 10,000 years, the conceptual model wherein stress concentrations on the top of a rigid pillar relieve stresses and reduce horizontal creep rates in the vicinity of that pillar provides an acceptable explanation for the simulated near term repository behavior during creep closure.

Room Porosity and Permeability. The slow rate at which halite would creep into and fill the void spaces between supercompacted AMWTF waste pucks and the slow degradation rates for that waste were cited by the Department as supporting the conclusion that the room scale porosity and permeability during the regulatory time frame would be at least as high for this type of waste as for standard waste. TEA agrees with this conclusion. Room-scale porosity and permeability would be expected to be higher than for standard waste in the near term because of the larger void spaces between and within the supercompacted waste containers. As the containers and waste degrade, the porosity and permeability would approach that of standard waste. See Section 4.2.1 for additional discussion.

Wicking. Brine wicking heights may be higher in the lower porosity, supercompacted AMWTF waste pucks than in standard waste and may lead to a more rapid degradation of supercompacted waste than was considered in the AMW performance assessment. The possible effect of an increased wicking height in supercompacted waste was not identified by the Department as a potentially relevant FEP. However, TEA's review determined that the wicking heights

incorporated into the standard waste model are adequately conservative. TEA concludes that use of the standard model wicking heights in the AMW performance assessment is acceptable.

8.2.3 Repository Chemical Conditions

Effects of MgO on Microbial Activity. At the November 18-19, 2003, Carlsbad meeting, the Agency requested a list of references used by Sandia to assess the potential effects of MgO on microbial activity. This list was transmitted to TEA from SNL by an email dated November 26, 2003.

CPR Degradation by Methanogenesis. The Department's initial analysis of CPR degradation did not take into account the natural sulfate minerals present in the Salado Formation. TEA believes that the presence of natural sulfate could significantly reduce the extent of CPR degradation by methanogenesis. This would result in a greater production of CO_2 than is presently expected by the Department. At the Agency's request, the effect of natural sulfate on CO_2 production was evaluated in a study by SNL. TEA believes that SNL's study did not adequately address all sources of natural sulfate that could be available to the repository. Until an adequately bounding study is provided, TEA believes that the Department should calculate MgO safety factors by assuming all carbon in the CPR in each waste panel would be converted to carbon dioxide.

Uncertainty in MgO Safety Factor Calculations. The Department proposed several possible panel loadings with AMWTF waste based on information available for other waste streams placed in Panel 1 when evaluating MgO safety factors. However, no information was provided to indicate that these assumed panel loadings are consistent with the expected shipments of waste from the AMWTF and other generator sites. In addition, the Department did not consider MgO safety factors for a scenario consistent with the shipment of only supercompacted AMWTF waste during the later stages of AMWTF operation. Consequently, TEA does not believe that the MgO safety factors for the panel loading scenarios provided by the Department are representative of realistic or conservative estimates of heterogeneous conditions in the WIPP repository. A final evaluation of the MgO safety factor for supercompacted waste cannot be made until the viability of the methanogenesis reaction is determined.

Uncertainty in CPR Inventory. The density of CPR in AMWTF waste could have a significant effect on the calculated MgO safety factor. However, the Department has not provided information regarding the uncertainties that could be associated with estimated CPR inventories. Without this information, MgO safety factors should be at least as great as the previously agreed upon value of 1.67 to ensure that sufficient MgO is available to react with carbon dioxide and adequately control repository chemical conditions.

Anoxic Corrosion Gas Generation Rates. Although the surface area of iron per unit repository volume for supercompacted AMWTF waste is approximately twice the value for standard waste, increased anoxic corrosion gas generation rates associated with this increased surface area were not accounted for in the AMW performance assessment calculations. Based on a study performed by SNL in which the anoxic corrosion rate was increased by a factors of 2.2 and 10, the Department concluded that not changing the anoxic corrosion rate in the AMW performance assessment was conservative because higher gas pressures were produced for only a short period

of time and the overall amount of gas generated was less. TEA considers SNL's study to be adequate and accepts the Department's conclusion. See Section 5.2.2 for additional information.

Implementation of Microbial Gas Generation Rates. Supercompacted AMWTF waste has significantly higher densities of CPR than average CH waste. However, the Department assumes that microbial degradation of CPR can be modeled by a zero-order reaction rate, which is independent of the CPR concentration. In evaluating this issue, TEA notes that the degradation rates for CPR in the AMW performance assessment are sampled across a range that accounts for uncertainty, and the sampled values conservatively represent the more rapid rates that would be expected in early times. TEA therefore believes that continuing to model CPR degradation as a zero-order reaction is reasonable. See Section 5.2.1.3 for additional information.

Organic Ligands. Crawford and Leigh (2003) indicate that organic ligands are documented in uncompacted AMWTF waste but not in the supercompacted waste. TEA believes that the concentration of ligands assumed for WIPP brine in the AMW performance assessment is conservatively high because it was based on the assumption that the entire ligand inventory in the repository would dissolve in the minimum amount of brine required for a release. The performance assessment calculations are therefore conservative and the possible presence of small quantities of ligands in AMWTF uncompacted waste should not affect repository performance. See Sections 3.2.1.5 and 5.2.4 for additional information.

Radiological Homogeneity. TEA accepts the Department's continuing assumption of radiological homogeneity for the WIPP waste for calculating releases of AMWTF waste because of its relatively low radionuclide concentration. See Section 3.1.1 for additional information.

Gas Viscosity. In a repository that is predominantly filled with CH_4, the gas viscosity can be up to two times greater than for H_2. An evaluation of this issue performed by SNL indicated that despite the higher viscosity of CH_4, exclusive use of the properties of H_2 in the AMW performance assessment does not significantly affect gas pressure in the repository. Because gas pressure is the main driver for spallings and direct brine releases, this result indicates that predicted releases would not be significantly affected by using the properties of hydrogen. TEA accepts this conclusion. See Section 5.2.3 for more information.

Supercompacted Waste Degradation. The Department assumed that degradation rates for supercompacted AMWTF waste will be lower than for standard waste because of the lower permeability of the supercompacted waste. TEA does not necessarily accept this conclusion because the Department has not demonstrated that the permeability of the supercompacted waste will be sufficiently low to significantly retard brine migration through it. However, TEA's conclusion that if degradation does occur, the supercompacted waste will become similar to standard waste, supports the Department's position that supercompacted waste can be treated as standard waste in performance assessment.

8.2.4 Waste Room Closure

Applicability of SANTOS to Rigid Pillar Concept. The SANTOS numerical modeling results presented by the Department indicate that the stacks of pucks will prevent horizontal stresses from closing the room. Although these results are consistent with the rigid pillar concept, TEA

questions the ability of the SANTOS code to accurately simulate waste room closure and the stresses applied to the waste. Although these concerns are currently being evaluated by SNL, TEA concludes that the SANTOS modeling results are generally consistent with the rigid pillar concept, particularly in the simulation of near-term behavior.

Integration of Waste Porosities into the Porosity Surfaces. In the CCA, the porosity of the waste was combined with the porosity of the room into a collective porosity. This conceptualization was considered to be an appropriate simplification because the waste was assumed to be fully degraded and room closure tightly encapsulated the wastes within a few hundred years. In the case of supercompacted AMWTF waste, however, the wastes have very low porosities and portions of the room may remain open. TEA therefore considered the possibility that the conceptualization of a single porosity to describe both the room and the wastes was inappropriate. However, the porosity surfaces developed by SANTOS are only used to simulate room-scale pore volumes during creep closure. While the combined, room-scale porosity and pore volume are used in BRAGFLO to calculate repository gas pressures, no direct use is made of the porosities of individual waste forms. TEA therefore concludes that under the present configuration of the performance assessment codes, the conceptualization of a single porosity to describe both the room and the waste is appropriate.

Porosity Surface Documentation. A preliminary draft of the Park and Hansen (2003b) report "Determination of the Porosity Surfaces of the Disposal Room Containing Various Waste Inventories for the WIPP PA" was provided by the Department on December 10, 2003, but a final report was also needed. The final version of this report was provided on December 24, 2003.

Heterogeneity in Room Closure Modeling. TEA was concerned that the Department's room closure modeling does not adequately capture the heterogeneity of the different waste forms and therefore biases the conclusions reached in the AMW performance assessment. In response to an Agency request, SNL evaluated the effects of a panel filled with supercompacted AMWTF waste on repository performance. The principal mechanical heterogeneity is related to the high rigidity of the supercompacted waste and the differences in porosity history during creep closure. The focus of SNL's study was therefore on the uncertainty in the porosity of the waste room during creep closure due to the high rigidity of the supercompacted waste. Waste room porosity is important because of its influence on repository gas pressure and brine saturation, and the close correlation of these parameters to spalling and direct brine releases. The results showed that spalling and direct brine releases would not be significantly affected by the differences in porosity. TEA concludes that repository performance is relatively insensitive to mechanical heterogeneities related to supercompacted AMWTF waste.

8.2.5 Features, Events, and Processes

The Department's FEPs analysis was poorly documented and justified, and did not adequately identify the FEPs that needed to be evaluated for the emplacement of AMWTF waste in the WIPP. However, because all significant AMWTF waste FEPs were addressed in the analyses presented in the Department's AMWTF report and AMW performance assessment, no additional FEPs evaluation is required.

8.2.6 AMW Performance Assessment

Clay Seam G. The room closure scenarios in the AMW performance assessment did not account for raising the waste panels to Clay Seam G and the effect of this was not discussed in the documentation provided by the Department. TEA expects the effects of a more rapid upper wall movement facilitated by a lower sliding friction along the clay seam to be small and largely limited to early time, before vertical room closure effectively blocks horizontal sliding along the clay seam. Studies performed by SNL also concluded that the effects on room closure would be small. TEA therefore concludes that raising the repository to Clay Seam G will not significantly affect disposal room closure. See Section 6.2 for additional information.

Porosity Surfaces. The AMW performance assessment was conducted using SANTOS-generated porosity surfaces for supercompacted AMWTF waste that may not have fully accounted for possible horizontal movement of the waste and may have exhibited long-term porosities that were unrealistically high. Higher porosities may not be conservative because they could lead to lower brine saturations, lower gas pressures, less waste inundation by brine, and possibly underestimated releases. In response to an Agency request, SNL evaluated the effects of uncertainty in the porosity of a panel filled with supercompacted AMWTF waste by using a range of constant porosities that were not developed from SANTOS calculations. The results showed that repository performance would be relatively insensitive to uncertainty in the room-scale porosity of supercompacted AMWTF waste. TEA accepts these results and conclusions.

Comparison of Results. The Department compared the AMW performance assessment results with the CRA1 results rather than with the Agency-approved PAVT baseline. In its letters of October 29 and December 9, 2003, 2003, the Agency requested a comparison of AMW performance assessment results with those of the PAVT. That comparison was received from the Department on December 24, 2003.

Single Replicate. The Department provided a single replicate of 100 CCDF curves for the AMW performance assessment rather than the three replicates required in a full performance assessment. Although three replicates are needed to fully address uncertainty in performance assessment, TEA considers the information presented in the single replicate to have adequately demonstrated the effects and identified the issues related to emplacement of supercompacted AMWTF waste.

Interbed Transport. The AMW performance assessment results provided by the Department did not include releases through radionuclide transport in the anhydrite interbeds in the Salado. Although transport of radionuclides into the anhydrites were stated by the Department to be limited, documentation to support this conclusion was required. The required documentation was received from the Department on December 24, 2003.

Sensitivity Analysis. The sensitivity analysis adequately assessed sensitivity to changes in the new AMW performance assessment parameters on an individual basis. However, the analysis did not assess sensitivity to combinations of conditions that could lead to low probability but high radioactivity releases. The behavior observed in Vector 22 of the initial AMW performance assessment provides an example of this. As discussed in Section 4.2.4, the Agency's rule addresses not only average behavior but also the degree of confidence in that behavior. The

possible low probability, high release events are examples of performance effects that are not captured when a homogeneous repository is assumed.

9.0 CONCLUSIONS

Based on the information available at this time, TEA believes that emplacement of supercompacted and uncompacted AMWTF wastes at WIPP is not likely to affect the ability of the repository to meet the Agency-mandated release limits. The ability of the repository to successfully isolate waste from the environment is substantial and releases resulting from intrusion events are expected to be lower for AMWTF waste than for standard waste. This is because of the higher strength of the supercompacted waste and the lower radionuclide inventories of both supercompacted and uncompacted AMWTF wastes. The remaining issues that have not been resolved concern the generation of CO_2 and the amount of MgO that must be added to the supercompacted waste to sequester it, and the effect of an increased room-scale permeability on direct brine releases. The accuracy of the SANTOS code is an additional issue that is important but is not limited to AMWTF wastes and can be addressed separately.

TEA believes that each of these currently unresolved issues can be successfully addressed. If an adequately bounding analysis for the generation of CO_2 cannot be provided, the Department can assume that all carbon in the CPR in each waste panel would be converted to CO_2 and enough MgO provided in that waste panel to provide the Agency's approved safety factor of 1.67. The effect of an increased room-scale permeability on direct brine releases is currently being evaluated by SNL. Although the effect may significantly increase such releases, they are expected to remain small relative to other types of releases and are not expected to affect overall repository performance.

The current status of TEA's concerns is summarized in Table 9.1. Summaries of these concerns are presented in Section 8.2 and more detailed discussions can be found in Sections 2 through 7 of this report.

Table 9.1. Current Status of TEA Concerns

Concern	Department Position Accepted	Department Position Rejected	Additional Information Required
Waste Inventory Issues			
Inventory change documentation	X		
Inventory accuracy documentation	X		
Mechanical and Emplacement Issues			
Waste strength	X		
Waste porosity and permeability	X		
Cuttings and cavings releases	X		
Spallings releases	X		
Stuck pipe and gas erosion releases	X		
Direct brine releases			X
Releases through the Culebra	X		
Ten drum overpacks	X		
Rigid pillar concept	X		
Room permeability	X		
Wicking	X		
Repository Chemical Conditions			
Effects of MgO on microbial activity	X		
CPR degradation by methanogenesis		X	
Uncertainty in MgO safety factor calculations		X	
Uncertainty in CPR inventory		X	
Anoxic corrosion gas generation rates	X		
Implementation of microbial gas generation rates	X		
Organic ligands	X		
Radiological homogeneity	X		
Gas viscosity	X		
Supercompacted waste degradation	X		
Waste Room Closure			
Applicability of SANTOS to rigid pillar concept	X		
Integration of waste porosities into the porosity surfaces	X		
Porosity surface documentation	X		
Heterogeneity in room closure modeling	X		
Features, Events, and Processes			
Incorporation of FEPs in analysis	X		
AMW Performance Assessment			
Clay Seam G	X		
Porosity surfaces	X		
Comparison of results	X		
Single replicate	X		
Interbed transport	X		
Sensitivity analysis	X		

REFERENCES

BNFL 2003. *Physical Information on AMWTF Supercompacted Wastes: Questions and Responses.* ERMS 532257. BNFL, Inc. May 22, 2003.

Brush, L.H., and Y. Xiong 2003a. *Calculation of Actinide Solubilities for the WIPP Compliance Recertification Application*. ERMS 529131. Sandia National Laboratories Carlsbad Programs Group, Carlsbad, New Mexico. May 8, 2003.

Brush, L.H., and Y. Xiong 2003b. *Calculation of Organic Ligand Concentration for the WIPP Compliance Recertification Application and for Evaluating Assumptions of Waste Homogeneity in WIPP PA*. ERMS 531488. Sandia National Laboratories Carlsbad Programs Group, Carlsbad, New Mexico. September 11, 2003.

Butcher, B.M. 1997. *A Summary of the Sources of Input Parameter Values for the WIPP Final Porosity Surface Calculations.* SAND97-0796. Sandia National Laboratories, Albuquerque, New Mexico.

Crawford, B., and C.D. Leigh 2003. *Estimate of Complexing Agents in TRU Waste for the Compliance Recertification Application.* ERMS 531107. Sandia National Laboratories Carlsbad Programs Group, Carlsbad, New Mexico. August 26, 2003.

DOE 1996. *Title 40 CFR Part 191 Compliance Certification for the Waste Isolation Pilot Plant.* DOE/CAO-1996-2184. U.S. Department of Energy, Carlsbad Area Office, Carlsbad, New Mexico.

DOE 2003. *Title 40 CFR Part 191 Compliance Recertification for the Waste Isolation Pilot Plant.* Draft. U.S. Department of Energy, Carlsbad Area Office, Carlsbad, New Mexico.

EPA 1998. *Technical Support Document for Section 194.23: Parameter Justification Report.* Office of Radiation and Indoor Air, Docket No. A-93-02, V-B-14.

EPA 2001. Letter from F. Marcinowski, Director, Radiation Protection Division, to Dr. I. Triay, Manager, Carlsbad Field Office. EPA Docket A-98-49, II-B-3-15. ERMS 519362. U.S. Environmental Protection Agency Office of Radiation and Indoor Air, Washington D.C. January 11, 2001.

EPA 2003. Letter from F. Marcinowski, Director, Radiation Protection Division, to Dr. I. Triay, Manager, Carlsbad Field Office, U.S. Department of Energy. U.S. Environmental Protection Agency Office of Radiation and Indoor Air, Washington D.C. March 21, 2003.

Hansen, C.W., L.H. Brush, M.B. Gross, F.D. Hansen, B. Thompson, J.S. Stein, and B-Y Park 2003a. *Effects of Supercompacted Waste and Heterogeneous Waste Emplacement on Repository Performance, Rev. 0.* Sandia National Laboratories Carlsbad Programs Group, Carlsbad, New Mexico. October 7, 2003.

Hansen, C.W., L.H. Brush, M.B. Gross, F.D. Hansen, B-Y Park, J.S. Stein, and B. Thompson 2003b. *Effects of Supercompacted Waste and Heterogeneous Waste Emplacement on Repository Performance, Rev. 1.* Sandia National Laboratories Carlsbad Programs Group, Carlsbad, New Mexico. October 17, 2003.

Hansen, F.D. 2003. *The Disturbed Rock Zone at the Waste Isolation Pilot Plant.* SAND2003-4307. Sandia National Laboratories, Albuquerque, NM.

Hansen, C.W., and A.C. Snider 2004. *Effect of TDOP Stacking Assumptions on Analysis of Supercompacted Waste (Revision 1).* Memorandum to Records. Sandia National Laboratories Carlsbad Programs Group, Carlsbad, New Mexico. March 2, 2004.

Hansen, C.W., J.S. Stein, and B. Zelinski 2004. *Effect of Waste Porosity Modeling on AMW Performance Assessment.* Sandia National Laboratories Carlsbad Programs Group, Carlsbad, New Mexico. Undated.

Kanney, J.F., W.P. Zelinski, and C.W. Hansen 2004. *Effect of Increased Gas Viscosity on Repository Pressures in the AMW Performance Assessment.* Memorandum to Records. Sandia National Laboratories Carlsbad Programs Group, Carlsbad, New Mexico. March 3, 2004.

Kanney, J.F., A.C. Snider, T.W. Thompson, and L.H. Brush 2004. *Effect of Naturally Occurring Sulfate on the MgO Safety Factor in the Presence of Supercompacted Waste and Heterogeneous Waste Emplacement.* Sandia National Laboratories Carlsbad Programs Group, Carlsbad, New Mexico. March 5, 2004.

Krieg, R.D. 1984. *Reference Stratigraphy and Rock Properties for the Waste Isolation Pilot Plant (WIPP) Project.* SAND83-1908. Sandia National Laboratories, Albuquerque, New Mexico. 1984.

Lambe, T.W., and R.V. Whitman 1969. *Soil Mechanics.* John Wiley and Sons, Inc., New York, New York. 553 pp.

Lambert, S.J. 1992. Geochemistry of the Waste Isolation Pilot Plant (WIPP) Site, Southeastern New Mexico, U.S.A. *Applied Geochemistry* 7:513-531.

Leigh, C.D. 2003a. *Estimate of Complexing Agent Masses in a Single Panel in the WIPP Repository in Support of AP-107, Supercedes ERMS 531113.* ERMS 531328. Sandia National Laboratories Carlsbad Programs Group, Carlsbad, New Mexico. September 4, 2003.

Leigh, C.D. 2003b. *Estimate of Oxyanion Masses in a Single Panel in the WIPP Repository in Support of AP-107, Supercedes ERMS 530988.* Revision 1. ERMS 531332. Sandia National Laboratories Carlsbad Programs Group, Carlsbad, New Mexico. September 4, 2003.

Leigh, C.D. 2003c. *Estimate of Cellulosics, Plastics, and Rubbers in a Single Panel in the WIPP Repository in Support of AP-107; Supercedes ERMS #530959.* ERMS 531324. Sandia National Laboratories Carlsbad Programs Group, Carlsbad, New Mexico. September 4, 2003.

Leigh, C.D. 2003d. *Radionuclide Densities in CH Waste Streams from TWBID Rev 2.1 Version 3.1.2 Data Version 4.09,* Letter Response to Dr. L.H. Brush. ERMS 531586. Sandia National Laboratories Carlsbad Programs Group, Carlsbad, New Mexico. September 19, 2003.

Leigh, C.D. 2004. *Waste Parameters for an Alternative TDOP Loading Assumption in the AMW Analysis; Revision 1.* Memorandum to Records. Sandia National Laboratories Carlsbad Programs Group, Carlsbad, New Mexico. February 26, 2004.

Leigh, C.D., and S. Lott 2003a. *Calculation of Waste Stream Volume, Waste and Container Material Densities, and Radionuclide Concentrations for INEEL Waste Stream IN-BN-510 for the Compliance Recertification Application.* ERMS 530666. Sandia National Laboratories Carlsbad Programs Group, Carlsbad, New Mexico. August 12, 2003.

Leigh, C.D., and S. Lott 2003b. *Calculation of Waste Stream Volumes, Waste and Container Material Densities, and Radionuclide Concentrations for Non-debris AMWTF Waste Streams an INEEL for the Compliance Recertification Application.* ERMS 530688. Sandia National Laboratories Carlsbad Programs Group, Carlsbad, New Mexico. August 12, 2003.

Long, J. 2003. *Execution of Performance Assessment for the Advanced Mixed Waste Calculations, Rev. 0.* ERMS 532564. Sandia National Laboratories Carlsbad Programs Group, Carlsbad, New Mexico. October 27, 2003.

Lott, S. 2003a. *Response to the Request for Waste Material and Container Material Densities from TWBID Revision 2.1, Version 3.12, Data Version D.4.08.* Letter to C.D. Leigh. ERMS 530767. Los Alamos National Laboratories Carlsbad Programs Group, Carlsbad, New Mexico. August 15, 2003.

Lott, S. 2003b *Response to the Request for Radionuclide Activities in TRU Waste Streams from TWBID Revision 2.1 Version 3.12, Data Version D.4.09,* Letter to C.D. Leigh, ERMS 532566, Los Alamos National Laboratories Carlsbad Programs Group, Carlsbad, New Mexico, September 19, 2003.

Ludwigsen, J.S., D.J. Ammerman, and H.D. Radloff 1998. *Analysis in Support of Storage of Residues in the Pipe Overpack Container.* SAND98-1003. Sandia National Laboratories, Albuquerque, New Mexico. April, 1998.

Park, B-Y, and F.D. Hansen 2003a. *Simulations of the Pipe Overpack to Compute Constitutive Model Parameters.* ERMS 533188, Sandia National Laboratories Carlsbad Programs Group, Carlsbad, New Mexico.

Park, B-Y, and F.D. Hansen 2003b. *Determination of the Porosity Surfaces of the Disposal Room Containing Various Waste Inventories for WIPP PA*. ERMS 533216, Sandia National Laboratories Carlsbad Programs Group, Carlsbad, New Mexico.

Park, B-Y, and J.F. Holland 2003. *Structural Evaluation of WIPP Disposal Room Raised to Clay Seam G.* SAND-2003-3409, Sandia National Laboratories Carlsbad Programs Group, Carlsbad, New Mexico.

Pfeifle, T.W., and L.D. Hurtado 1998. *Permeability of Natural Rock Salt From the Waste Isolation Pilot Plant (WIPP) During Damage Evolution and Healing*. SAND-98-0417C CONF-980620, Sandia National Laboratories, Albuquerque, New Mexico.

Snider, A.C. 2003a. *Calculation of the Quantities of MgO Required for the Consumption of CO_2 for the WIPP Compliance Recertification Application*. ERMS 530220. Sandia National Laboratories Carlsbad Programs Group, Carlsbad, New Mexico. June 30, 2003.

Snider, A.C. 2003b. *Calculation of MgO Safety Factors for the WIPP Compliance Recertification Application and for Evaluating Assumptions of Homogeneity in WIPP PA*. ERMS 531508. Sandia National Laboratories Carlsbad Programs Group, Carlsbad, New Mexico. September 11, 2003.

SNL 1997a. *Summary of EPA-Mandated Performance Assessment Verification Test (Replicate 1) and Comparison with the Compliance Certification Application Calculations (Rev 1).* WPO 46674. Sandia National Laboratories, Albuquerque, New Mexico. September, 1997.

SNL 1997b. *Supplemental Summary of EPA-Mandated Performance Assessment Verification Test (All Replicates) and Comparison with the Compliance Certification Application Calculations.* WPO 46702. Sandia National Laboratories, Albuquerque, New Mexico. August, 1997.

SNL 1997c. *Quality Assurance Document, Version 1.0 for SANTOS.* WPO 37673. Sandia National Laboratories, Albuquerque, New Mexico.1997.

SNL 1997d. *Verification and Qualification Document for SANTOS.* WPO 35675. Sandia National Laboratories, Albuquerque, New Mexico. 1997.

SNL 2002. *Sandia National Laboratories FEPs Assessment of Advanced Mixed Waste Treatment Facility Wastes at the WIPP.* ERMS 524771. Sandia National Laboratories Carlsbad Programs Group, Carlsbad, New Mexico. December 2, 2002.

Stein, J.S., and W.P. Zelinski 2004. *Effect of Increased Iron Surface Area from Supercompacted AMWTP Waste on Long-Term Repository Conditions as Modeled in Performance Assessment of the WIPP.* Sandia National Laboratories Carlsbad Programs Group, Carlsbad, New Mexico. Undated.

Stone, C.M. 1997a. *Final Disposal Room Structural Response Calculations.* SAND97-0795. Sandia National Laboratories, Albuquerque, New Mexico. 1997.

Stone, C.M. 1997b. *SANTOS-A Two-dimensional Finite-Element Program for the Quasi-Static, Large Deformation, Inelastic Response of Solids*. SAND90-0543. Sandia National Laboratories, Albuquerque, New Mexico. 1997.

Wagner, S.W., and G.R. Kirkes 2002. *FEPs Assessment Analysis Plan, AP-090.* ERMS 522779. Sandia National Laboratories Carlsbad Programs Group, Carlsbad, New Mexico. June 2002.

Wang, Y. and L.H. Brush 1996. *Estimates of Gas-Generation Parameters for the Long-Term WIPP Performance Assessment.* Memorandum to M.S. Tierney. ERMS 231943. Sandia National Laboratories, Albuquerque, New Mexico. January 26, 1996.

Appendix A

FEPs Identified by SNL as Related to Accepting AMWTF Waste at WIPP

Table A-1. FEPs Identified by SNL as Related to Accepting AMWTF Waste at WIPP

EPA FEP No.	FEP Name	FEP Base Assumption	Screening Classification (see legend)	Comments on Classification	CCA Cross References
W2	Waste inventory	The quantity and type of radionuclides emplaced in the repository will dictate performance requirements	UP		SCR.2.1.2 Section 4.1 Section 6.4.3.5 Section 6.4.3.3 Appendix BIR Appendix WCA, Sections 3.2, 8.2 and 8.3 Appendix PAR, Table PAR-41
W3	Heterogeneity of waste forms	The distribution of radionuclides within the different waste types could affect release patterns	DP		SCR.2.1.2 Section 6.4.7 Section 6.4.12.4 Appendix WCA, Section 3.2.1
W4	Container form	The type and shape of waste container will affect heat dissipation and container strength	SO-C		SCR.2.1.3 Appendix DVR, Section 12.2
W5	Container material inventory	Steel and other materials will corrode and affect the amount of gas generated	UP		SCR.2.1.3 Chapter 4, Table 4-4 Section 6.4.3.3 Appendix BIR Appendix SOTERM, Section 2.2.3 Appendix PAR, Parameter 1, Table PAR-43
W12	Radionuclide decay and ingrowth	Radioactive decay of waste will change and decrease the inventory with time	UP		SCR.2.2.1 Section 6.4.12.4 Section 6.4.5.4.2 Appendix BIR, Section 3.2 Appendix NUTS, Section 4.3.7 Appendix SECOTP2D, Section 2 Appendix PANEL, Section 4.6
W13	Heat from radioactive decay	Radioactive decay of waste will generate heat in the repository	SO-C		SCR.2.2.2

W14	Nuclear criticality: heat	A sustained fission reaction would generate heat	SO-P		SCR.2.2.3 *Section 6.4.6.2* *Section 6.4.5.2* *Appendix MASS*
W15	Radiological effects on waste	Radiation can change the physical properties of many materials	SO-C		SCR.2.2.4 *Section 6.4.3.4* *Section 6.4.3.5* *Section 6.3.3.6*
W16	Radiological effects on containers	Radiation can change the physical properties of many materials	SO-C		SCR.2.2.4 *Section 6.4.3.4* *Section 6.4.3.5* *Section 6.3.3.6*
W17	Radiological effects on seals	Radiation can change the physical properties of many materials	SO-C		SCR.2.2.4 *Section 6.4.3.4* *Section 6.4.3.5* *Section 6.3.3.6*
W25	Disruption due to gas effects	Increased gas pressures may lead to fracturing of Salado interbeds	UP		SCR.2.3.5 Section 6.4.5.2 Appendix BRAGFLO, Section 4.10 Appendix MASS, Section 13.3 and Attachment 13-2 Appendix PAR, Table PAR-36
W26	Pressurization	Increased gas pressures may slow the rate of salt creep	UP		SCR.2.3.5 Section 6.4.3.1 Appendix BRAGFLO, Section 4.11 Appendix PORSURF, Attachment PORSURF-6
W27	Gas explosions	Explosion of gas mixtures in the repository could affect the DRZ	UP		SCR.2.3.6 Section 6.4.5.3 Appendix PCS, Section 2.2.3 Appendix PAR, Table PAR-37
W28	Nuclear explosions	A critical mass of plutonium in the repository could explode if rapidly compressed	SO-P		SCR.2.3.6
W29	Thermal effects on material properties	Temperature rises could lead to changes in porosity and permeability	SO-C		SCR.2.3.7 Appendix SEAL, Section 7.4

W30	Thermally-induced stress changes	Elevated temperatures could change the local stress field and alter the rate of salt creep	SO-C		SCR.2.3.7
W31	Differing thermal expansion of repository components	Stress distribution and strain changes can depend on differing rates of thermal expansion between adjacent materials	SO-C		SCR.2.3.7
W32	Consolidation of waste	Salt creep and room closure will change waste permeability	UP		SCR.2.3.8 Section 6.4.3.1 Section 6.4.3.2 Appendix WCA, Section 5.2 Appendix PAR, Table PAR-38 Appendix PORSURF, Attachment PORSURF-6
W33	Movement of containers	Density differences or temperature rises could lead to movement of containers within the salt	SO-C		SCR.2.3.8
W34	Container integrity	Long-lived containers could delay dissolution of waste	SO-C	Beneficial SO-C	SCR.2.3.8 Section 6.5.4

W44	Degradation of organic material	Microbial breakdown of cellulosic material in the waste will generate gas	UP		SCR.2.5.1.1 Section 6.4.3.3 Appendix SOTERM, Section 2.2.2 Appendix WCA, Section 5.1 Appendix BRAGFLO, Section 4.13 Appendix MASS, Section 8 and Attachment 8-2
W49	Gases from metal corrosion	Anoxic corrosion of steel will produce hydrogen	UP		SCR.2.5.1.2 Section 6.4.3.3 Appendix SOTERM, Section 2.2.3 Appendix WCA, Section 5.1 Appendix BRAGFLO, Section 4.13 Appendix MASS, Section 8 and Attachment 8-2
W50	Galvanic coupling	Potential gradients between metals could affect corrosion rates	SO-P		SCR.2.5.1.2 *Appendix GCR*
W51	Chemical effects of corrosion	Corrosion reactions will lower the oxidation state of brines and affect gas generation rates	UP		SCR.2.5.1.2 *Section 6.4.3.3* Appendix WCA, Section 4.1.1 Appendix PAR, Parameter 1, Table PAR-43
W52	Radiolysis of brine	Alpha particles from decay of plutonium can split water molecules to form hydrogen and oxygen	SO-C		SCR.2.5.1.3 Section 6.4.3.3 *Section 6.4.3.5* *Section 6.4.3.6* Appendix MASS, Section 8
W53	Radiolysis of cellulose	Alpha particles from decay of plutonium can split cellulose molecules and affect gas generation rates	SO-C		SCR.2.5.1.3
W54	Helium gas production	Reduction of alpha particles emitted from the waste will form helium	SO-C		SCR.2.5.1.3 *Section 6.4.3.3* *Appendix BIR*

W55	Radioactive gases	Radon will form from decay of plutonium. Carbon dioxide and methane may contain radioactive ^{14}C	SO-C		SCR.2.5.1.3 Appendix BIR
W56	Speciation	Speciation is the form in which elements occur under particular conditions. This form controls mobility and the reactions that are likely to occur	UP	UP in disposal rooms and Culebra. SO-C elsewhere, and beneficial SO-C in cementitious seals.	SCR.2.5.2 Section 6.4.3.4 Section 6.4.3.5 Section 6.4.6.2.1 Appendix SOTERM, Sections 3 AND 4 Appendix PAR, Parameters 36 to 47, 52 to 57, Table PAR-39
W57	Kinetics of speciation	Reaction kinetics control the rate at which particular reactions occur thereby dictating which reactions are prevalent in non-equilibrium systems	SO-C		SCR.2.5.2
W58	Dissolution of waste	Dissolution of waste controls the concentrations of radionuclides in brines and groundwaters	UP		SCR.2.5.3 Section 6.4.3.5 Appendix PAR, Parameters 36 to 47, Table PAR-39
W59	Precipitation [secondary minerals]	Precipitation of secondary minerals could affect the concentrations of radionuclides in brines and groundwaters	SO-C	Beneficial SO-C	SCR.2.5.3
W60	Kinetics of precipitation and dissolution	The rates of dissolution and precipitation reactions could affect radionuclide concentrations	SO-C	Kinetics of waste dissolution is a beneficial SO-C	SCR.2.5.3
W61	Actinide sorption	Actinides may accumulate at the interface between a solid and a solution. This affects the rate of transport of actinides in brines and groundwaters	UP	UP in the Culebra and Dewey Lake. Beneficial SO-C elsewhere	SCR.2.5.4 *Chapter 3* Section 6.4.3.6 Section 6.4.6.2.1 Section 6.4.6.6 *Appendix SEAL* Appendix MASS, Section 15.2 and Attachment 15-1 Appendix SECOTP2D, Section 2

W62	Kinetics of sorption	The rate at which actinides are sorbed can affect radionuclide concentrations	UP		SCR.2.5.4 Appendix MASS, Section 15.2, Attachment 15-1 Appendix PAR, Parameters 47 and 52 to 57, Table PAR-39
W63	Changes in sorptive surfaces	Changes in mineralogy along fracture walls could change the extent of sorption	UP		SCR.2.5.4 Appendix MASS, Section 15.2, Attachment 15-1 Appendix PAR, Parameters 47 and 52 to 57, Table PAR-39
W64	Effect of metal corrosion	Metal corrosion will have an effect on chemical conditions in the repository by absorbing oxygen	UP		SCR.2.5.5 Section 6.4.3.5 Appendix SOTERM, Sections 2.2.3 and 4 Appendix WCA, Section 4.1.1 Appendix PAR, Parameters 36 to 47, Table PAR-39
W65	Reduction-oxidation fronts	Redox fronts may affect the speciation and hence migration of radionuclides	SO-P		SCR.2.5.5
W66	Reduction-oxidation kinetics	Reduction-oxidation reactions may not be in thermodynamic equilibrium thereby affecting speciation	UP		SCR.2.5.5 Section 6.4.3.5 Appendix SOTERM, Sections 2.2.3 and 4 Appendix PAR, Parameters 36 to 47, Table PAR-39
W67	Localized reducing zones	Localized reducing zones, bounded by reduction-oxidation fronts, may develop on metals undergoing corrosion	SO-C		SCR.2.5.5
W68	Organic complexation	Aqueous complexes between radionuclides and organic materials may enhance the total dissolved radionuclide load	SO-C		SCR.2.5.6 Section 6.4.3.5 Appendix SOTERM, Section 5 Appendix WCA, Section 4.1.3

W69	Organic ligands	Increased concentrations of organic ligands favor the formation of complexes	SO-C		SCR.2.5.6 Section 6.4.3.5 Appendix SOTERM, Section 5 Appendix WCA, Sections 4.1.3, 8.11 and 8.12 Appendix BIR
W70	Humic and fulvic acids	High molecular weight organic ligands, including humic and fulvic acids may be present in soil waste	UP		SCR.2.5.6 Section 6.4.3.6 Section 6.4.6.2.2 Appendix SOTERM, Section 6.3.3 Appendix PAR, Parameter 46, Table PAR-39
W71	Kinetics of organic complexation	The rates of complex dissociation may affect radionuclide uptake and other reactions	SO-C		SCR.2.5.6
W72	Exothermic reactions	Exothermic reactions, including concrete and backfill hydration, and aluminum corrosion, may raise the temperature of the disposal system	SO-C		SCR.2.5.7 *Section 6.4.3.5* Appendix WCA, Section 5.3.1
W73	Concrete hydration	Hydration of concrete in seals will enhance rates of salt creep and may induce thermal cracking	SO-C		SCR.2.5.7 Appendix SEAL, Section 7.4.1.1
W74	Chemical degradation of seals	Reaction of cement with brine and groundwater may affect seal permeability	UP		SCR.2.5.8 Section 6.4.4 Appendix SEAL, Appendix A Appendix PAR, Parameter 10, Table PAR-19
W75	Chemical degradation of backfill	Reaction of the MgO backfill with CO_2 and brine may affect disposal room permeabilities	SO-C		SCR.2.5.8 Appendix BACK, Section 3.2

W77	Solute transport	Radionuclides may be transported as dissolved species or solutes	UP		SCR.2.6.1 Section 6.4.5.4 Section 6.4.6.2.1 Appendix MASS, Sections 13.5 and 15.2 Appendix NUTS, Section 4.3 Appendix SECOTP2D, Section 2
W78	Colloid transport	Colloid transport, with associated radionuclides, may occur at a different rate to dissolved species	UP		SCR.2.6.2 Section 6.4.6.2.2 Appendix MASS, Section 15.3 and Attachments 15-2 and 15-8 Appendix SECOTP2D, Section 2

W79	Colloid formation and stability	The formation and stability of colloids is dependent upon chemical conditions such as salinity	UP		SCR.2.6.2 Section 6.4.3.6 Appendix SOTERM, Section 6 Appendix BACK, Section 3.4 Appendix WCA, Section 4.2 Appendix PAR, Parameter 46, Table PAR-39
W80	Colloid filtration	Colloids with associated radionuclides may be too large to pass through pore throats in some media	UP		SCR.2.6.2 Section 6.4.6.2.2 Appendix MASS, Section 15.3 and Attachments 15-8 and 15-9
W81	Colloid sorption	Colloids with associated radionuclides may be physically or chemically sorbed to the host rock	UP		SCR.2.6.2 Section 6.4.6.2.2 Appendix SECOTP2D, Section 2 Appendix MASS, Section 15.3 and Attachment 15-8 Appendix PAR, Parameters 52-57
W82	Suspensions of particles	Rapid brine flow could transport active particles in suspension	DP	SO-C for undisturbed conditions	SCR.2.6.3 Section 6.4.7.1 Appendix CUTTINGS, Appendix A.2
W83	Rinse	Rapid brine flow could wash active particulates from waste surfaces	SO-C		SCR.2.6.3

W84	Cuttings	Waste material intersected by a drill bit could be transported to the ground surface	DP	Repository intrusion only	SCR.2.6.3 Section 6.4.7.1 Appendix CUTTINGS, Appendix A.2
W85	Cavings	Waste material eroded from a borehole wall by drilling fluid could be transported to the ground surface	DP	Repository intrusion only	SCR.2.6.3 Section 6.4.7.1 Appendix CUTTINGS, Appendix A.2
W86	Spallings	Waste material entering a borehole through repository depressurization could be transported to the ground surface	DP	Repository intrusion only	SCR.2.6.3 Section 6.4.7.1 Appendix CUTTINGS, Appendix A.2
W87	Microbial transport	Radionuclides may be bound to or contained in microbes transported in groundwaters	UP		SCR.2.6.4 Section 6.4.6.2.2 Appendix SOTERM, Section 6.3.4 Appendix MASS, Section 15.3 and Attachment 15-9
W88	Biofilms	Biofilms may retard microbes and affect transport of radionuclides	SO-C	Beneficial SO-C	SCR.2.6.4
W89	Transport of radioactive gases	Gas phase flow could transport radioactive gases	SO-C		SCR.2.6.5 SCR.2.5.1.3
W90	Advection	Dissolved and solid material can be transported by a flowing fluid	UP		SCR.2.7.1 Section 6.4.5.4 Section 6.4.6.2 Appendix NUTS, Sections 4.3.1 and 4.3.2 Appendix SECOTP2D, Section 2
W91	Diffusion	Dissolved and solid material can be transported in response to Brownian forces	UP		SCR.2.7.2 Section 6.4.6.2 Section 6.4.5.4 Appendix MASS, Attachment 15-3 Appendix SECOTP2D, Section 2 Appendix NUTS, Section 4.3.3

W92	Matrix diffusion	Dissolved and solid material may be transported transverse to the direction of advection in a fracture and into the rock matrix	UP		SCR.2.7.2 Section 6.4.6.2 Appendix MASS, Attachment 15.6 Appendix SECOTP2D, Sections 2, 3.5 and 3.6
W93	Soret effect	There will be a solute flux proportional to any temperature gradient	SO-C		SCR.2.7.3
W95	Galvanic coupling	Potential gradients may be established between metal components of the waste and containers and affect radionuclide transport	SO-P		SCR.2.7.4 Appendix GCR
W96	Electrophoresis	Charged particles and colloids can be transported along electrical potential gradients	SO-C		SCR.2.7.4
W97	Chemical gradients	Chemical gradients will exist at interfaces between different parts of the disposal system and may cause enhanced diffusion	SO-C	p. SCR-87 incorrectly states that gradients are UP.	SCR.2.7.5
W98	Osmotic processes	Osmosis may allow diffusion of solutes across a salinity interface	SO-C	Beneficial SO-C	SCR.2.7.5
W99	Alpha recoil	Recoil of the daughter nuclide upon emission of an alpha-particle during radioactive decay at the surface of a solid may eject the daughter into groundwater	SO-C		SCR.2.7.5
W100	Enhanced diffusion	Chemical gradients may locally enhance rates of diffusion	SO-C		SCR.2.7.5

Modified from SNL 2002, Table 2

Table A.1 Key:

UP FEP accounted for in the assessment calculations for undisturbed performance for 40 CFR 191.13 (as well as 40 CFR 191.15 and Subpart C of 40 CFR Part 191).

DP FEP accounted for (in addition to all UP FEPs) in the assessment calculations for disturbed performance for 40 CFR 191.13.

SO-R FEP eliminated from performance assessment calculations on the basis of regulations provided in 40 CFR Part 191 and criteria provided in 40 CFR Part 194.

SO-C FEP eliminated from performance assessment (and compliance assessment) calculations on the basis of consequence.

SO-P	FEP eliminated from performance assessment (and compliance assessment) calculations on the basis of low probability of occurrence.
NA	FEP not applicable to the particular category.
HCN	Historical, Current and Near-Future human-initiated events and processes (EPs)
Future	Future human-initiated EPs